YANCHAO YUE

UNIVERSITÀ DEGLI STUDI DI TRENTO

Doctoral School in Engineering of Civil and Mechanical Structural Systems

IMPACT OF SEISMIC VULNERABILITY ON BRIDGE MANAGEMENT SYSTEMS

YANCHAO YUE

IMPACT OF SEISMIC VULNERABILITY ON BRIDGE MANAGEMENT SYSTEMS

May 2012

University of Trento
University of Brescia
University of Padua
University of Trieste
University of Udine
University IUAV of Venice

Yanchao Yue

IMPACT OF SEISMIC VULNERABILITY ON BRIDGE MANAGEMENT SYSTEMS

Tutor: Dr. Daniele Zonta

Co-Tutor: Dr. Matteo Pozzi

2011

UNIVERSITY OF TRENTO
Doctoral School of Engineering of Civil and Mechanical Structural Systems

Head of Doctoral School: Prof. Davide Bigoni

Dissertation Defense on 25th November 2011

Board of Examiners:

Prof. Paolo E. Pinto	University of Rome 'La Sapienza', Italy
Prof. Daniel Straub	Technical University of Munich, Germany
Dr. Daniele Zonta	University of Trento, Italy

SUMMARY

Motivated by the potential vulnerability of their road infrastructure, many national authorities and local Departments of Transportation are incorporating seismic risk assessment in their management systems. This Dissertation aims to develop methods and tools for seismic risk analysis that can be used in a Bridge Management System (BMS); helping bridge owners to assess the costs of repair, retrofit and replacement of the bridges under their responsibility.

More specifically, these tools are designed to offer estimates of:
(1) the seismic risk to single components of bridges and their expected performance after an earthquake.
(2) the impact *a priori* (i.e. before an earthquake) of a given earthquake on the operation of a road network, in terms of connectivity between different locations.
(3) the damage *a posteriori* (i.e. after an earthquake) to road network operation, based on prior knowledge of network vulnerability and on the observed damage to a small number of single bridges.

The effectiveness of these methods is tested and validated in a specific case study, the bridge stock of the Autonomous Province of Trento (APT) in Italy.

To address the first point, I will first introduce the fragility curve method for risk assessment of individual bridges. The Hazus model is chosen as the most appropriate and is applied to the bridges of the APT stock. Once the fragility curves for all the bridges have been generated, a risk analysis is performed for three earthquake scenarios (with return periods of 72, 475 and 2475 years) and four condition states (operational, damage, life safety and collapse limit state). Next, I will extend the results of the component level analysis to the network level: the APT road network is modeled in the form of a graph and the problem of connectivity between two locations is analyzed. A shortest path algorithm is introduced and implemented to identify the best path between any two given places. Correlation in capacity and demand among bridges is not considered at this stage.

After reiterating the fundamentals of probability theory, the theory of Bayesian Networks is introduced. The Bayesian Network approach is used to incorporate mutual correlation in capacity and demand, in risk assessment of a bridge stock. The concept is first formulated and illustrated on a simple case (the ‘twin bridge problem’), then extended to the general case of a full stock. I will show how the

same framework can be used in post-earthquake assessment problems, where the evidence of the state of one or more bridges affects the prediction of the performance of another bridge. The outcomes and the limits of this work are discussed at the end of the Thesis.

DEDICATION

To my parents, my wife and Elena:

Thank you for your constant belief in me and unconditional support in the pursuit of my dream. It is you that give me the force, courage and confidence to face happiness and sadness, chances and challenges. I love you all forever!

ACKNOWLEDGEMENTS

My first and utmost gratitude is to my tutor, Dr. Daniele Zonta for his invaluable supervision and support during my PhD study. His profound knowledge of the research field and his manner of viewing this world have always inspired me, not only in the way of conducting my research work but also in the way of striving in my life. His generous encouragements and great enthusiasm in my job have and will always stimulate me to face challenges with confidence, all my life. I am lucky to have the honor of being his student in my life.

I wish to express my special thanks to Dr. Matteo Pozzi and Dr. Francesca Bortot. The extensive discussions and close cooperation with them resulted in many of the innovative ideas presented in this Thesis. Especially, I need to thank my co-tutor Dr. Matteo Pozzi, who reviewed and checked every detail of my Thesis.

My thanks also go to Prof. Riccardo Zandonini, Prof. Maurizio Piazza and Prof. Oreste S. Bursi for their instructions and support in Trento and to my friends and colleagues, Huayong Wu, Chuanguo Jia, Davide Trapani, Emiliano Debiasi, Federico Larcher, Paolo Esposito, Anil Kumar, Leqia He, and Zhen Wang, who made my stay here feel as if it were my home.

Finally thanks to all those who have contributed with their efforts and enthusiasm to the realization of this Thesis.

CONTENTS

SUMMARY 3
DEDICATION 5
ACKNOWLEDGEMENTS 7
CONTENTS 9
LIST OF TABLES 13
LIST OF FIGURES 15
1 Introduction 19
1.1 Motivation 19
1.2 Objectives of the Thesis 21
1.3 Introducing the APT BMS 21
1.4 Method 24
1.5 Outline of Thesis 25
2 Fragility curves 27
2.1 Introduction 27
2.1.1 Expert Based Fragility Functions 28
2.1.2 Empirical fragility curves 28
2.1.3 Analytical fragility curves 29
2.2 HAZUS model 30
2.2.1 Formulation of fragility curves 30
2.2.2 Capacity-spectrum approach 31
2.2.3 Analysis of bridge capacity 33
2.2.4 Accounting for 3D effects 34
2.3 Application of Hazus model to APT-BMS 36
2.3.1 Example of a bridge with weak bearings and strong piers 36
2.3.2. Example of a bridge with strong bearings and weak piers 37
2.4 Results and conclusions 40
2.5 Other methods for generating fragility curves 43
2.5.1 The maximum likelihood method (Shinozuka et al. 2000b) 43
2.5.2 Fragility curves for highway bridges (Karim and Yamazaki 2003) 44

2.5.3 Fragility curves for bridge piers based on numerical simulation (Karim and Yamazaki 2001) 45
2.5.4 Seismic fragility methodology for bridges using component level approach (Nielson and DesRoches 2007) 47
3 Network level assessment 49
3.1 Introduction 49
3.2 Connectivity analysis in APT-BMS 50
3.2.1 Definition of network connectivity 50
3.2.2 Description of algorithms ORDER and ORDER-II 52
3.2.3 Network simulation 54
3.2.4 Implementation in APT-BMS 58
3.3 Identifying the safest path in the network 63
3.3.1 Calculation procedure of Dijkstra's algorithm 63
3.3.2 Algorithm implementation and results 64
3.4 Existing methods for network level assessment 65
3.4.1 Probability-Based Bridge Network Performance Evaluation (Liu and Frangopol 2006) 65
3.4.2 Prioritization based on system reliability analysis (Nojima 1998) 66
3.4.3 Vulnerability and importance based prioritization (Basöz and Kiremidjian 1995) 68
3.4.4 Bridge Network maintenance optimization using stochastic dynamic programming (Frangopol and Liu 2007) 69
3.4.5 Minimal link set and minimal cut set formulations (Bensi 2010) 69
4 Bayesian Network 71
4.1 Introduction 71
4.2 Basics of Probability Theory 72
4.2.1 Conditional probability and independence 72
4.2.2 Conditional independence 72
4.2.3 The law of total probability 72
4.2.4 Bayes' Theorem 73
4.3 Bayesian networks 76
4.3.1 Definition of Bayesian Networks 76
4.3.2 The Chain Rule for Bayesian Networks 77
4.4 Junction trees 78
4.4.1 Moralization 78
4.4.2 Triangulation 79
4.5 Bayesian networks with conditional Gaussian distributions 80
4.5.1 Conditional Gaussian potentials 80
4.5.2 Marginals 82
4.5.3 Direct combination 82
4.5.4 Complements 83
4.5.5 General combination 84

4.5.6 Assignment of potentials to cliques 85
4.5.7 Collecting message 86
4.5.8 Distributing messages from the root 87
4.5.9 Entering evidence 89
4.6 Software packages for Bayesian networks 89
4.6.2 Bayesian Network Toolbox (BNT) 91
4.6.2 Hugin 91
4.6.3 BayesiaLab 93
4.6.4 Netica 94
4.6.5 MSBNX 94
4.6.6 GeNIe & SMILE 95
5 Post-earthquake analysis using Bayesian Networks 97
5.1 Introduction 97
5.1.1 BNs in civil engineering 97
5.1.2 BNs in seismic risk analysis 98
5.2 Proposed framework 101
5.2.1. The demand model 102
5.2.2 Capacity Model 104
5.2.3 The uncertainties terms 105
5.2.4 BN framework for individual bridges 107
5.2.5 BN framework for twin bridges 109
5.3 Operations on the framework 112
5.3.1 Prior distribution of earthquake magnitude 112
5.3.2 Entering evidence in the BN framework 113
5.4. Case study 116
5.4.1 Bridges with strong piers and weak bearings 116
5.4.1.1 Initialization 118
5.4.1.2 Entering evidence 118
5.4.2 Bridges with strong bearings and weak piers 119
5.4.2.1 Initialization 120
5.4.2.2 Entering evidence 121
5.5. Conclusions 122
6 Network-level analysis using Bayesian Networks 123
6.1 Description of the framework 123
6.2 Computation procedures 130
6.3 Application 131
6.4 Identifying the best path 137
6.4.1 The link value 137
6.4.2 The sum of different link values 139
6.4.3 Application 140
6.4.4 Results 144
6.5 Conclusions 145

7 Conclusions and Future work 147
Appendix A: Joint distribution for uncertainties in two sites 151
Appendix B: Earthquake return period 155
Appendix C: Gaussian random fields 157
Appendix D: Monte Carlo simulation 159
Appendix E: How to consider the correlation between global variables 161
References 163
Publications 171

LIST OF TABLES

Table 1.1 Deadliest Earthquakes 1990 - 2011 (USGS, 2011).....20
Table 2.1 Definition of damage states (FEMA, 2003).....31
Table 2.2 Drift and displacement limits (Basöz and Mander, 1999) 32
Table 2.3 Values for strength reduction factor Q (Dutta, 1999) 33
Table 2.4 Friction coefficients of the bearings in the transverse direction (Basöz and Mander 1999).....34
Table 2.5 3D effect factor for bridges seated on strong bearings with weak piers (Dutta and Mander 1998).....35
Table 2.6 3D effect factor for single span bridge (Basöz and Mander 1999).....35
Table 2.7 The required parameters for calculating median spectral accelerations 36
Table 2.8 Seismic probability of Ponte Nogarè SP83 for different limit states.....37
Table 2.9 Spectral parameters at the SP90 Adige Bridge location 38
Table 2.10 parameters of the SP90 Bridge on the Adige River 38
Table 2.11 parameters of the pier.....39
Table 3.1 probabilities in operational mode.....50
Table 3.2 all the network states in Fig. 3.1 51
Table 3.3 Geographical coordinates of nodes in Trento to Ala road network 55
Table 3.4 Descriptions of links in Trento to Ala road network.....57
Table 3.5 Expected connectivity of between Trento to Ala given different m values 60
Table 3.6 Connectivity between Passo Lavazè and Riccomassimo for different m values for return period of 475 years.....61
Table 3.7 Connectivity between Passo Lavazè and Riccomassimo for different m values for return period of 72 years.....62
Table 3.8 Connectivity between Passo Lavazè and Riccomassimo given different m values for return period of 2475 years.....62
Table 4.1 States of the variables (Neapolitan, R.E. 2003).....75
Table 4.2 List of all the software package for BNs 90
Table 5.1 Parameters for calculating the median spectral acceleration in Eq (5.4).117
Table 5.2 Results after initialization 118

Table 5.3 Results given the evidence 118
Table 5.4 Parameters for calculating median spectral acceleration 119
Table 5.5 Prior distribution of variables after initialization 120
Table 5.6 Posterior distributions of variables given the evidence 121
Table 5.7 Posterior distributions of the physical parameters given the evidence 121
Table 6.1 Prior distribution of the global variables 131
Table 6.2 Posterior distributions of the global variables based on the evidence that bridge 1 has collapsed 134
Table 6.3 Posterior distributions of the global variables based on evidence that bridge 2 has collapsed 135
Table 6.4 Posterior distributions of the global variables based on the evidence that bridge 3 is safe 135

LIST OF FIGURES

Fig. 1.1 Bridge age distribution (a); typological distribution (b) in APT-BMS (Zonta. et al 2007) 22
Fig. 1.2 Flowchart for the APT-BMS showing its main components and information paths (Zonta. et al 2007) 22
Fig. 2.1 Graphical representation of fragility function (Nielson 2005).....28
Fig. 2.2 Two failure modes for single span bridges (Basöz, and Mander. 1999) 33
Fig. 2.3 (a) Overview of the SP83 Bridge on the Nogarè River; (b) Plan view, elevation and cross-section of the deck 36
Fig. 2.4 Fragility curves of Ponte Nogarè SP83 37
Fig. 2.5 Overview of the SP90 Bridge on the Adige River at Villa Lagarina.....37
Fig. 2.6 The fragility curves of the pier 38
Fig. 2.7 The fragility curves due to the sliding of bearings 39
Fig. 2.8 Seismic vulnerability of APT stock for the return period of 475 years in damage states (a), OLS (b), DLS (c), LLS (d), CLS 40
Fig. 2.9 Seismic vulnerability of APT stock for the return period of 72 years in damage states (a), OLS (b), DLS (c), LLS (d), CLS 41
Fig. 2.10 Seismic vulnerability of APT stock for the return period of 2475 years in damage states (a), OLS (b), DLS (c), LLS (d), CLS 41
Fig. 2.11 Seismic vulnerability distribution of the APT stock.....42
Fig. 2.12 PGA value of APT region with 475 years' return period (DPC-INGV).....42
Fig. 2.13 Example of empirical fragility curves reported by Shinozuka et al. (2000b) 44
Fig. 3.1 Simple network with two nodes and three bridges.....50
Fig. 3.2 Google Earth map from Trento to Ala.....55
Fig. 3.3 Simulated transportation graph between Trento-Ala.....56
Fig. 3.4 The simplified graph between Trento-Ala.....56
Fig. 3.5 Google Earth map of the APT-BMS network.....58
Fig. 3.6 Graph representation of Trento to Ala road network with individual bridges 59
Fig. 3.7 Graph representation of Trento to Ala road network indicating the

probability of link failure.....59
Fig. 3.8 Locations of Passo Lavaz è and Riccomassimo in APT road network 61
Fig. 3.9 Calculation procedures of a simple graph using Dijkstra's algorithm 64
Fig. 3.10 Simulated network and the safest path between Passo Lavaz è and Riccomassimo.....65
Fig. 4.1 A Bayesian Network for the example in Section 4.2.4.....77
Fig. 4.2 Junction tree structure for the Bayesian Network in Fig 4.1.....78
Fig. 4.3 Moralization procedures for the Bayesian Network in Fig 4.1 79
Fig. 4.4 Triangulation procedures for the Bayesian Network in Fig 4.3 79
Fig. 4.5 A conditional Gaussian BN 81
Fig. 4.6 Graphical representation of the direct combination of two potentials 83
Fig. 4.7 Example of Bayesian Network.....86
Fig. 4.8 Assignments of the potentials to the cliques 86
Fig. 4.9 The order of collecting messages 87
Fig. 4.10 Order of distributing messages.....88
Fig. 4. 11 Example of graph structure 90
Fig. 4.12 Graphical representation of the 'Sick Dilemma' example in Hugin 92
Fig. 4.13 Prior distribution of the 'Sick Dilemma' example after initialization in Hugin 92
Fig. 4.14 Graphical representation of the 'Sick Dilemma' example in BayesiaLab .93
Fig. 4.15 Node editor in BayesiaLab 93
Fig. 4.16 Software window of Netica.....94
Fig. 4.17 The software window of MSBNX.....94
Fig. 5.1 Conceptual framework of BN in Bensi et al. (2010).....100
Fig. 5.2 The conceptual BN that contains the three main parts in the framework ..101
Fig. 5.3 The closest distance to the surface projection of the fault (Bensi, 2010)...104
Fig. 5.4 Bayesian Network for bridge type 1.....108
Fig. 5.5 Bayesian Network for bridge type 2.....108
Fig. 5.6 Bayesian Network for two bridges with strong piers and weak bearings ..110
Fig. 5.7 Bayesian Network for two bridges with strong bearings and weak piers ..111
Fig. 5.8 5-component MoG Approximation of the truncated exponential distribution 113
Fig. 5.9 CDFs of the truncated exponential distribution and MoG Approximation 113
Fig. 5.10 How to incorporate into the framework the evidence about the bridge state 114
Fig. 5.11 Procedures to generate the random number X_1 114
Fig. 5.12 SP135 Bridge on River Fersina-Canezza (a) overview (b) Plan view, elevation and cross-section of the deck 116
Fig. 5.13 SP31 Bridge on River Avisio (a) overview (b) Plan view, elevation and cross-section of the deck.....117
Fig. 5.14 Viadotto Pianello: (a) overview (b) plan view, elevation and cross-section of deck 119

Fig. 5.15 Viadotto San Silvestro(a) overview (b) plan view, elevation and cross-section of deck.....119
Fig. 6.1 The BN framework for the network with n bridges 125
Fig. 6.2 BN model for intra-event error (Bensi, 2010).....126
Fig 6.3 Line layout, circle layout and grid layout for numerical investigation (Bensi, 2010).....127
Fig. 6.4 Error measures for different configurations at different distances based on the methods in Bensi (2010).....128
Fig. 6.5 The BN framework for a network with n bridges 129
Fig. 6.6 Distance between two bridges A and B at different locations. 132
Fig. 6.7 Prior seismic vulnerability in APT bridge stock for a 7.0 magnitude earthquake with epicenter in Salò (E10.519935,N45.603110.).....133
Fig. 6.8 Prior distribution of probability of collapse in APT bridge stock for a 7.0 magnitude earthquake with epicenter in Salò (E10.519935,N45.603110).....134
Fig. 6.9 Posterior seismic vulnerability in APT bridge stock for a 7.0 magnitude earthquake with the epicenter in Salò (E 10.519935,N 45.60311).....136
Fig. 6.10 Posterior distribution of probability of collapse in APT bridge stock for a 7.0 magnitude earthquake with the epicenter in Salò (E10.519935, N45.603110) .136
Fig. 6.11 Link composed by bridge A and bridge B in series.....137
Fig. 6.12 Link formed by n bridges in series.....138
Fig. 6.13 Different links between two nodes.....139
Fig. 6.14 The network between Trento and Ala.....141
Fig. 6.15 The link between node 2 and node 4.....141
Fig. 6.16 The BN used to calculate the value of P(B425|B424).....142
Fig. 6.17 The BN used to calculate the value of P(B426|B425·B424) 143
Fig. 6.19 The best path between Passo Lavazè and Riccomassimo 144
Fig. D.1 The integral of f(x) using the Monte Carlo method.....160

1 Introduction

1.1 Motivation

The recent Magnitude 9.0 earthquake near the East Coast of Honshu, Japan, causing 28050 deaths (USGS 2011), again heightens our awareness of the great damage that can be caused by earthquakes. There are about five million earthquakes per year, worldwide. They can cause fires, floods, toxic gas leaks, the spread of bacteria and radio-active materials and can also cause tsunamis, landslides, avalanches, cracks and other secondary disasters. Table 1.1, taken from USGS (2011), gives a quantitative idea of how enormous the damage produced by earthquakes to human society in the last twenty years has been.

Bridges, in particular, play a vital role in modern transportation: they are the key nodes of various road networks and the main components of three-dimensional city traffic. Bridges are also the reflection of a country's development, economic strength, technology and productivity. Bridge Management Systems (BMS) are tools designed to help bridge managers keep track of their bridge stock: providing information on the bridge stock characteristics, condition and serviceability (Thompson et al. 1998, Astudillo 2002, Frangopol Neves 2004, and Bortot 2006). Based on the analysis of single bridges, the BMS helps bridge managers develop programs to determine the best allocation of resources to maximize the safety and functionality of the road network. Originally, the function of BMS was to facilitate the day-to-day management of bridges. Gradually, the functions of BMS became more and more powerful (Bortot 2006). More recently, bridge management systems have been used as tools to improve the overall condition of bridges and to prevent excessive structure deterioration (Bortot, 2006).

We have learned from recent experience how earthquakes can seriously damage highway systems, even in those countries which are supposed to be prepared for such events. Many authors (see, for example, Ghasemi et al., 1996) report the

example of the 1995 Kobe Earthquake, when at least 60% of the bridges in the Kobe area were damaged and the Hanshin Expressway, the major transportation route between Osaka and Kobe, collapsed.

Motivated by the potential vulnerability of their road infrastructure, many national authorities and local Departments of Transportation are incorporating seismic risk assessment in their management systems (FEMA 2003, Shinozuka et al. 2000). Therefore, there is growing demand for tools that help assess seismic bridge vulnerability and can predict bridge performance under a given earthquake scenario. Of critical importance to strategic decision making by transportation and civil protection agencies, is the ability to predict the operational state of the road network in a post-earthquake scenario; this can help minimize the impact of possible network downtimes on the rescue operations.

Table 1.1 Deadliest Earthquakes 1990 - 2011 (USGS, 2011)

Date	Magnitude	Fatalities	Region
1990/06/20	7.4	50,000	Iran
1991/10/19	6.8	2,000	Northern India
1992/12/12	7.8	2,519	Flores Region
1993/09/29	6.2	9,748	India
1994/06/06	6.8	795	Colombia
1995/01/16	6.9	5,530	Kobe, Japan
1996/02/03	6.6	322	Yunnan, China
1997/05/10	7.3	1,572	Northern Iran
1998/05/30	6.6	4,000	Afghanistan-Tajikistan Border Region
1999/08/17	7.6	17,118	Turkey
2000/06/04	7.9	103	Southern Sumatera, Indonesia
2001/01/26	7.7	20,023	India
2002/03/25	6.1	1,000	Hindu Kush Region, Afghanistan
2003/12/26	6.6	31,000	Southeastern Iran
2004/12/26	9.1	227,898	Off West Coast of Northern Sumatra
2005/10/08	7.6	80,361	Pakistan
2006/05/26	6.3	5,749	Java, Indonesia
2007/08/15	8.0	514	Near the Coast of Central Peru
2008/05/12	7.9	87,587	Eastern Sichuan, China
2009/09/30	7.5	1,117	Southern Sumatra, Indonesia
2009/04/06	6.3	308	L'Aquila, Italy
2010/01/12	7.0	222,570	Haiti
2011/03/11	9.0	28050	Near the East Coast of Honshu, Japan

1.2 Objectives of the Thesis

This Dissertation aims to develop methods for seismic risk analysis that can be incorporated in a BMS and so help bridge owners to assess the costs of repair, retrofit and replacement of the bridges under their responsibility. More specifically, these tools address the following points:

1. Estimating the seismic risk of the individual components of a bridge stock, and their expected performance after an earthquake.
2. Evaluating *a priori* (i.e. before an earthquake) the impact of a given earthquake on the operation of a road network, in terms of connectivity between different locations.
3. Evaluating *a posteriori* (i.e. after an earthquake) the damage state of a road network and its operability, based on the prior knowledge of the network vulnerability and the posterior evidence of damage observed on one or more individual bridges.

The effectiveness of these tools is tested and validated on a specific case study, the bridge stock of the Autonomous Province of Trento (APT) in Italy. The APT bridge stock and the Bridge Management Systems currently used by the Department of Transportation are briefly introduced in the next Section.

1.3 Introducing the APT BMS

Due to the political devolution process in Italy since the nineteen seventies, many administrative responsibilities have been transferred to local authorities. During this process, the number of bridges under Autonomous Province of Trento (APT) responsibility doubled, without an adequate transition period. The clear need for a management tool which could help make decisions on maintenance, rehabilitation or replacement of bridges in the APT led to the APT Bridge Management System (BMS). This was is developed in collaboration between the University of Trento (UniTN) and the APT Department of Transportation (DoT) (Zonta. et al 2007).

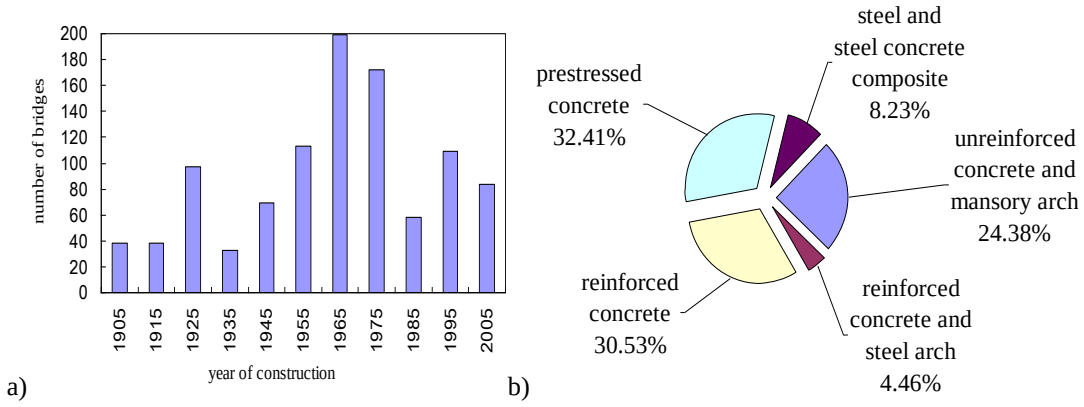

Fig. 1.1 Bridge age distribution (a); typological distribution (b) in APT-BMS (Zonta. et al 2007)

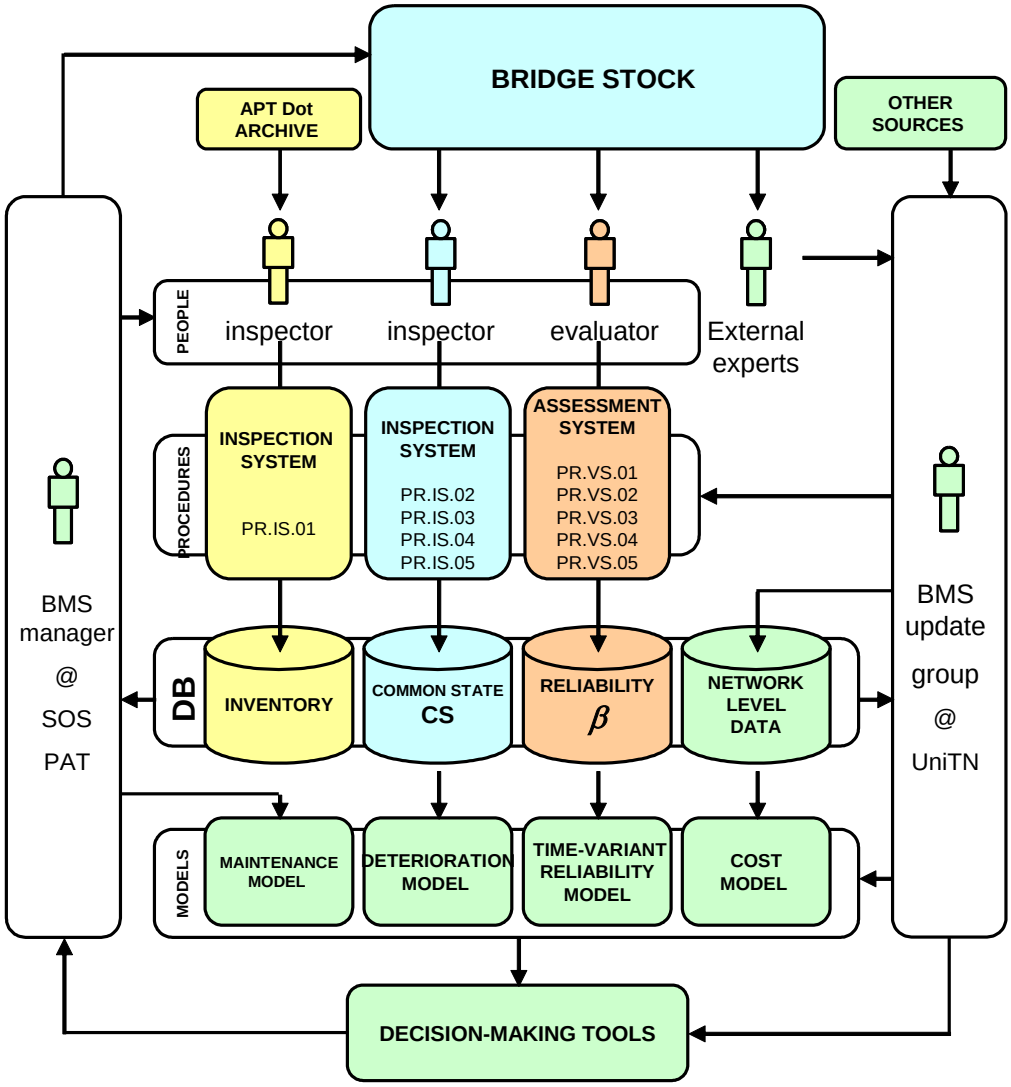

Fig. 1.2 Flowchart for the APT-BMS showing its main components and information paths (Zonta. et al 2007)

The APT-BMS has been operational since 2004; it manages 986 bridges and approximately 2400 kilometers of roads. Most of the APT bridges were built after the Second World War; the peak construction period being the 70s (Fig. 1.1(a)). As for construction type (Fig. 1.1(b)), 62.93% of APT bridges are reinforced concrete and prestressed concrete, and 28.84% are arch bridges, while the remaining 8.23% includes steel and steel-concrete composite bridges.

The APT-BMS is based on an SQL database, which includes all the data for the whole stock of bridges. The main characteristics of the systems are:

- The system is fully operative on the web; inspectors and evaluators upload data to the system through a web-based interface and the managers access the results of the analysis using the same web interface.
- All personnel including DoT (Department of Transportation) managers, DoT inspectors and professional engineers involved in management can directly interact with the system.
- All information is provided in real-time.
- For each bridge, the system not only gives a clear indication of the condition state but also its safety level expressed as a reliability index.
- System maintenance and upgrade are continuous and transparent to the users.

As shown in Fig. 1.2, the APT-BMS has four major components: 'Data Storage', 'Maintenance and Cost Model', 'Deterioration Model' and 'Decision Making Algorithms'. These components are divided into modules; each module having a specific task. The module can be at project level or network level. The former focuses on a single bridge while the latter concerns the bridge stock as a whole.

In APT-BMS, the bridge is considered as a set of Structural Units (SU), such as deck, piles and abutments, which are characterized by common attributes (such as length, material, typology etc.). The spatial arrangement of SUs is defined through connections (C). Each SU and C includes a set of Standard Elements (SE). The APT system currently recognizes 22 types of Structural Unit. For more details of APT-BMS, see Zonta et al. (2007).

1.4 Method

Objective 1 is addressed using a classical fragility curve approach. Fragility curves are conditional probability statements which give the likelihood of a bridge reaching, or exceeding, a particular damage level for an earthquake of a given intensity level (Shinozuka et al. 2000a, Nielson 2005). Much research has been devoted to generating fragility curves. Because of the characteristics of APT-BMS, managing a large number and variety of bridge types, a systematic and quick method is required to develop fragility curves. The Hazus model (FEMA, 2003) meets this requirement and was chosen for application to the case study: in contrast with other methods, such as empirical fragility curves or analytical fragility curves that require much previous damage data or extensive computation, only limited information is needed for this model. Using the Hazus model, the fragility curves for all the bridges in the APT stock are generated. Next, the seismic risks for a number of earthquake scenarios are evaluated. I considered 3 earthquake scenarios, with return periods of 72, 475 and 2475 years, and four possible limit states of the bridge: operational (OLS), damage (DLS), life safety(LLS) and collapse (CLS).

After an earthquake, the ability to decide the best path to distribute the available human and material rescue resources to the disaster centre is of paramount importance to decision makers. Addressing **Objective 2** means solving the problem of determining the best path between any two given locations after an earthquake, where 'best' means the lowest risk of exposure to operational problems in a given damage scenario. This problem is addressed by Dijkstra's algorithm (Dijkstra, 1959). In the analysis, bridges are first regarded simply as independent components. Next, their mutual correlation in demand and capacity are taken in to account. For example, nearby bridges are likely to have a similar site condition, thus their seismic demands are somehow correlated. Also, some of the bridges have very similar characteristics, such as type, material, and construction year. In this case, it is reasonable to find the correlations between these bridges and so provide a dynamic assessment of seismic risk.

To address **Objective 3**, I propose to model the logical connection between the bridges in the stock with Bayesian Networks (BN), (Jensen and Nielsen 2007). A limit of classical BN algorithms is that they are normally thought to handle discrete variables, while the quantities involved in post-earthquake assessment are continuous. To overcome this limitation, all the continuous variables are assumed to have conditional Gaussian distribution; in this case it is demonstrated that there is exact inference in hybrid BNs, which include both discrete and continuous variables (Lauritzen and Jensen, 2001). The BN incorporates the seismic demand model, the capacity model and the fragility function. The uncertainty terms are considered both in the capacity model and the demand model. First, the BN is applied to the

individual bridges and the prior probabilities of the bridge being in any one of the limit states are calculated during the initialization procedures. After an earthquake, the data on the bridge is entered into the network using the Monte-Carlo method and the probabilities of other variables are updated. Next, this framework is easily extended from individual bridges to the whole network; all the bridges in the network are correlated through the demand model and the capacity model. When an earthquake happens, the data on one or more of the bridges can be propagated throughout the network, so as to provide an updated assessment on the performance of the other bridges and the whole network. Finally, the best path search between any two given network nodes is reformulated, now accounting for bridge correlations in demand and capacity.

1.5 Outline of Thesis

The rest of the Thesis is organized in the following Chapters, in detail:

- In Chapter 2, the fragility curve method for risk assessment is introduced. The Hazus model is chosen as the most appropriate and is applied to the bridges of the APT stock. Once the fragility curves for all the bridges have been generated, risk analysis is performed for three earthquake scenarios (with return periods of 72, 475 and 2475 years) and four damage states (OLS, DLS, LLS, and CLS).
- In Chapter 3, I extend the results of the component analysis to the network level; the APT road network is modeled in the form of a graph and the problem of connectivity between two locations is analyzed. A shortest path algorithm is introduced and implemented, to identify the best path between any two given places. Correlation in capacity and demand among bridges is not accounted for at this stage.
- Chapter 4 describes basic Bayesian Networks theory. After reiterating the fundamentals of probability theory, the definition of the Bayesian Network is given. The general operations on Bayesian Networks are introduced and the computation scheme with conditional Gaussian distributions is explained in detail.
- Chapter 5 presents a seismic risk assessment framework both for individual bridge and twin bridges based on the BN methodology. In this system, two bridges are correlated through the demand and capacity models. It is shown how evidence of the state of one bridge can affect the prediction performance of another bridge. Two case studies are used to illustrate the procedures.

- In Chapter 6, the concept introduced in Chapter 5 for two bridges is extended to all the bridges in the network of the post-earthquake assessment system. Now, all the bridges are correlated through the demand model and capacity model. Given the data on one or more variables, the performance of the whole network can be updated. The best path given any two nodes within the network is identified again. Correlations between different bridges are now considered and the results are compared with those in Chapter 3.
- Finally, in Chapter 7, the outcomes and limits of this Thesis are summarized and necessary future work is discussed.

2 Fragility curves

2.1 Introduction

Fragility curves are conditional probability statements which give the likelihood of a bridge reaching, or exceeding, a particular damage level, for an earthquake of a given intensity level (Shinozuka et al. 2000a, Nielson 2005). The conditional probability is given by the following equation:

$$\text{Fragility}\,(x) = P(LS \mid IM = x) \tag{2.1}$$

where LS is the limit state of the bridge, IM is the ground motion intensity measure of the bridge, and x is the realization of the intensity measure. This equation shows that when the earthquake intensity is x, the probability of the bridge exceeding the limit state LS is Fragility(x). Fig. 2.1 is the graphical representation of Equation (2.1).

As an effective tool in seismic risk analysis, fragility curves have become more and more popular. Fragility curves are not only useful in seismic risk assessment, but also in bridge retrofit prioritization and post earthquake response. When updating a bridge network, fragility curves can be used to highlight the most vulnerable bridges so as to maximize the functionality of the whole bridge network system. In a real time post earthquake situation, fragility curves can assist decision makers to make rapid decisions on bridge closures.

Based on information found in the literature, Shinozuka et al. (2000b) classifies four methods for developing fragility curves: professional judgment; quasi-static and design code consistent analysis; utilization of damage data associated with past earthquakes, and numerical simulation of the seismic response of structures based on dynamic analysis. According to the generation methodology, Nielson (2005) defines three kinds of fragility curve: expert based, empirical and analytical.

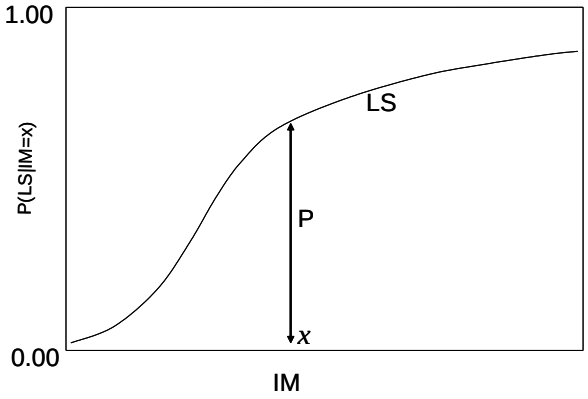

Fig. 2.1 Graphical representation of fragility function (Nielson 2005)

2.1.1 Expert Based Fragility Functions

One example of Expert-based Fragility Functions is ATC-13 (ATC, 1985), developed by the Applied Technology Council (ATC) and reported by Nielsen (2005). The ATC put together 42 experts to give information on the various components of infrastructures. The experts were asked to give the probability of a bridge being in one of seven damage states for a given intensity value. These results were compiled as the damage probability matrices (DPM) for bridges in the ATC-13 report (ATC, 1985). Nielsen (2005) raised several major concerns with this methodology: first, the procedure is subjective in that it is based solely on the experience of the experts; next, the DPM were created for only two classes of bridges, major and conventional. He concluded that this method presents a very high level of uncertainty. See Nielsen (2005) for more details.

2.1.2 Empirical fragility curves

Empirical fragility curves are generated from actual earthquake data. This methodology has been presented and demonstrated by several groups, for example Prof. Kiremidjian's group (Basöz and Der Kiremidjian, 1995) and Prof. Der Kiureghian's group (Gardoni et al. 2002). Although there are some slight variations in the methods used by the researchers, they are conceptually the same. During the procedure, first a post earthquake damage state assessment is performed for all the bridges that belong to the considered bridge class, and then ground motion intensity, in terms of a measure such as peak ground acceleration (PGA), is assigned to each bridge. Then a damage state and a given ground intensity motion are given for each bridge in a damage matrix. The percentage of the overall bridge class inventory will be displayed for each damage state and at each ground motion intensity level. There are several of ways to generate fragility curves. See the maximum likelihood method proposed by Shinozuka et al. (2000b) in section 2.5.1.

Although the generation methods for empirical fragility curves are relatively straightforward, they have some drawbacks and limitations as pointed out by Basöz and Kiremidjian (1995). First, it is difficult to get enough information on bridges belonging to a specific bridge class that lie in a particular damage level. Second, it is very difficult to get the ground motion intensities for the target bridges. Finally, the empirical fragility curves are too subjective. There is often a discrepancy between the damage levels assigned by two different inspectors. Further details of this discussion are found in Basöz and Kiremidjian (1995).

2.1.3 Analytical fragility curves

Because of the limitations of empirical fragility curves, more research is devoted to the implementation of analytical fragility curves. When actual bridge damage and ground motion data are not available, analytical fragility curves must be used to assess the performance of bridges under earthquakes. There are many researchers who have developed analytical fragility curves for bridges using a variety of different methodologies.

According to the definition of the fragility curves (Shinozuka et al. 2000a, Nielson 2005), it is obvious that fragility curves are related to both structural demand (D) and structural capacity (C). The fragility can be described as:

$$P_f = P[D \geq C] = P[\ln D - \ln C \geq 0] \tag{2.2}$$

In addition, when the structural demand and capacity fit a lognormal distribution - if we assume that: $C \sim \ln N(\mu_C, \sigma_C^2)$; $D \sim \ln N(\mu_D, \sigma_D^2)$, then the reliability index β is:

$$\beta = -\frac{\mu_P}{\sigma_P} \tag{2.3}$$

where $\mu_P = \mu_D - \mu_C$, $\sigma_P^2 = \sigma_C^2 + \sigma_D^2$.

Based on the above, it can be seen that the structural demand and capacity must be modeled to generate analytical fragility curves. Researchers use a number of methods to accomplish this task. In order to facilitate reading, and to separate out other researchers' methods from the method that will be used in this Thesis, the methods of other researchers will be introduced at the end of this chapter, see section 2.5. Although the general procedures used by different researchers are conceptually the same, there are some differences in how the tools are actually employed to accomplish each step.

2.2 HAZUS model

HAZUS (FEMA 2003) is a geographic information system (GIS) based, standardized, nationally applicable multi-hazard loss estimate methodology and software that was developed for the National Institute of Building Science (NIBS) under a cooperative agreement with the Federal Emergency Management Agency (FEMA). Hazus is intended to develop guidelines and procedures for making earthquake loss estimates. It can be used by local, state and regional officials to help them to reduce risks from earthquakes, and to prepare for emergency response and recovery. This package was developed by a team of earthquake loss experts including earth scientists, engineers, architects, economists, emergency planners, social scientists and software developers. It provides damage and loss estimate for thirteen major components or subcomponents, for example general building stock, transportation systems, airport transportation systems, and so on.

The HAZUS model (FEMA, 2003) is a rapid approach seeking to establish dependable fragility curves (Mander, 1999). In contrast to other methods that have been used in the past, such as empirical fragility curves or analytical fragility curves that require much previous damage data or extensive computation, only limited information is needed for this model.

Because of the characteristics of the APT bridge stock, illustrated in Section 1.2, with a large number and variety of bridge types, a systematic and quick method is required to develop fragility curves. Given the level of information stored in the APT-BMS database, HAZUS seems the most suitable model for this application. Its implementation in the APT-BMS is explained in here.

2.2.1 Formulation of fragility curves

The probability of being in or exceeding a damage state in HAZUS is modeled as:

$$[P_f(S_a)]_i = \Phi[\frac{1}{\mathrm{A}}\ln(\frac{S_a}{(a_g)_i})] \quad i=1,2,3, \tag{2.4}$$

where Φ is the standard normal cumulative distribution function; S_a is the spectral acceleration amplitude (for a period of T=1 sec); $(a_g)_i$ is the median spectral acceleration that causes the i^{th} damage level; and A is the normalized composite log-normal standard deviation. There are five possible damage states defined in APT-BMS: no-damage, OLS, DLS, LLS, and CLS; these five states are associated with the five damage state defined in Hazus according to Table 2.1. The normalized standard deviation A takes account of uncertainty and randomness for both capacity

and demand. As justified by Basöz and Mander (1999), the uncertainty factor for seismic demand can be assumed to be 0.5 (Pekcan, 1998), the uncertainty factor for capacity is assumed to be 0.25 (Dutta, 1999), and an analysis uncertainty factor is assumed to be 0.2. Therefore the recommended value of A =$(0.5^2+0.25^2+0.2^2)^{0.5}$ = 0.6. Therefore, in Equation (2.4), the only unknown parameter is $(a_g)_i$, which can be calculated using a capacity-spectrum approach.

Table 2.1 Definition of damage states (FEMA, 2003)

	Damage state	Failure Mechanisms
1	No damage	First yield
2	Operational limit state (OLS)	Cracking, spalling
3	Damage control limit state (DLS)	Bond, abutment back wall collapse
4	Life safety limit state (LLS)	Pier concrete failure
5	Collapse limit state (CLS)	Deck unseating, pier collapse

2.2.2 Capacity-spectrum approach

According to the Italian code (D.M.14 Jan 2008), which is largely based on Eurocode 8 (Eurocode 8, 2004), the seismic demand is given by:

$$(C_d)_S = a_g \cdot S \cdot \eta \cdot F_0 \tag{2.5a}$$

$$(C_d)_L = a_g \cdot S \cdot \eta \cdot F_0 \cdot \left[\frac{T_C}{T}\right] \tag{2.5b}$$

where $(C_d)_S$, $(C_d)_L$ are the seismic demands of short and long periods; a_g is the design ground acceleration (normalized with respect to gravitational acceleration, g); S is the coefficient dependent on the soil type; η is the damping correction factor with a reference value of η=1 for 5% viscous damping; F_0 is the spectral amplification factor; T_C is the upper limit of the period of the constant spectral acceleration branch; and T is the effective period of the structure given by:

$$T = 2\pi \cdot \sqrt{\frac{W}{g \cdot k}} = 2\pi \cdot \sqrt{\frac{W \cdot \Delta}{g \cdot F_y}} = 2\pi \cdot \sqrt{\frac{\Delta}{C_c \cdot g}} \tag{2.6}$$

where W is the weight of the bridge; F_y is the lateral force on the pier; $C_c = F_y / W$ is the base shear capacity; and Δ is maximum displacement response. For example, for a collapse mechanism involving bridge pier bending collapse, the ultimate displacement can be calculated using:

$$\Delta = \theta \cdot H \tag{2.7}$$

where θ is the column drift, and H is the column height (Basöz and Mander 1999). Basöz and Mander (1999) also propose values of θ and Δ as in Table 2.2.

Under the capacity-spectrum approach, the capacity is assumed to be equal to the demand:

$$C_d = C_c \tag{2.8}$$

Table 2.2 Drift and displacement limits (Basöz and Mander, 1999)

Damage State	Drift limits (θ) for Weak Pier & Strong Bearings		Displacement Limits (Δ) for Weak Bearings & Strong Pier (m)
	Non-seismic	Seismic	
2	0.005	0.010	0.05
3	0.010	0.025	0.100
4	0.02	0.05	0.175
5	0.05	0.075	0.300

Substituting Equation (2.6) and Equation (2.8) into Equation (2.5), the required spectral accelerations can be obtained as the greater of $(a_g)_S$ and $(a_g)_L$:

$$(a_g)_S = \frac{C_C}{S \cdot \eta \cdot F_0} \tag{2.9a}$$

$$(a_g)_L = \frac{2\pi}{S \cdot \eta \cdot F_0} \cdot \sqrt{\frac{C_C \cdot \Delta}{g}} \cdot \frac{K_{3D}}{T_C} \tag{2.9b}$$

In Equations (2.9), the only parameter to be calculated is the normalized capacity C_C which will be obtained in the following section.

2.2.3 Analysis of bridge capacity

Based on Dutta and Mander (1998), the capacity of a bridge can be divided into two parts: base shear capacity under lateral loading and arching action under transverse shaking. For a bridge with strong bearings and weak piers, the capacity is assumed to be from piers only. For a bridge with weak bearings and strong piers, or a single span bridge, the capacity is dependent on the bearings.

Dutta and Mander (1998) have shown that the pier capacity can be defined as:

$$C_{cp} = \lambda_Q \cdot k_P \cdot \frac{D}{H} \tag{2.10}$$

where $K_p = \zeta \cdot j \cdot (1+0.64 \cdot \rho_t \cdot f_y / f_c \cdot \psi)$; $\psi = W_D / f_c \cdot A_g$ = the average dead load axial stress ratio in the column; D = column diameter; H = column height; ρ_t = volumetric ratio of longitudinal reinforcement (assumed to be 0.01 for non-seismic design and 0.02 for seismic design); ζ = fixity factor, taken as 1 for multi-column bends, and 0.5 for single column cantilever action; j = internal lever arm coefficient normally assumed to be 0.8; f_y = yield stress of the longitudinal reinforcement; f_c = strength of the concrete; W_D = the deck weight; A_g = the cross section area of the column; and λ_Q is a strength reduction factor that occurs due to cyclic loading. For different damage states, the values are given as Table 2.3.

Table 2.3 Values for strength reduction factor Q (Dutta, 1999)

Damage State	Non-seismically designed	Seismically Designed
1	1	1
2	1	1
3	0.6	0.9
4	ζ / K_p	0.8
5	$\zeta \cdot j / K_p$	0.7

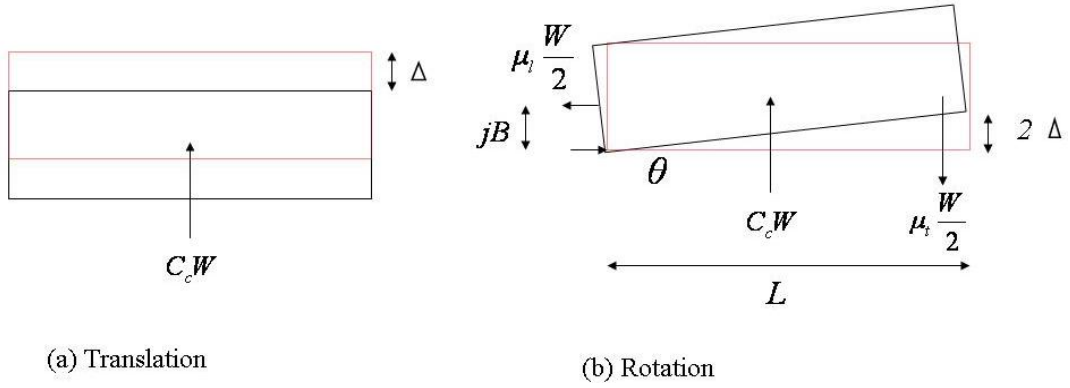

Fig. 2.2 Two failure modes for single span bridges (Basöz, and Mander. 1999)

For single span bridges or bridges seated on strong piers with weak bearings, the capacity is assumed to arise from bearings only. There are two mechanical modes to compute the capacity of bearings: translation and rotation (Fig. 2.2). The mechanism with lower capacity governs. The following calculates the capacity using principles of virtual work plastic analysis, where the external work done (EWD) by the seismic loads is equal to the internal work (IWD) done by the resisting mechanism.

For the translation mode: the external work is $EWD = C_c W\Delta$, and the internal work is $IWD = \mu_t W\Delta$; according to principles of virtual work plastic analysis, we have $C_c = \mu_t$. μ_t is the coefficient of sliding friction of the bearings in the transverse direction.

For the rotation mode, the external work is $EWD = C_c W\Delta$, and the internal work is $IWD = \mu_t W\Delta + \mu_l W j B\theta/2$, so $C_c = \mu_t + \mu_l jB\theta/2\Delta$. Since $\mu_t < \mu_t + \mu_l jB\theta/2\Delta$, $C_c = \mu_t$. The μ_t values for different bearings in every damage state are shown in Table 2.4.

Table 2.4 Friction coefficients of the bearings in the transverse direction (Basöz and Mander 1999)

Damage State	Rubber, fixed, or mobile mechanical bearings	Other bearings
2	0.85	0.8
3	0.75	0.7
4	0.75	0.7
5	0.75	0.7

2.2.4 Accounting for 3D effects

K_{3D} is the factor that considers the 3D arching action when the displacement is sufficiently large (Basöz and Mander 1999). In Equation (2.9a), the 3D effects are omitted because the seismic displacement has not yet developed. Coefficient K_{3D} depends on the failure mechanism, as explained in the following.

Case 1: For bridges seated on strong bearings with weak piers, based on the work of Dutta and Mander (1998), the definition is:

$$K_{3D} = 1 + \frac{k_{3D}}{n-1} \tag{2.11}$$

where n represents the number of spans in the bridge, and k_{3D} is a factor related to span continuity and bearing type as given in table 2.5.

Table 2.5 3D effect factor for bridges seated on strong bearings with weak piers (Dutta and Mander 1998)

Bridge Type	Bearing type	k_{3D}
Simply supported	Neoprene Pads	0.25
	High steel rocker bearings	0.09
	Low steel rocker bearings	0.20
Continuous Bridges	all bearing types	0.33

Case 2: For bridges seated on weak bearings with strong piers, based on Dutta and Mander (1998), K_{3D} is defined as:

$$K_{3D} = 1 + \frac{f_{3D}}{n} \tag{2.12}$$

where f_{3D} is given as follows:
f_{3D} = 0.05 for high steel rocker bearings with a span length larger than 20m;
f_{3D} = 0.10 for low steel sliding bearings with a span length not larger than 20m;
f_{3D} = 0.21 for neoprene pads.

Case 3: for bridges with monolithic abutments, the abutment strength is assumed to be the same as the pier strength, and the pier capacity is defined in terms of pier strength and weight. For the bridge with *n* spans, the capacity is defined as:

$$C_c = C_{cp} \cdot (1 + \frac{1}{n}) \tag{2.13}$$

Therefore the 3D factor is given by:

$$K_{3D} = \sqrt{\frac{C_{cp} \cdot (1 + 1/n)}{C_{cp}}} \approx 1 + 0.5/n \tag{2.14}$$

Case 4: for bridges with single span, the 3D factors are listed in Table 2.6.

Table 2.6 3D effect factor for single span bridge (Basöz and Mander 1999)

Deck Type	Bearing Type	K_{3D}
Concrete Deck	Neoprene Pads	1.2
Steel Girder L > 20m	High steel rocker bearings	1.05
Steel Girder L <= 20m	Low steel rocker bearings	1.1

2.3 Application of Hazus model to APT-BMS

2.3.1 Example of a bridge with weak bearings and strong piers

The SP83 Bridge on the Nogarè river (Fig. 2.3) is a typical bridge in APT-BMS. It is a 3 span pre-stressed reinforced concrete bridge with wall piers and non monolithic abutments. The column parameters are *D*=5m, *H*=13.4m. Its geographical location is Long=11.2132(*E*), Lat= 46.1025(*N*), and the elastic spectra parameters are: *S*=1, F_0 =2.6835, T_C =0.33393.

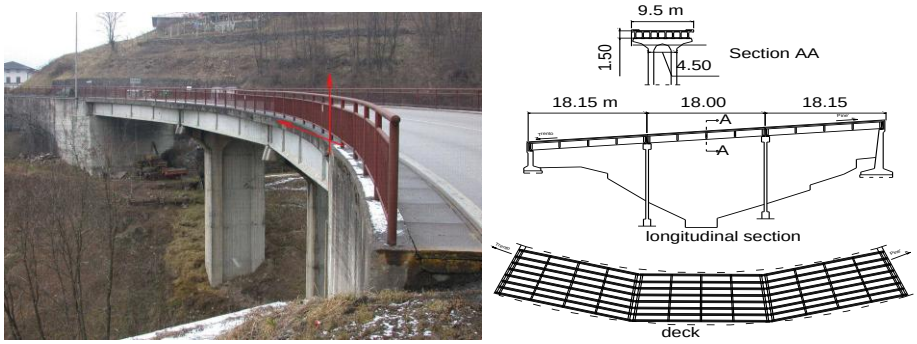

Fig. 2.3 (a) Overview of the SP83 Bridge on the Nogarè River; (b) Plan view, elevation and cross-section of the deck

Since the bridge has wall piers, the capacity is assumed to arise from bearings only, so $Cc = \mu_t$=[0.85, 0.75, 0.75, 0.75]. Substituting *Cc* into Equations (2.9), the required median spectral acceleration $(a_g)_i$ is obtained. Table 2.7 gives the results. Given $(a_g)_i$, from Equation (2.4), the fragility curves of Ponte Nogarè SP83 under different damage states are calculated as shown in Fig. 2.4. Assuming a spectral acceleration S_a =0.071g, which is the earthquake intensity with a return period of 475 years, the seismic probabilities of the SP83 Nogarè Bridge in every damage state are calculated as shown in Table 2.8. In table 2.8, the second column gives the probability of exceeding each limit state, and the third column gives the probabilities of exceeding or being in each limit state.

Table 2.7 The required parameters for calculating median spectral accelerations

Damage State	μ_t	η	Δ(m)	$(a_g)_S$ (g)	$(a_g)_L$ (g)	a_g (g)
2	0.85	0.6325	0.05	0.5008	0.8829	0.8829
3	0.75	0.6325	0.1	0.4419	1.1728	1.1728
4	0.75	0.6325	0.175	0.4419	1.5515	1.5515
5	0.75	0.6325	0.3	0.4419	2.0314	2.0314

Table 2.8 Seismic probability of Ponte Nogar è SP83 for different limit states

Damage State	$P[D>DS_i\|Sa]$	$P[D=DS_i\|Sa]$
2	1.2885×10^{-5}	1
3	1.4262×10^{-6}	1.1459×10^{-5}
4	1.3195×10^{-7}	1.2942×10^{-6}
5	1.0922×10^{-8}	1.2103×10^{-7}

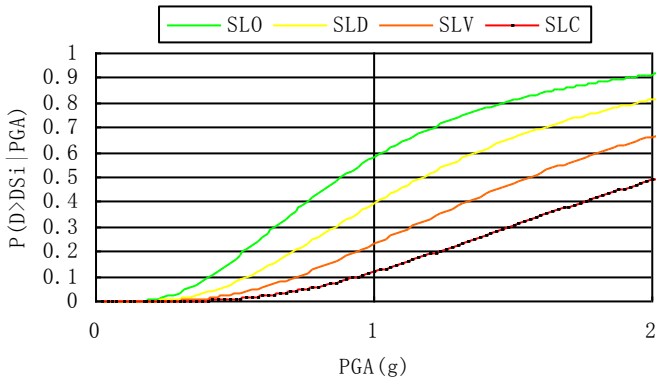

Fig. 2.4 Fragility curves of Ponte Nogar è SP83

2.3.2. Example of a bridge with strong bearings and weak piers

The SP90 Bridge on the Adige River at Villa Lagarina is a simply supported, pre-stressed concrete girder bridge with four spans. It was built in 1966. The column parameters are D=1.5m, H=10.45m. The elastic spectra parameters are given in Table 2.9.

Fig. 2.5 Overview of the SP90 Bridge on the Adige River at Villa Lagarina

Table 2.9 Spectral parameters at the SP90 Adige Bridge location

Long	Lat	S_a (Return period of 475 years)	Fo	Tc	S
11.038	45.913	0.116 g	2.484	0.286	1.00

The capacity of the bridge is calculated as the smaller of the two resisting mechanisms, pier collapse or sliding of bearings. If the pier capacity is critical, the capacity coefficient is given by:

$$C_c = \lambda_Q \cdot k_p \cdot \frac{D}{H} \tag{2.15}$$

Conversely, if sliding of bearings is critical, the capacity coefficient is simply:

$$C_c = \mu_t \tag{2.16}$$

For computation simplicity, the smaller of the two is used here as the capacity value of this bridge. The parameters of the pier are given in Table 2.10.

Since this is a simple supported bridge, the 3D effects coefficient is given by:

$$K_{3D} = 1 + \frac{k_{3D}}{n-1} = 1.08$$

Table 2.10 parameters of the SP90 Bridge on the Adige River

Damage states	η	λ_Q	θ	a_g	F(PGA)
OLS	0.745	1.0	0.005	0.513	6.66×10^{-3}
DLS	0.674	0.8	0.010	0.718	1.21×10^{-3}
LLS	0.649	0.7	0.020	0.986	1.83×10^{-4}
CLS	0.367	0.6	0.050	1.472	1.16×10^{-5}

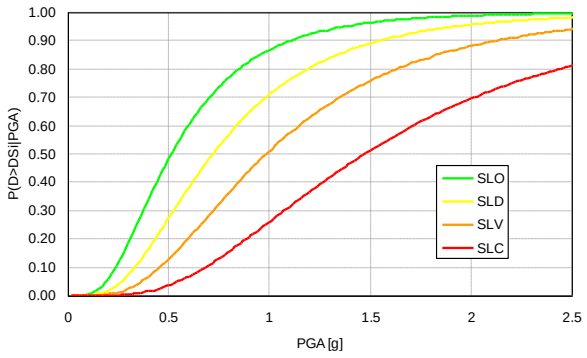

Fig. 2.6 The fragility curves of the pier

Finally, the fragility curves for the four limit states are given in Fig. 2.6. Similarly, Table 2.11 gives the parameters related with the sliding mechanism, while the corresponding fragility curves are depicted in Fig. 2.7. By comparing the parameters of the two mechanisms, it is evident how in this case the pier mechanism is the more critical, and the corresponding fragility curves are used to represent the bridge vulnerability.

Table 2.11 parameters of the pier

Damage states	η	μ_t	Δ(m)	A_i(g)	F(PGA)
OLS	0.632	0.85	0.050	1.1124	8.38×10^{-5}
DLS	0.632	0.75	0.100	1.4777	1.13×10^{-5}
LLS	0.632	0.75	0.175	1.9548	1.28×10^{-6}
CLS	0.632	0.75	0.300	2.5595	1.29×10^{-7}

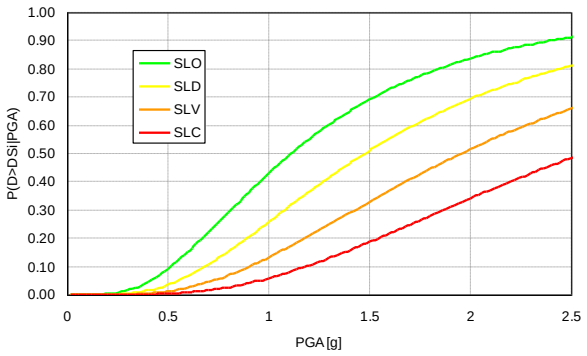

Fig. 2.7 The fragility curves due to the sliding of bearings

2.4 Results and conclusions

Using the above methods, the fragility curves for all the bridges in the APT stock are generated. Thus, given an earthquake scenario, seismic vulnerability for all damage states can be calculated, for the same three return periods and four limit states.

The results with return periods of 475 years, 72 years, and 2475 years are shown in Google Earth maps in Figs 2.8, 2.9, and 2.10 respectively. Bridges are denoted by dots of different colors, according to their probability P of exceeding the limit state: green ($P<10^{-5}$), yellow ($10^{-5}<P<10^{-4}$), orange ($10^{-4}<P<10^{-3}$) and red ($P>10^{-3}$). This is a very straightforward way to show bridge managers and users the seismic risk of every bridge. The histogram of Fig. 2.11 gives the number of bridges in each probability class for a return period of 475 years.

The results show that the seismic risk for a return period of 475 years in the APT stock is moderate. For limit states OLS and DLS, some bridges have relatively high failure probabilities as shown in Fig. 2.8 (a) and Fig. 2.8 (b). As for limit states LLS and CLS, 99% of the bridges in the APT stock have a very low probability as shown in Fig. 2.8 (c) and Fig. 2.8 (d). This can be explained by the seismic activity of the APT region. Fig 2.12 gives the PGA values of the APT region in the 475 year return period. From Fig. 2.11, we can see that for the 475 year return period, PGA values in most areas of APT region are about 0.075g, which is a very low value. Only in the south east part of APT region, there is a higher PGA value. This region is classified as a low seismic zone.

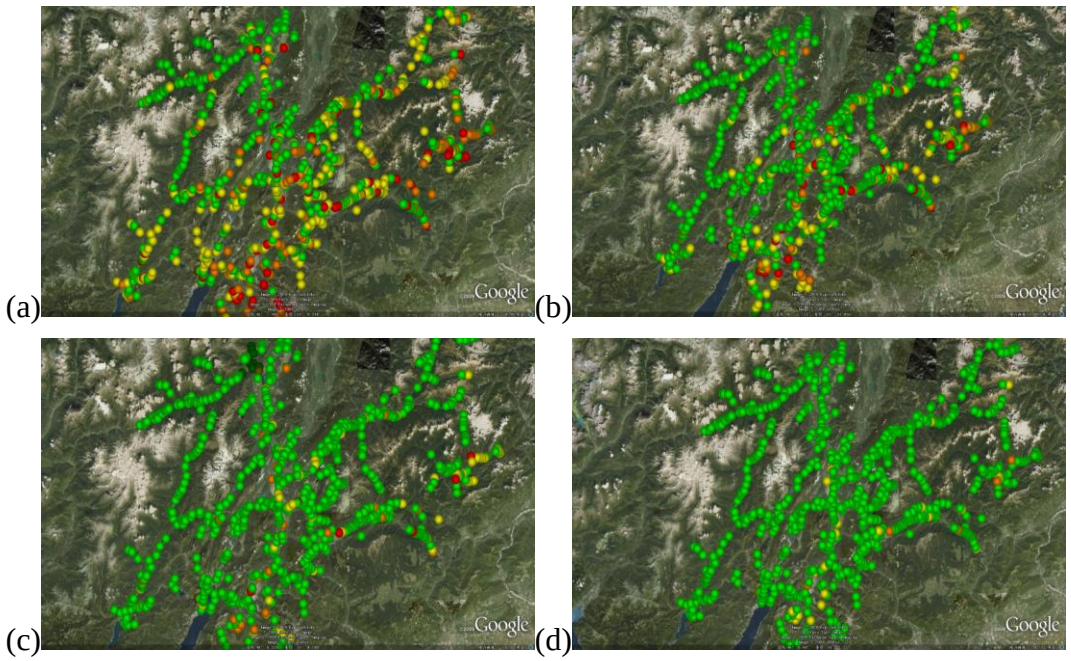

Fig. 2.8 Seismic vulnerability of APT stock for the return period of 475 years in damage states (a), OLS (b), DLS (c), LLS (d), CLS

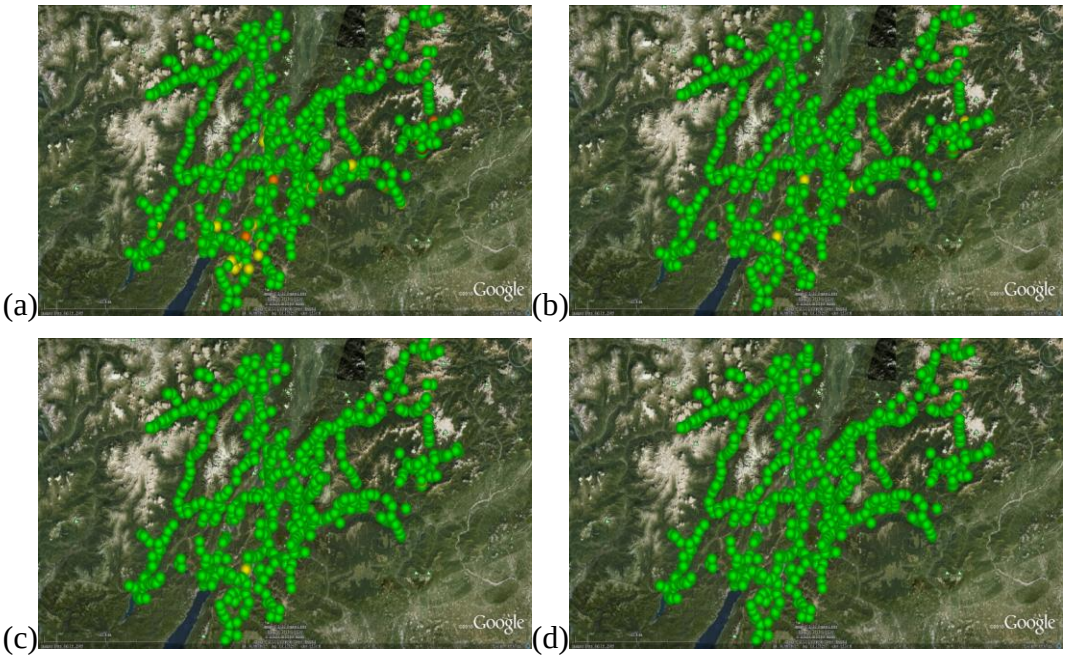

Fig. 2.9 Seismic vulnerability of APT stock for the return period of 72 years in damage states (a), OLS (b), DLS (c), LLS (d), CLS

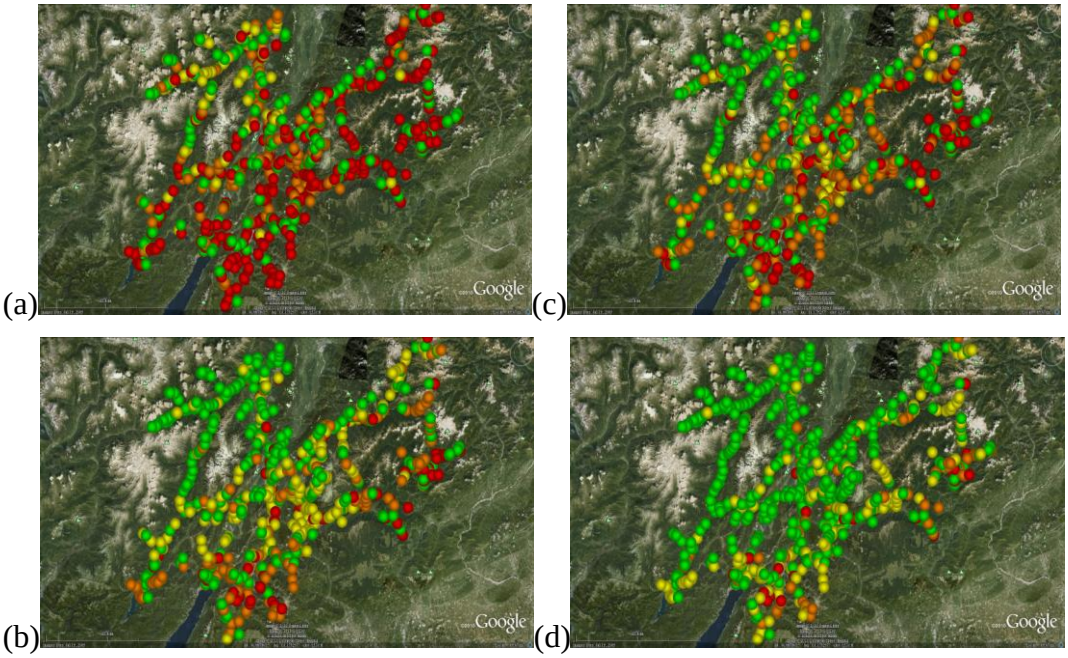

Fig. 2.10 Seismic vulnerability of APT stock for the return period of 2475 years in damage states (a), OLS (b), DLS (c), LLS (d), CLS

Although the direct seismic risk involving collapse or loss of life is moderate, system operation at network level is of concern in a post earthquake situation. From fig 2.11, we find that there are about 150 red bridges for operation limit state, so approximately 15% of the bridges in the APT stock have a relatively high risk of

suffering operational problems. It is therefore necessary to identify the safest path between any two given points after an earthquake. Here 'the safest' means the lowest risk of exposure to operational problems in a given earthquake scenario. After an earthquake, the ability to decide quickly is of great help to decision makers who need to best distribute the available human and material rescue resources to the disaster center. This problem is addressed in the next section.

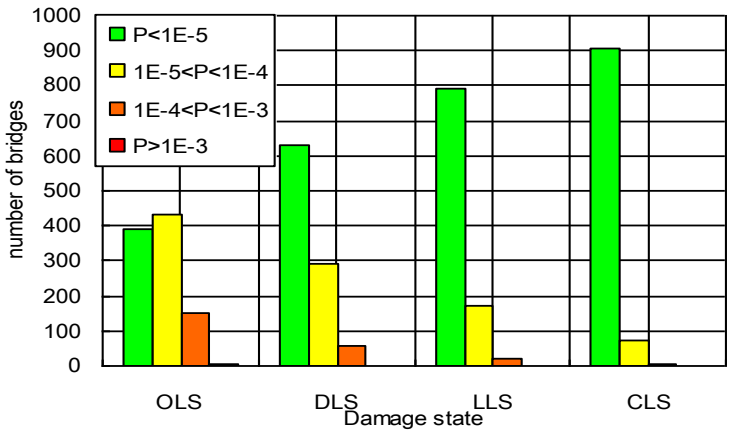

Fig. 2.11 Seismic vulnerability distribution of the APT stock

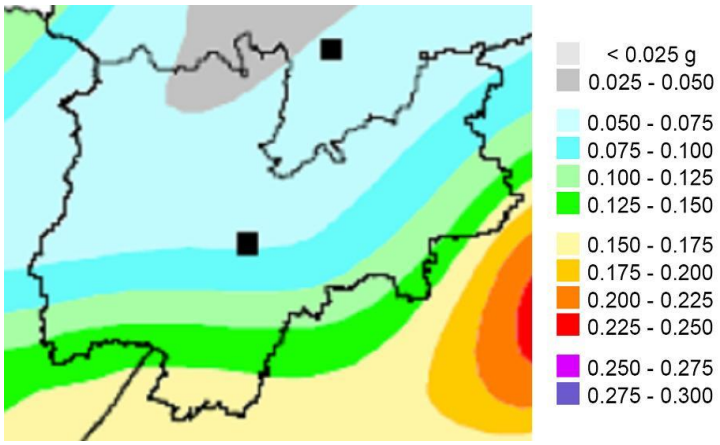

Fig. 2.12 PGA value of APT region with 475 years' return period (DPC-INGV)

2.5 Other methods for generating fragility curves

A review of the literature identified a state-of-the-art method to calculate fragility curves, and I report this here.

2.5.1 The maximum likelihood method (Shinozuka et al. 2000b)

In Shinozuka et al. (2000b), the empirical fragility curves are developed based on the bridge damage data, obtained from the 1995 Hyogo-ken Nanbu (Kobe) earthquake, and on the two-parameter lognormal distribution functions which were used for fragility curve construction. The estimate of the two parameters (median and log-standard deviation) is performed using maximum likelihood method. The peak ground acceleration (PGA) is used to represent the seismic ground motion intensity. The likelihood function is expressed as follows:

$$L = \prod_{i=1}^{N} \left[F(a_i)\right]^{x_i} \left[1 - F(a_i)\right]^{1-x_i} \tag{2.17}$$

where $F(\cdot)$ represents the fragility curve for a specific state of damage; a_i = PGA value to which bridge i is subjected; x_i = 1 or 0 depending on whether or not the bridge sustains the state of damage; and N = total number of bridges inspected after the earthquake. $F(a_i)$ takes the following analytical form:

$$F(a) = \Phi\left[\frac{\ln(\frac{a}{c})}{\zeta}\right] \tag{2.18}$$

where a represents PGA, and $\Phi[\cdot]$ = the standard normal cumulative function. The two parameters c and ζ in (2) are computed satisfying the following equations to maximize L:

$$\frac{d\ln L}{dc} = \frac{d\ln L}{d\zeta} = 0 \tag{2.19}$$

This equation is solved by using the optimization algorithm. Using the maximum likelihood method, three fragility curves are constructed as shown in Fig. 2.13.

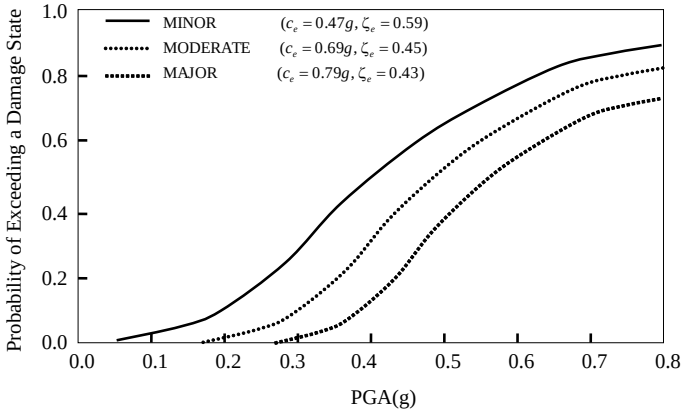

Fig. 2.13 Example of empirical fragility curves reported by Shinozuka et al. (2000b)

2.5.2 Fragility curves for highway bridges (Karim and Yamazaki 2003)

This method develops analytical fragility curves for highway bridges considering the variation of structural parameters based on numerical simulation. Based on the observed correlation between the fragility curve parameters and the over-strength ratio of the structures, this method constructs the fragility curves using 30 non-isolated highway bridges in Japan, which fall within the same group and have similar characteristics.

It is assumed that there might be a correlation between the fragility curve parameters and the structural parameters, like the over-strength ratio θ of the structure, height of the pier (h), span length (L), and weight (W) of the superstructure. However, for simplicity, only θ is considered in the current analysis as it is one of the key structural parameters and provides information on the reserve strength of the structure when designed. The over-strength ratio θ of the structure is defined as:

$$\theta = \frac{P_{\mu}}{k_{he} W} \tag{2.20}$$

where P_u is the horizontal capacity of the structure, W is the equivalent weight, which is calculated as the weight of the superstructure and a 50% weight of the substructure, and k_{he} is the equivalent lateral force coefficient.

$$k_{he} = \frac{k_{hc}}{\sqrt{2\mu_a - 1}} \tag{2.21}$$

where $k_{hc}$is the design lateral force coefficient, and μ_a is the allowable ductility

factor of the substructure. The design lateral force coefficient k_{hc} is defined as

$$k_{hc} = c_z k_{hco} \tag{2.22}$$

where c_z is the zonation factor, and k_{hco} is the standard design lateral force coefficient. The value of k_{hco} can be obtained by knowing the natural period of the structure and ground conditions.

The regression model used to obtain the relationship between fragility curves λ and ζ with the over-strength ratio τ is given as:

$$\lambda_\theta = b_0 + b_1 \tau \tag{2.23}$$

$$\xi_\theta = c_0 + c_1 \tau \tag{2.24}$$

where λ_θ and ζ_θ are the mean and standard deviation of the fragility curves with respect to τ, τ is the over-strength ratio of the structure, and b_0 and b_1 are the regression coefficients.

2.5.3 Fragility curves for bridge piers based on numerical simulation (Karim and Yamazaki 2001)

This method presents a numerical analysis to construct fragility curves for bridge piers of a specific bridge based on static sectional and pushover analysis, and non-linear dynamic analysis. The analyses of fragility curves for special piers designed under the 1964 and 1998 Japanese highway bridge codes were constructed with respect to both PGA and PGV. The input motions were selected from the strong records of the 1995 Kobe, 1994 Northridge, 1993 Kushiro and the 1987 Chiba-ken earthquakes.

The steps for constructing analytical fragility curves are as follows.

a. Select the earthquake ground motion records.
b. Normalize PGA of the selected records to different excitation levels.
c. Make an analytical model of the structure.
d. Obtain the stiffness of the structure.
e. Select a hysteretic model for the non-linear dynamic response analysis.
f. Perform the non-linear dynamic analysis using the selected records.
g. Obtain the ductility factors of the structure.
h. Obtain the damage indices of the structure at each excitation level.
i. Calibrate the damage indices for each damage rank.

j. Obtain the number of occurrences of each damage rank in each excitation level and get the damage ratio.
k. Construct the fragility curves using the obtained damage ratio and the ground motion indices for each damage rank.

For the assessment of the bridge piers, the damage index *DI* is expressed as

$$DI = \frac{\mu_d + \beta \mu_h}{\mu_u} \tag{2.25}$$

where μ_d and μ_u are the displacement and ultimate ductility of the bridge piers, β is the cyclic loading factor taken as 0.15 and μ_h is the cumulative energy ductility. The ultimate ductility μ_u is defined as the ratio of maximum displacement (obtained from the static analysis) to the yield displacement (obtained from the static analysis). The displacement ductility is defined as the ratio of the maximum displacement (obtained from dynamic analysis) to the displacement at the yield point (obtained from static analysis). The cumulative energy ductility μ_h is defined as the ratio of the hysteretic energy (obtained from dynamic analysis) to the energy at yield point (obtained from static analysis).

The damage indices obtained for the selected input ground motion are calibrated to get the relationship between the DI and damage rank (DR).

Using the relationship between DI and DR, the number of occurrences of each damage rank is obtained. These numbers are then used to obtain the damage ratio of each damage rank.

To count the number of occurrences of each damage rank, the PGA for selected records were normalized to different excitation levels. Then, the ground motions records were applied to the structure to obtain the damage indices. Using these damage indices, the number of occurrences of each damage rank is obtained for each excitation level. Finally, using the numbers, the damage ratio is obtained for each damage rank.

1. Fragility curves. Fragility curves are constructed with respect to both PGA and PGV. The damage ratio for each damage rank in each excitation level is obtained by calibrating the DI. Based on this data, fragility curves for the bridge piers are constructed assuming a lognormal distribution. The cumulative probability P_R of the occurrence of the damage to be equal or higher than rank *R*, is given as

$$P_R = \Phi\left[\frac{\ln X - \lambda}{\zeta}\right] \tag{2.26}$$

where Φ is the standard normal distribution, *X* is the ground motion index (PGA and

PGV), and λ and ζ are the mean and standard deviation of ln$X$. Two parameters of the distribution are obtained by the least square method on lognormal probability paper. Using these probability papers, the two parameters of the distribution are obtained to construct the fragility curves of the bridge piers.

2.5.4 Seismic fragility methodology for bridges using component level approach (Nielson and DesRoches 2007)

This methodology considers the contribution of the major components of the bridge, such as the columns, bearings and abutments, to its overall bridge system fragility. In particular, probability tools are used to estimate directly the bridge system fragility from the individual component fragilities.

A probability distribution is developed for the demand, conditioned on the IM, also known as a probabilistic seismic demand model (PSDM), and convolving it with a distribution for the capacity. The estimate for the median demand (S_d) can be represented by a power model:

$$S_d = aIM^b \tag{2.27}$$

where IM is the seismic intensity measure of choice, and both a and b are regression coefficients. Thus, the PSDM can be written as

$$P\left[D \geq d \,|\, IM\right] = 1 - \Phi\left(\frac{\ln(d) - \ln(aIM^b)}{\beta_{DIM}}\right) \tag{2.28}$$

The generation of the PSDMs follows the procedure outlined below.

1. Assemble a suite of N ground motions which are applicable to the geographical area of interest. This suite should represent a broad range of values for the chosen intensity measure.
2. Generate N statistical samples of the subject structure. These samples should be generated by sampling various modeling parameters which may be deemed significant. Thus, N statistically different yet nominally identical bridge samples are generated.
3. Perform a full non-linear time history analysis for each ground motion-bridge pair. Key responses should be monitored throughout the analysis.
4. For each analysis, peak responses are recorded and plotted versus the peak value of the intensity measure for that ground motion. A regression analysis of these data is then performed to estimate a, b and $\beta_{D|IM}$.

Step 4 is repeated for all major vulnerable components in the bridge. Thus, the

seismic demand on each of the bridge components can be modeled.

The capacity level (limit states) for the various bridge components can be assessed using a physics (prescriptive) approach and a judgmental (descriptive) approach.

The distributions of the component capacities are assumed to be lognormal. The lognormal parameters for limit state (S_c, β_c) of each bridge component used are developed using a Bayesian approach that incorporates physics-based assessments with judgmental assessments.

The general assessment of the seismic vulnerability for the bridge as a whole must be made by combining the effects of the various bridge components. The probability that the bridge is at, or beyond, a particular limit state is the union of the probabilities of each of the components being in that same limit state.

The estimate of the system or bridge level fragility is facilitated through the development of a joint probabilistic seismic demand model (JPSDM). This approach recognizes that there is some level of correlation between the demands placed on the various bridge components during a given earthquake.

Specifically, this methodology is designed to consider all major bridge components when assessing seismic vulnerabilities. The demand on the bridge is quantified by using a JPSDM. The fragility of the bridge is calculated by integrating overall failure domains of the joint PSDM.

3 Network level assessment

3.1 Introduction

Bridges in highway networks are crucial to the essential function of connectivity. Highway bridges provide effective links that connect the nodes of interest in a geographical region. Therefore, it is a fundamental requirement to maintain highway bridges at, or above, a minimum level of service and safety during their entire life (Liu and Frangopol 2006). Compared with the seismic assessment of individual bridges, network level seismic assessment normally involves network prioritization, which is always related to the distribution of limited financial, material and human resources to bridge maintenance, repair, and rehabilitation in an best manner.

A clear objective is needed before selecting the prioritization method. Safety, minimum cost, and minimum travel time are all reasonable and desirable aims. Different targets can lead to different solutions and methods. Normally, the prioritization methods function can be expressed as (Nuti, 2004):

$$P_b = f(F_b, R_b, C_b) \tag{3.1}$$

where P_b is the prioritization value for every bridge in a stock, f is the function dependent on the prioritization method, F_b is the seismic hazard on the bridge, R_b is the resistance of the bridge, and C_b is the cost of bridge failure. Based on Equation (3.1), the bridge with a higher prioritization value deserves a higher priority in seismic retrofitting.

The outline of this chapter is as follows: in section 3.2, the connectivity analysis is carried out in APT-BMS; in section 3.3 the safest path is identified in the APT-BMS network; finally, the existing methods for network level assessment are introduced in section 3.4.

3.2 Connectivity analysis in APT-BMS

From chapter 2, we learned that the seismic risk in the APT stock is moderate. However, the system operation at network level is of concern in a post earthquake situation. Approximately 15% of the bridges in the APT stock have a relatively high risk of suffering operational problems. It is therefore necessary to identify the safest path between any two given points after an earthquake. Here 'the safest' means the lowest risk of exposure to operational problems in a given earthquake scenario. Before identifying the shortest path between any two given points, we need to check the connectivity of the two points. The connectivity reliability of a network states the probability that the traffic can reach the destination from the origin (Liu and Frangopol, 2006). In this Chapter, it is assumed that the bridge elements are the only vulnerable parts of the network, and that the roads between any two bridges will never fail. In Chapter 4, I will explain the graph theory in detail.

3.2.1 Definition of network connectivity

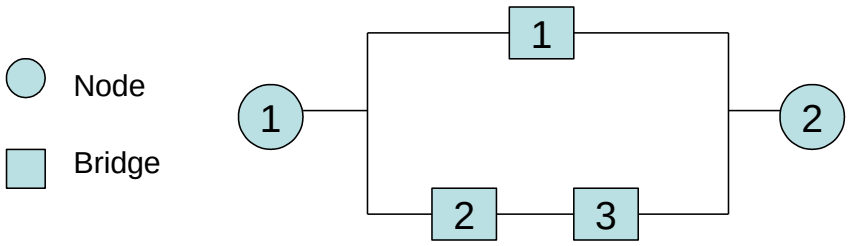

Fig. 3.1 Simple network with two nodes and three bridges

Fig. 3.1 is a simple network with two nodes and three bridges. Bridge i, for i = 1, 2, 3, is in the operational mode with probability p_i, and in the failed mode with probability q_i =1- p_i. Table 3.1 gives the values of p_i and q_i for each bridge. In this example, I assume that there is no correlation between these bridges; they are all independent of each other.

Table 3.1 probabilities in operational mode

Bridge	p_i	q_i
1	0.7	0.3
2	0.8	0.2
3	0.9	0.1

The links between the nodes and the bridges are assumed to be safe. A bridge mode vector V is used to denote the state mode of the bridges:

$$V_i = \begin{cases} 1 & \text{if bridge } i \text{ is in failed mode} \\ 0 & \text{if bridge } i \text{ is in operational mode} \end{cases} \quad (3.2)$$

Given a specific mode vector, if there is at least one path connecting node 1 and node 2, then we say that node 1 and node 2 are connected; otherwise they are disconnected. Table 3.2 gives all the network states and the corresponding probability for each network state.

Table 3.2 all the network states in Fig. 3.1

Network state	Bridge mode vector *V*	Probability for this vector	*Connectivity*
1	110	0.054	Disconnected
2	101	0.024	Disconnected
3	011	0.014	Connected
4	100	0.216	Connected
5	001	0.056	Connected
6	010	0.126	Connected
7	000	0.504	Connected
8	111	0.006	Disconnected

Table 3.2 shows that there are five network states that are connected. The sum of the probabilities for these five states is 0.916. In this case, we say that the connectivity for the network is 0.916. From this example, the connectivity can be defined as the sum of the probabilities of the network states that are connected.

In this simple network, there are only 3 bridges and 2 nodes, therefore it is very easy to check the connectivity between two nodes. For a complex network with a large number of nodes, it is extremely difficult to check the connectivity between any two nodes; below I describe the procedure to solve this problem.

Assume that there is a graph with *n* nodes and *m* links. To check the connectivity between any two nodes:

Step 1: Rank all the nodes from 1 to *n* randomly, and assuming a need to check the connectivity between node 1 and node *n*, set node 1 as the start node.

Step 2: If there is a direct link between node *i* and the start node, then node *i* is called the linked node; find all the linked nodes, and mark the other nodes as unlinked nodes.

Step 3: For each of the linked nodes, repeat step 2 until the linked nodes set and the unlinked nodes set become unchanged. Finally, if node *n* is in the linked nodes set, then node 1 and node n are connected, otherwise they are disconnected.

Using this method, the connectivity for a specific network state can be obtained. However, due to the exponential effect, it is difficult to enumerate the state space for

a network with more than a few nodes. For a network with 50 bridges, the number of network states is 2^{50} =1.13 ×10^{15}, which is a huge number. On the other hand, in many cases, it is not necessary to enumerate all the possible states. In some cases, for all the connected states, there are only a finite number of states that account for the majority of the probability of being connected, while the probabilities of other states are very low. Take the network in Fig. 3.1 for example; network states 3, 4, 5, 6, and 7 are connected. The sum of probabilities of states 4, 6, and 7 is 0.846, which accounts for 92.4% of all the probabilities being in connected states. Therefore, below we can restrict our attention to the most likely states and give bounds on the network performance. In order to enumerate the most likely states, algorithm ORDER (Li 1984) and algorithm ORDER-II (Lam 1986) are introduced in the next section.

3.2.2 Description of algorithms ORDER and ORDER-II

Algorithm ORDER was proposed by Li and Silvester (1984), and is used to enumerate the most probable states in a network, *m*, with *n* failure-prone components. Here the failure-prone component means that the probability in operational mode p_i is larger than the probability in fair mode q_i. There are the following assumptions for this algorithm:

1. Component *i* is in the operational mode with probability p_i, and in the failed mode with probability q_i =1- p_i, all the components are independent.
2. $p_i \geq q_i$.
3. Components are renamed such that $R_1 \geq R_2 \geq \ldots \geq R_n$ where $R_i = q_i / p_i$.

The state of the system is denoted by S_k, k =1, 2, …, 2^n. The probability of S_k is given by

$$P_k = \prod_i^n p_i (q_i / p_i)^{V_i} \tag{3.3}$$

where V_i is defined as in Equation (3.2). Obviously, when V_i = 0, for i = 1, 2, …, n, P_k has the largest value. So the most probable state, S_1, corresponds to no failures, and the next most probable state is the one in which there is only one failed component. This failed component has the largest R_i, i.e., component 1. In this algorithm, the state S_i, i = 1, 2, …, m, is identified by the identities of the failed components in S_i ; thus, $S_1 = \varnothing$, $S_2 = \{1\}$, etc.

Let A = $\{S_1, S_2, ..., S_m\}$ denote an ordered set of failure states such that $P(S_1) \geq P(S_2) \geq \ldots \geq P(S_m)$. There are three operations in this algorithm.

The first operation is called appends, denoted as ||, and is defined as follows:

$$A \| \{i\} = \{S_1 \cup \{i\}, S_2 \cup \{i\}, \cdots, S_m \cup \{i\}\}$$

The element *i* is inserted into each network state of A.

The second operation is called insert, denoted as $B \rightarrow A$, and defined as:

$B \rightarrow A$ = the ordered set which results when each element of B is inserted into the ordered set A.

The last operation is called select, denoted $T(A)$, and is defined as:

$T(A)$ = the ordered set which contains the first m elements of the ordered set A.

The algorithm consists of two phases and n stages, with stage i corresponding to failure-prone component i. First we find t, where t is the smallest integer such that $2^t \geq m$.

Phase 1:

1) Initialize: $S_1 = \varnothing$, $A_0 = \{ S_1 \}$.
2) For $i = 1, 2, \ldots, t$, repeat 2.1), 2.2).

2.1) $B_{i-1} = A_{i-1} \parallel \{i\}$

2.2) $A_i = B_{i-1} \rightarrow A_{i-1}$

Phase 2:

3) Initialize: $A_{t+1} = T(A_t)$.
4) For $i = t+1, \ldots, n$, repeat 4.1), 4.2), 4.3).

4.1) $B_{i-1} = A_{i-1} \parallel \{i\}$

4.2) $A_i = B_{i-1} \rightarrow A_{i-1}$

4.3) $A_i = T(A)$

A_n contains, in decreasing order, the m most probable states.

Algorithm ORDER has the disadvantage that it can only generate exactly m (a pre-assigned number) most probable states. To get more states one has to run the algorithm from the beginning, using a larger m. This limits algorithm flexibility, and it is difficult to make a good choice of m before running the algorithm (Lam 1986). In Lam (1986), Lam and Li proposed an updated algorithm, ORDER-II, which can generate states in the appropriate order, and does not require a fixed number of states beforehand. The algorithm can be run until a desired degree of accuracy is obtained, thus optimizing the use of computational resources.

The problem in ORDER-II is formulated in a more general context as follows. We are given a set $S = \{e_1, e_2, \ldots, e_n\}$ of n elements, sorted such that $w(e_i) \geq w(e_j)$ for all $i > j$, where $w(e_i)$is the weight of element e_i. We want to generate subsets SS_1, $SS_2, \ldots$, such that $w(SS_i) \geq w(SS_j)$ for all $i > j$, where $w(SS_i)$ is the total weight of all elements in subset SS_i. The following are the notations for ORDER-II:

$e_L(SS_i) = \text{last element (the one with largest weight) in subset } SS_i$

$n(e_i) = \text{the next element after } e_i \text{ in set } S, \text{ that is } e_{i+1}$

$Tree$ = the structure for storing candidate subsets

SSR_i = the subset at the root of the heap at stage i

$SS_i - \{e_j\}$ = the subset SS_i with element e_j deleted

$SS_i + \{e_j\}$ = the subset SS_i with element e_j added

The procedures of the algorithm are as follows:

Initialize: i: = 1; SS_1: = $\{e_1\}$; Tree: = Φ;
Repeat
If $e_L(SS_i) \neq e_n$ then
begin
add SS_i - $\{e_L(SS_i)\}$+ $\{n\{e_L(SS_i)\}\}$ to Tree;
add SS_i + $\{n\{e_L(SS_i)\}\}$ to Tree;
end;
SS_{i+1} : = SSR_i;
Delete SSR_i from Tree;
i: = i + 1;
until enough subsets have been generated.

After describing the algorithms ORDER and ORDER-II, the next section will introduce the network in APT-BMS, and the algorithm will be implemented.

3.2.3 Network simulation

There are 983 bridges in the APT stock, located along SP (province owned) roads and SS (state owned) roads. The whole APT road network, including all bridges and roads, is simulated as a graph.

The key phase of network simulation is identifying all the nodes of the graph. The following points are defined as nodes: the intersections or endpoints of SP and SS roads. Each node has 3 variables: ID number, longitude, latitude.

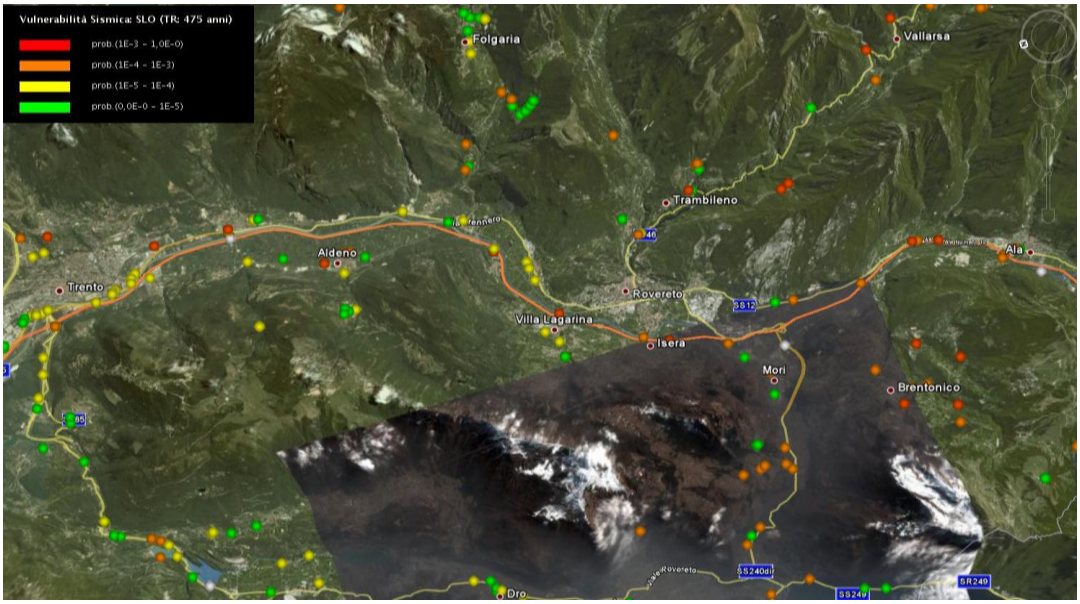

Fig. 3.2 Google Earth map from Trento to Ala

Table 3.3 Geographical coordinates of nodes in Trento to Ala road network

Node	Longitude[°]	Latitude[°]
1	11.11209	46.05268
2	11.11474	46.04633
3	11.11213	46.04482
4	11.1277	46.00896
5	11.12003	46.00924
6	11.09432	45.93155
7	11.07568	45.92801
8	11.03576	45.90218
9	11.03545	45.91406
10	11.03381	45.88712
11	11.00792	45.88184
12	11.03117	45.87281
13	10.99713	45.86327
14	11.00514	45.76261
15	10.99979	45.76708
16	11.00032	45.75776

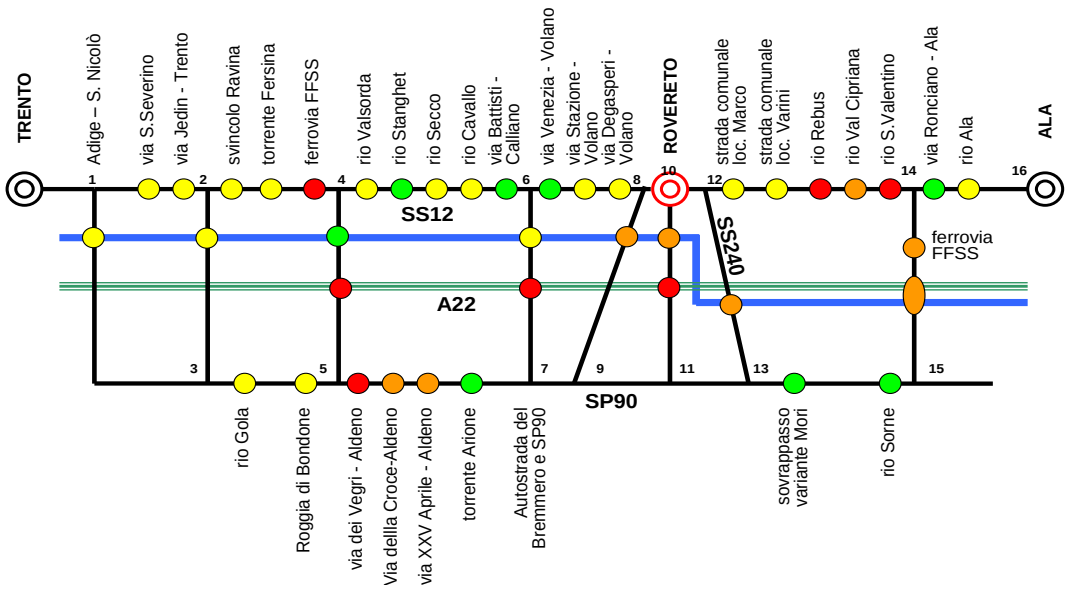

Fig. 3.3 Simulated transportation graph between Trento-Ala

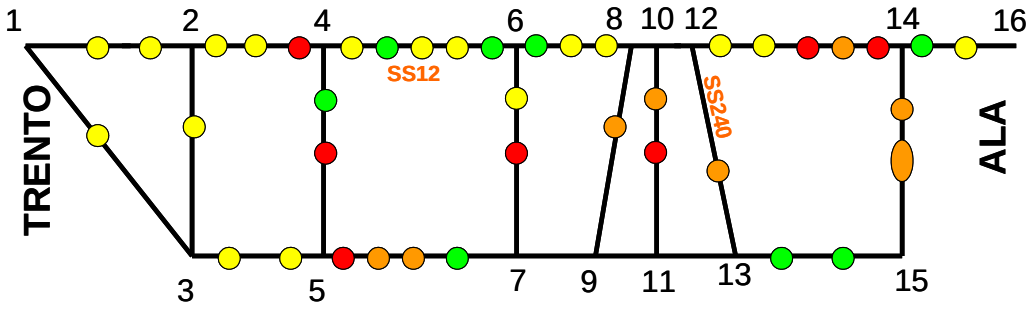

Fig. 3.4 The simplified graph between Trento-Ala

Fig. 3.2 is the Google Earth map from Trento to Ala. Trento is the capital city of the APT region, while Ala is an important town in the south of the APT, near the high risk seismic zones in Northern Italy. Fig. 3.3 is the simulated graph from Trento to Ala. There are 40 bridges with differing probabilities of being in operational limit state, as represented by the colored dots. SS12 and SP90 are two main roads connecting Trento and Ala. The Adige River and the A22 highway are between SS12 and SP90. In the APT network, we consider only the SS and SP roads, and only the intersections and the endpoints of SS and SP roads can be identified as nodes, so A22 is not included in the simulated graph. Based on this definition, there are 16 nodes in this graph. All the nodes are shown in Fig. 3.4. Each node has 3 variables: ID number, longitude, latitude. For example, the parameters of node 1 are 1, 11.11209, and 46.05268 respectively.

After identifying all the Nodes, the next step is to identify all the Links. Not all connections between two nodes can be regarded as links; these must be along the SP or SS roads. There are 22 links in Fig. 3.4.

Table 3.4 gives descriptions of every link. Each link has 6 variables: ID number, start node ID, end node ID, ID of the road forming the link, the relative position of the start node on the road, and the relative position of the end node on the road. For example, the parameters of link 1 are 1, 1, 2, 250, 377.03, and 376.246; this means that the number of this link is 1, the endpoints of this link are node 1 and node 2, the link belongs to road 250 which is ss12 in the database, the relative position of node 1 in ss12 is 377.03 km and the relative position of node 2 in ss12 is 376.246 km. After identifying all the links, the APT stock network is simulated as a graph in Google.

When all the nodes and links are identified, the whole APT network is simulated as a graph in Google Earth as shown in Fig. 3.5. The small red points represent the nodes, and the red lines represent the links. In total, there are 558 nodes and 740 links in the APT stock. All the bridges are located on the links. Now the algorithms can be performed on the APT network.

Table 3.4 Descriptions of links in Trento to Ala road network

Path	Start Node	End Node	Road Name	Road ID	Start Km	End Km
1	1	2	ss12	250	377.03	376.246
2	2	4	ss12	250	376.246	371.441
3	4	6	ss12	250	371.441	361.19
4	6	8	ss12	250	361.19	355.715
5	8	10	ss12	250	355.715	354.095
6	10	12	ss12	250	354.095	352.415
7	12	14	ss12	250	352.415	337.71
8	14	16	ss12	250	337.71	337.052
9	1	3	ss12	250	377.03	377.45
10	2	3	sp90 part 2	126	25.35	25.11
11	3	5	sp90 part 2	126	25.11	20
12	4	5	sp21	27	3.1	2.8
13	5	7	sp90 part 2	126	20	12
14	6	7	sp59	73	1.01	0.1
15	7	9	sp90 part 1	123	22.9	22.7
16	8	9	sp90 dir ss12	128	0	0.5
17	9	11	sp90 part 1	123	22.7	22.5
18	10	11	sp90 dir Rovereto	127	0	2.3
19	11	13	sp90 part 1	123	22.5	22
20	12	13	ss240	269	0	3.5
21	13	15	sp90 part 1	123	22	11
22	14	15	sp90 part 1 dir Ala	125	0.3	0

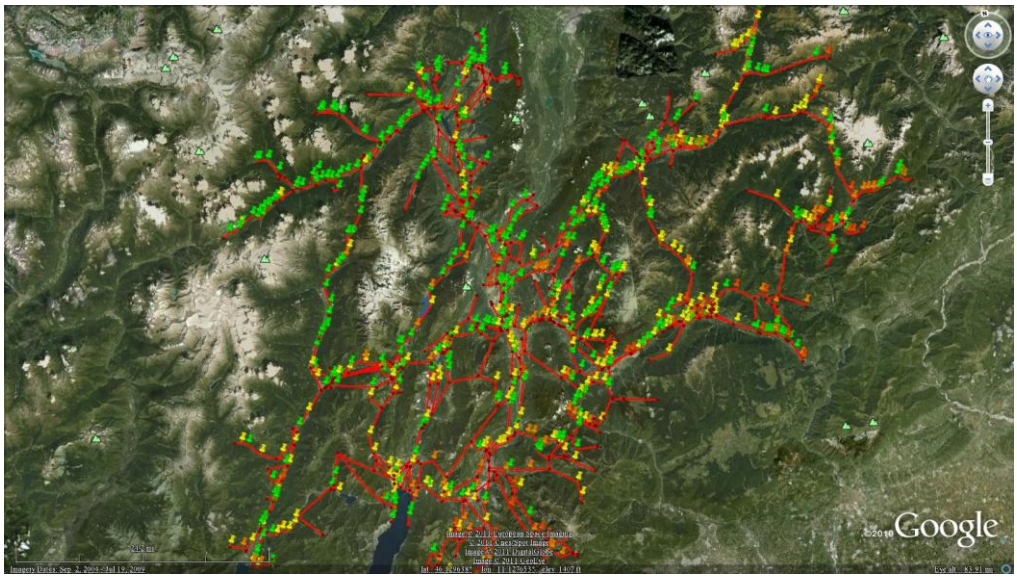

Fig. 3.5 Google Earth map of the APT-BMS network

3.2.4 Implementation in APT-BMS

After simulating the network, the algorithms ORDER and ORDER-II are used to find *m*, the most probable states of the network. Let's start with the simple network from Trento to Ala in Fig. 3.3. Fig. 3.6 shows the probability of each bridge having operational problems. Since there are 40 bridges in this network, there will be $2^{40} = 1.1 \times 10^{12}$ states for this network. For the whole network in APT-BMS, there are 984 bridges, and so the number of network states will be 2^{984}, which is an enormous number. In order to simplify the computation, all the bridges within one link are combined into one bridge, and the probability of this new bridge having operational problems is the sum of probabilities of all the bridges having an operational problem. It must be noted that here we make an approximation: considering an example with two bridges (A and B) on the link, as we know, the probability of the link being disconnected is $P_{fail}(link) = P_{fail}(A) + P_{fail}(B) - P_{fail}(AB)$. If we neglect the correlation between bridges A and B, we have $P_{fail}(AB) = P_{fail}(A) \cdot P_{fail}(B)$, so $P_{fail}(link) = P_{fail}(A) + P_{fail}(B) - P_{fail}(A) \cdot P_{fail}(B)$. Since the values of $P_{fail}(A)$ and $P_{fail}(B)$ are very small, their product is negligible. Therefore $P_{fail}(link) = P_{fail}(A) + P_{fail}(B)$. The results are shown in Fig. 3.7. In Fig. 3.7, the components have been reduced to 17, so the total network states number becomes $2^{17} = 1.3 \times 10^5$.

In this example, the number of components is $n = 17$, and we want to consider the *m* most probable states for this network. For each network state, we calculate the connectivity of the network. If there is at least one path to connect node 1 and node 16, then the connectivity for this state is 1, otherwise 0. After considering all the m most probable states, the approximate total connectivity for this network is:

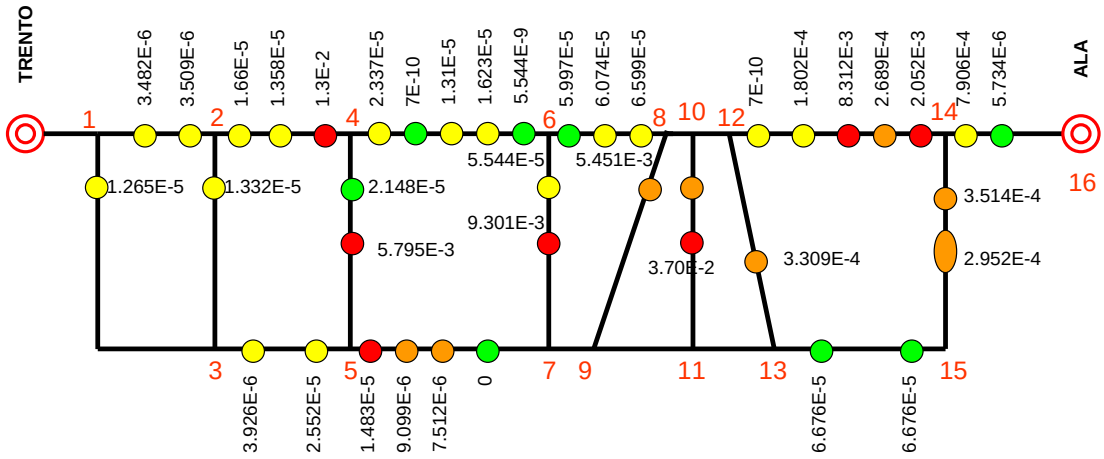

Fig. 3.6 Graph representation of Trento to Ala road network with individual bridges

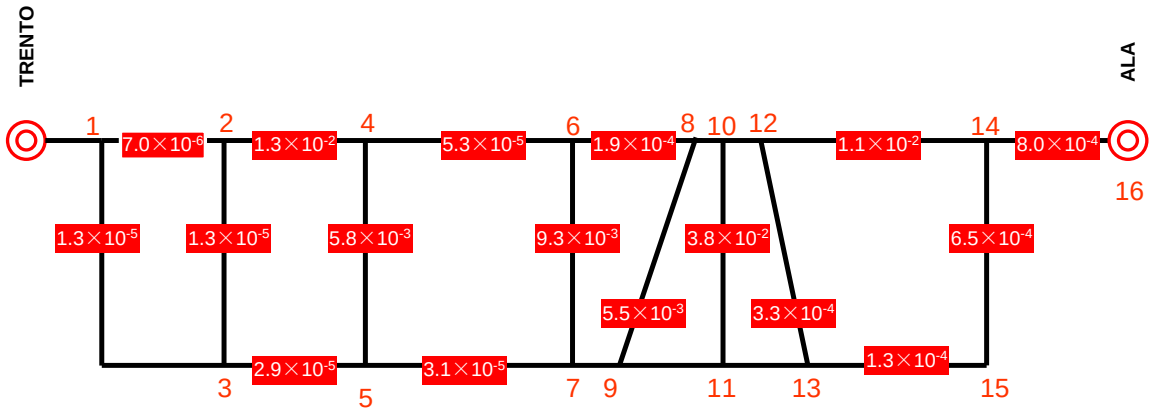

Fig. 3.7 Graph representation of Trento to Ala road network indicating the probability of link failure

$$C \approx \sum_{i=0}^{m} C_i \cdot P_i \tag{3.4}$$

where P_i is the probability of the i-th network state, and C_i is the connectivity for the i-th network state. $C_i = 1$, if there is at least one path from node 1 to node 16; $C_i = 0$, if not. Obviously,

$$C_{2^n} \le C_i \le C_1 \qquad i = 1, 2, \cdots, 2^n \tag{3.5}$$

where C_1 is the connectivity when all the components are in operational mode, and $C_2{}^n$ is the connectivity when all the components are in failure mode. So $C_1 = 1$, and

$C_2^n = 0$. If we consider the m most probable states, we have:

$$C = \sum_{i=1}^{m} C_i \cdot P_i + \sum_{i=m+1}^{2^n} C_i \cdot P_i \tag{3.6}$$

From Equation (3.5), we have:

$$\sum_{i=m+1}^{2^n} C_{2^n} \cdot P_i \le \sum_{i=m+1}^{2^n} C_i \cdot P_i \le \sum_{i=m+1}^{2^n} C_1 \cdot P_i \tag{3.7}$$

Since $C_1 = 1$, and $C_2^n = 0$, Equation (3.7) becomes

$$0 \le \sum_{i=m+1}^{2^n} C_i \cdot P_i \le \sum_{i=m+1}^{2^n} P_i = 1 - \sum_{i=1}^{m} P_i \tag{3.8}$$

Substituting Equation (3.8) into (3.6), we get:

$$\sum_{i=0}^{m} C_i \cdot P_i \le C \le \sum_{i=0}^{m} C_i \cdot P_i + 1 - \sum_{i=0}^{m} P_i \tag{3.9}$$

Table 3.5 gives the connectivity of the network when considering different m values. When the 5 most probable states are considered, the real network connectivity C is between 9.7568×10^{-1} and 1. If the 10 most probable states are considered, the range becomes [9.9448×10^{-1}, 9.9869×10^{-1}]. As the value of m increases, the upper and lower bounds of C converge quickly. From this example, we can say that the connectivity for this network is 9.9448×10^{-1}.

Table 3.5 Expected connectivity of between Trento to Ala given different m values

Number of states (m)	$\sum_{i=0}^{m} P_i$	$\sum_{i=0}^{m} C_i \cdot P_i$	$\sum_{i=0}^{m} C_i \cdot P_i + 1 - \sum_{i=0}^{m} P_i$
5	0.9757	0.9757	1
10	0.9958	0.9945	0.9987
100	0.9987	0.9945	0.9958
1000	0.9998	0.9945	0.9946
5000	0.9999	0.9945	0.9946
10000	0.9999	0.9945	0.9945
50000	1	0.9945	0.9945

After performing the algorithm on the network from Trento to Ala, we want to consider the connectivity of the whole network in APT-BMS - this has already been simulated in section 3.2.3.

Lavaz è Pass and Riccomassimo are two remote places in Trentino Province (see Fig. 3.8) located to the north and south of the APT region, respectively. Given the start node as Riccomassimo and the end node as Lavaz è Pass, the connectivity, using the algorithm ORDER-II, is analyzed below.

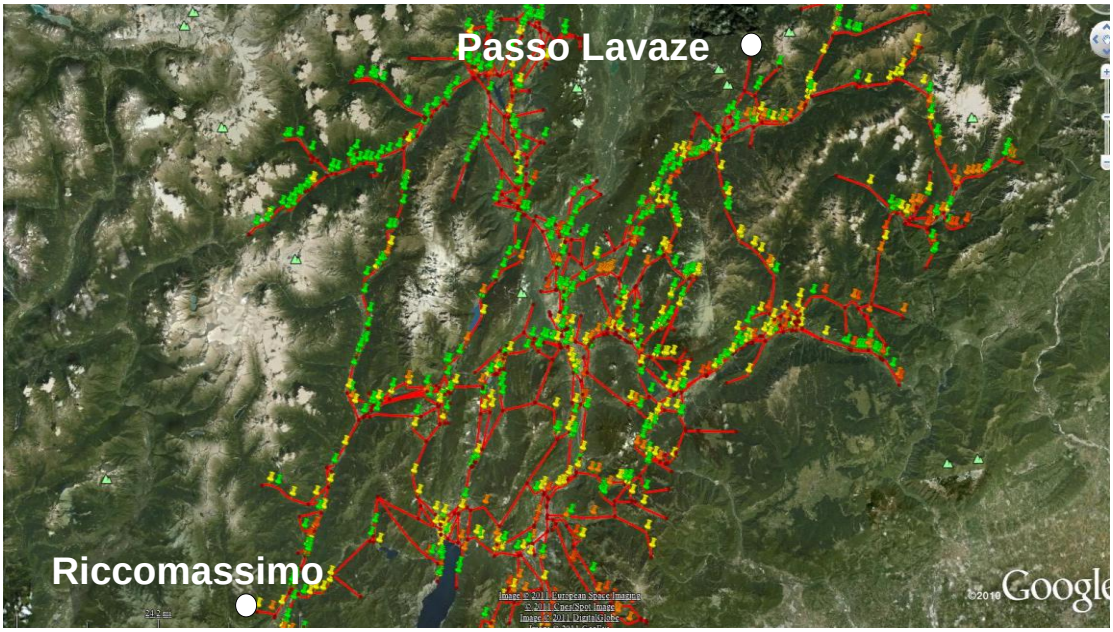

Fig. 3.8 Locations of Passo Lavaz è and Riccomassimo in APT road network

Table 3.6 Connectivity between Passo Lavaz è and Riccomassimo for different m values for return period of 475 years

Number of states (m)	$\sum_{i=0}^{m} P_i$	$\sum_{i=0}^{m} C_i \cdot P_i$	$\sum_{i=0}^{m} C_i \cdot P_i + 1 - \sum_{i=0}^{m} P_i$
10	0.5666	0.5666	1
10^2	0.7394	0.7313	0.9919
10^3	0.7899	0.7313	0.9414
10^4	0.7952	0.7313	0.9361
10^5	0.7978	0.7313	0.9334
10^6	0.7997	0.7313	0.9316

From Table 3.6, we can see that the 100 most probable states account for 73.9% of the whole states. After that, the sum of the probabilities for the m most probable states increases very slowly. However, the approximate connectivity remains the same after m = 100. Therefore, it can be concluded that after the most 100

probable states, the network is disconnected between the Lavaz è Pass node and the Riccomassimo node. From Table 3.6, we can conclude that the connectivity between the Lavaz è Pass node and the Riccomassimo node is between 7.3128×10^{-1} and 9.3163×10^{-1}, and more likely to be 7.3128×10^{-1}.

Similarly, the connectivities for return periods of 72 years and 2475 years are given in Table 3.7 and 3.8 respectively. For a return period of 475 years, the connectivity of the two nodes is about 9.9987×10^{-1}. While for a return period of 2475 years, the cumulative probability of the 10^6 most probable states is less than 1%, so the upper bound of the connectivity is very high, which is nearly 1. But the lower bound of the connectivity remains the same after $m = 10^3$. This can be explained by the fact that the network is disconnected for other states after $m = 10^3$. It is likely that the connectivity is about 3.4484×10^{-4}. It means that these two nodes are disconnected under this scenario. This can be explained by the reason that most bridges are collapsed after an earthquake with a return period of 2475 years.

Table 3.7 Connectivity between Passo Lavaz è and Riccomassimo for different m values for return period of 72 years

Number of states (m)	$\sum_{i=0}^{m} P_i$	$\sum_{i=0}^{m} C_i \cdot P_i$	$\sum_{i=0}^{m} C_i \cdot P_i + 1 - \sum_{i=0}^{m} P_i$
10	0.9982	0.9982	1
10^2	0.9999	0.9999	0.9999
10^3	0.9999	0.9999	0.9999
10^4	0.9999	0.9999	0.9999
10^5	0.9999	0.9999	0.9999
10^6	0.9999	0.9999	0.9999

Table 3.8 Connectivity between Passo Lavaz è and Riccomassimo given different m values for return period of 2475 years

Number of states (m)	$\sum_{i=0}^{m} P_i$	$\sum_{i=0}^{m} C_i \cdot P_i$	$\sum_{i=0}^{m} C_i \cdot P_i + 1 - \sum_{i=0}^{m} P_i$
10	0.60859×10^{-5}	6.0859×10^{-5}	1
10^2	1.8776×10^{-4}	1.8776×10^{-4}	1
10^3	5.8397×10^{-4}	3.4484×10^{-4}	0.9998
10^4	1.5619×10^{-3}	3.4484×10^{-4}	0.9988
10^5	4.2256×10^{-3}	3.4484×10^{-4}	0.9961
10^6	9.3840×10^{-3}	3.4484×10^{-4}	0.9910

In this section, the connectivity between two places was analyzed. In the following, the safest path between these two places is identified.

3.3 Identifying the safest path in the network

After an earthquake, the ability to quickly identify the safest path between two places is of great help to decision makers aiming to best distribute the available human and material rescue resources to the disaster centre. This is addressed by Dijkstra's algorithm (Dijkstra, 1959), which is a classic algorithm used to find the shortest path.

3.3.1 Calculation procedure of Dijkstra's algorithm

Dijkstra's algorithm is a graph search algorithm, used to solve the shortest path problem in a non-directional graph, with non-negative path cost. It was proposed by Dutch computer scientist Edsger Dijkstra in 1959. This algorithm is often used in transportation routing.

Given a graph with n nodes and m links, an $n \times n$ diagonal square matrix M is created. Each element of the matrix is the distance value between two nodes. For example, M_{ij} is the edge cost of the link between node i and node j. Given a graph, the input matrix is obtained under these rules:

- For each link, a value is assigned to it as the edge cost;
- The distance between the node and itself is zero, so all the diagonal elements M_{ij} equal zero;
- If there is no direct link between nodes i and j in the graph, then the matrix element M_{ij} is assigned as infinite.

After creating the input matrix, for a given start node in the graph, the algorithm can find the shortest paths between the start and every other node. Given the start node, let vector d be the temporary distances from other nodes to the start node, and let vector D be the final shortest distances from other nodes to the start node, which are also our target solution set. Dijkstra's algorithm will assign some initial values to d and try to improve them step-by-step:

Step 1: Assign the initial values to d. The initial distance between the start node and itself is zero, and the initial distances from all other nodes to the start node are infinite. Mark all nodes as unvisited.

Step 2: Set the node with the smallest distance as the current node, and use this smallest distance as the final distance between that node and the start node. For the current node, consider all its unvisited neighbors, and calculate the distances from the start node to the unvisited neighbor nodes directly, through the current node. If the new distance is smaller than the previous one, then change the distance; otherwise do not change.

Step 3: After considering all neighbor nodes of the current node, mark the current node as visited. A visited node will not be checked again, and its distance

value in distance vector *d* is replaced with infinite.

Step 4: Repeat step 2 and step 3 until all the nodes have been visited.

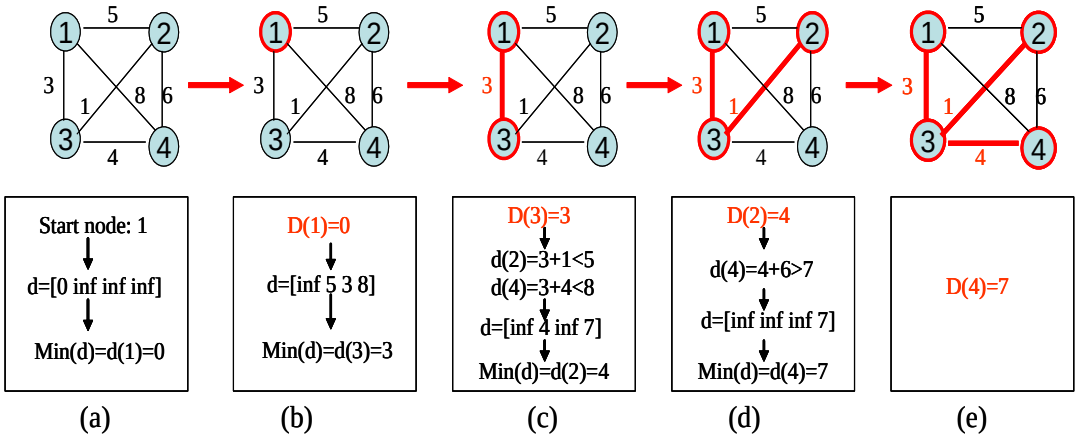

Fig. 3.9 Calculation procedures of a simple graph using Dijkstra's algorithm

Fig. 3.9 gives the calculation procedure for a simple graph with 4 nodes and 6 links. Each link has an edge cost indicated by the number near it. The input matrix of this graph is:

$$M = \begin{bmatrix} 0 & 5 & 3 & 8 \\ 5 & 0 & 1 & 1 \\ 3 & 1 & 0 & 4 \\ 8 & 1 & 4 & 0 \end{bmatrix}.$$

Based on the previous calculation procedure, the shortest distances, D, between the start node 1 and the other nodes are calculated, and the shortest paths are also identified with bold red lines in Fig. 3.9.

After introducing the calculation procedures of the Dijkstra algorithm, the following section will perform the algorithm using the APT network.

3.3.2 Algorithm implementation and results

Once the network has been simulated as a graph, the only data needed before running the algorithm is the edge cost for every link. The edge cost for every link is the sum of probabilities of being in the operational damage state for all the bridges along the link. When we have the edge cost for every link, the input matrix, which is a 558 × 558 diagonal matrix, is obtained, and then Dijkstra's algorithm can be implemented on the graph.

We now want to calculate the best path between Lavaz è Pass and Riccomassimo. Given that the start node is Riccomassimo and the end node is Lavaz è Pass, MATLAB program can generate the KML file automatically. It can then be loaded in Google Earth to show the simulated network and the outlined safest path. Fig.

3.10 shows the results for a return period of 475 years in a Google Earth map. The red lines represent the simulated network, while the white lines represent the safest path between Lavaz è Pass and Riccomassimo. In the same way, all the safe paths between any two given places can be identified in Google Earth. For the results of return periods of 2475 years and 72 years, the identified path is the same as in Fig. 3.10.

These results are very helpful for bridge managers and government officials in understanding the network status, and can assist them to make rapid decisions in near-real time, under post earthquake conditions.

Fig. 3.10 Simulated network and the safest path between Passo Lavaz è and Riccomassimo

3.4 Existing methods for network level assessment

The following details some state-of-the-art methods for network level assessment.

3.4.1 Probability-Based Bridge Network Performance Evaluation (Liu and Frangopol 2006)

This method aims to identify the best maintenance actions from a cost benefit analysis. Three different criteria are used to evaluate the overall performance of a

bridge network: network connectivity, user satisfaction and structural reliability of the critical bridges.

Bridge network connectivity is evaluated by using an event tree technique. A bridge network is considered to be disconnected if any nodes of interest are isolated from the other nodes of interest, due to the failure of any individual bridge in the network. Otherwise, the bridge network is considered to be connected. The reliability of the network is simply the sum of the reliabilities of all the paths of the network. The system reliabilities of the individual bridges in the network are assumed to be independent. The probability associated with the occurrence of an event on a specified path is simply the product of the probabilities of all the subsequent events on the path. In the network, this probability is:

$$P_{path} = \prod_{\text{all bridges on path}} P_{\text{fail or safety}} \tag{3.10a}$$

$$P_{connected} = \sum_{all\ paths\ with\ connection} P_{path} \tag{3.10b}$$

The unit traffic costs are calculated as the sum of travel time and vehicle operation costs.

$$w_{ij} = C_{\text{travel time}} + C_{\text{vehicle operation}} = \frac{D_{ij}}{V_{ij}} \times \alpha + D_{ij} \times \gamma \tag{3.11}$$

where D_{ij} is the distance between nodes i and j; V_{ij} is the traffic speed on link (i, j); α is unit cost for travel time per hour; and γ is unit cost for vehicle operation per mile.

The probability of unsatisfactory performance of the bridge network, $P_{f\text{-}us}$ is expressed as:

$$P_{f-us} = \frac{TFC}{TTC} \tag{3.12}$$

where *TFC* is total failure costs and *TTC* is total traffic costs in the bridge network.

3.4.2 Prioritization based on system reliability analysis (Nojima 1998)

This research proposes the concept of performance-based prioritization in upgrading the seismic reliability of road networks.

First, the performance measure is defined as the system flow capacity of road networks subject to failure. Given a network configuration and a set of flow

capacities on each link $C = \{c_1, c_2, \ldots, c_n\}$, the system flow capacity is defined as the maximum flow between a specific pair of source and terminal nodes. When a seismic event happens, the functional degradation is evaluated on the basis of the pre earthquake capacity of individual links, and the post earthquake structural damage pattern.

Then a binary performance index is defined to compute the system reliability. The binary state variables x_i (i = 1, 2, .., n) denote the state of survival (1) and failure (0) of the i-th link, and n-vector S = $\{x_{1,} x_{2\ldots,} x_n\}$ denotes the overall state of n links. Obviously, the maximum flow F_0 is obtained when x_i =1 for i = 1, 2, .., n. Then a binary variable $B(S)$ is used to compute the system reliability corresponding to satisfying (1) or not satisfying (0) a pre-assigned requirement level r ($0 < r < 1$) of maximum flow F_0.

$$B(S) = \begin{cases} 0 & (F_{\max}(S) < rF_0) \\ 1 & (F_{\max}(S) \geq rF_0) \end{cases} \tag{3.13}$$

where $F_{\max}$ (S) is the maximum flow of state S. The overall state of the system is denoted by S^k (k = 1, 2, .., 2^n). The probability of occurrence of each state S^k is denoted by $Q(S^k)$ and the expected value of the performance measure, which is denoted by E[G(S)], is derived as:

$$E[G(S)] = \sum_{k=1}^{2^n} Q(S^k)G(S^k) \tag{3.14}$$

where the upper and lower bounds of the system performance measure, G_U and G_L, are obtained using algorithm ORDER (1984, 1986), which will be introduced in the following section:

$$G_U = \sum_{k=1}^{m} Q(S^k)G(S^k) + [1 - \sum_{k=1}^{m} Q(S^k)]G_b \tag{3.15a}$$

$$G_L = \sum_{k=1}^{m} Q(S^k)G(S^k) + [1 - \sum_{k=1}^{m} Q(S^k)]G_w \tag{3.15b}$$

where G_b and G_w are the best (no components fail) and worst (all components fail) performance states, respectively.

At last, the importance measure of every component is calculated as follows. Let P(p) denote the system reliability as a function of the component reliability

vector p= {p_1, p_2, …, p_n}. The conditional system reliability given that a specific component i fails or not are written as $P(0_i, p)$ and $P(1_i, p)$ respectively. According to the total probability theorem, the system reliability $P(p)$ is a linear function of p_i:

$$P(p) = p_i \cdot P(1_i, p) + (1-p_i) \cdot P(0_i, p) \tag{3.16}$$

So the importance measure of component i can be obtained as the derivative of system reliability:

$$I_i^B = \frac{\partial P(p)}{\partial p_i} = P(1_i, p) - P(0_i, p) \tag{3.17}$$

Then the performance-based prioritization order can be determined by the rank of importance measures.

3.4.3 Vulnerability and importance based prioritization (Basöz and Kiremidjian 1995)

This report presents a prioritization method for seismic retrofitting of bridges which can identify the bridges that are in most need of retrofitting and rank the bridges based on their vulnerability and importance. The relationship is described as follows:

$$R_i = f(V_i, I_i) \tag{3.18}$$

where R_i is the ranking of bridge *i*; V_i is the vulnerability of bridge *i*; and I_i is the importance of bridge *i*.

Vulnerability *R* is expressed as a function of seismicity, which can describe the direct effect of ground motion on damage. Vulnerability assessment includes:

- Seismic hazard analysis at the bridge site;
- Classification of bridges based on their structural characteristics
- Fragility analysis.

The importance I of the bridge is defined as follows:

$$I = f(S, E, G, Q, L, H) \tag{3.19}$$

where *S* is public safety, *E* is emergency response, *G* is long term economic impact, *Q* is defense route, *L* is interaction with other lifelines, and *H* is historical significance.

3.4.4 Bridge Network maintenance optimization using stochastic dynamic programming (Frangopol and Liu 2007)

This paper presents a stochastic dynamic programming (DP) procedure for multi objective optimization of bridge networks, using a two-phase DP approach. Phase 1 identifies the best maintenance plans for individual bridges that have minimum life-cycle maintenance costs. It is solved using a specific DP optimization algorithm along with the Monte Carlo simulation. The best maintenance plan is:

$$\text{Minimize: } C_{lm} = \sum_{i=1}^{N} \frac{C_i}{(1+D_r)^{T_i}} \tag{3.20}$$

where C_{lm} is the life-cycle maintenance cost, C_i = cost associated with maintenance action; D_r = discount rate; and T_i = application time of maintenance action *i*.
Phase II allocates the limited annual maintenance budget such that the identified best maintenance plans for individual bridges can be satisfied for as many bridges as possible. The Phase 2 optimization problem for a certain year *k* is:

$$\text{Maximize: } \sum_i \sum_j D_{ij} \times \text{RIF}_i \times P_{ij} \tag{3.21a}$$

$$\text{Subject to } \sum_i \sum_j D_{ij} \times C_j \le C_{\text{budget}} \tag{3.21b}$$

where D_{ij} = binary design variable; RIF_i = reliability importance factor of bridge *i* at year *k* (0 means maintenance action *j* will not be applied to bridge *i*, and 1 means maintenance action *j* is selected to be applied to bridge *i*); P_{ij} = probability that the maintenance action *j* is applied to bridge *i* at year *k*; C_j = cost of maintenance action *j*; and C_{budget} = annual maintenance budget at year *k*.

3.4.5 Minimal link set and minimal cut set formulations (Bensi 2010)

A minimal link set (MLS) is a minimum set of components whose joint survival constitutes survival of the system, while the minimal cut set BN formulation introduces intermediate nodes corresponding to the system MCSs. In Bensi (2010) , the MLS and MCS BN formulations are described.

4 Bayesian Network

4.1 Introduction

A Bayesian Network (BN) is a directed acyclic graph (traditionally abbreviated DAG) consisting of a set of nodes and a set of directed edges (Jensen and Nielsen 2007). The nodes represent variables and the edges represent condition relationships between the variables. The BN originates from the field of artificial intelligence and incorporates graph theory and probability theory. It is a useful tool that helps perform uncertainty analysis in complex systems. For an extensive explanation of BN, see Jensen and Nielsen (2007). Due to their generality, such as incorporation of graph theory and probabilistic inference, accounting for the evolving nature of available information, BNs have been widely used in many areas in the last two decades.

The objective of this chapter is to introduce the basic theory of Bayesian Networks that the next chapter will further explore. The remainder of this chapter is as follows: in Section 2, the basic probability theories, such as conditional probability, conditional independence, and Bayes' theorem, are introduced; the definition of a Bayesian Network is given in Section 3; in Section 4, the junction tree structure is introduced, and the procedures used to construct a junction from the Bayesian Network are explained. Following this, the general inference algorithms on the junction tree are introduced in Section 5. Finally, the propagation scheme for Bayesian networks with conditional Gaussian distributions in Lauritzen and Jensen (2001) is introduced.

4.2 Basics of Probability Theory

4.2.1 Conditional probability and independence

In order to illustrate the usefulness of BNs, let us begin with two important concepts in probability theory, which are conditional probability and independence, as explained in Neapolitan (2003).

Let A and B be events such that $P(B)\neq 0$. Then the conditional probability of A given B, denoted $P(A|B)$, is given by $P(A|B)=P(A\cap B) / P(B)$. $P(A|B)$ means the probability of A happening given that event B has occurred.

Two events A and B are independent if one of the following holds:

(1). $P(A|B) = P(A)$ and $P(A) \neq 0$, $P(B) \neq 0$.

(2). $P(A) = 0$ or $P(B) = 0$.

From the definitions of conditional probability and independence, it is straightforward to prove that A and B are independent if and only if $P(A\cap B) = P(A) P(B)$.

4.2.2 Conditional independence

Having examined the concepts of conditional probability and independence, let us look at a very important concept in BNs, which is conditional independence.

Two events A and B are conditionally independent given C if $P(C) \neq 0$, and one of the following holds:

(1). $P(A| B\cap C) = P(A|C)$ and $P(A|C) \neq 0$, $P(B|C) \neq 0$.

(2). $P(A|C) = 0$, $P(B|C) = 0$.

4.2.3 The law of total probability

Events $E_1, E_2, \ldots, E_n$ are mutually exclusive and exhaustive, such that $E_i\cap E_j=\varnothing$ for $i \neq j$ and $E_1 \cup E_2 \cup ... \cup E_n = \Omega$. For any other event F, we have:

$$P(F) = \sum_{i=1}^{n} P(F \cap E_i) \tag{4.1}$$

If $P(E_i) \neq 0$, then $P(F\cap Ei) = P(F|Ei)\ P(E_i)$. Therefore, Equation (4.1) can be written as:

$$P(F) = \sum_{i=1}^{n} P(F \mid E_i)P(E_i) \tag{4.2}$$

4.2.4 Bayes' Theorem

Given two events E and F such that $P(E) \neq 0$ and $P(F) \neq 0$, we have

$$P(E \mid F) = \frac{P(F \mid E)P(E)}{P(F)} \tag{4.3}$$

For exclusive and exhaustive events E_1, E_2, …, E_n such that $P(E_i) \neq 0$ for all i, we have

$$P(E_i \mid F) = \frac{P(F \mid E_i)P(E_i)}{P(F \mid E_1)P(E_1) + P(F \mid E_2)P(E_2) + ... + P(F \mid E_n)P(E_n)} \tag{4.4}$$

Bayes' theorem is used to compute conditional probabilities of events of interest from known probabilities. Equation (4.3) can be used to compute $P(E|F)$ if we know $P(F|E)$, $P(E)$, and $P(F)$, while Equation (4.4) can be used to compute $P(E_i|F)$ if we know $P(F|E_j)$ and $P(E_j)$ for $1 \leq j \leq n$. Computing a conditional probability using Bayes' theorem is also called Bayesian inference. The following is a classic example from Neapolitan (2003) to illustrate Bayes' theorem.

Tom has a routine X-ray chest test in the hospital, and the result is positive for lung cancer. Tom is then convinced that he has lung cancer. But when his doctor tells him that the test is not invariably accurate, Tom decides to investigate the accuracy of the test. The following conditional probabilities give the accuracy of the test:

$$P(Test = positive \mid LungCancer = present) = 0.6 \tag{4.5a}$$

$$P(Test = positive \mid LungCancer = absent) = 0.02 \tag{4.5b}$$

From Equation (4.5), Tom feels a little bit better, but he still does not know the exact probability that he has lung cancer. The probability that Tom needs to know is $P(LungCancer = present|Test = positive)$. In this case, Tom realizes that Bayes' theorem can be used to get it.

$$P(LungCancer = present \mid Test = positive)$$

$$= \frac{P(Test = positive \mid LungCancer = present)P(LungCancer = present)}{P(Test = positive)} \tag{4.6}$$

In order to apply Equation (4.6), Tom needs to know $P(LungCancer = present)$, which is the information before the test. At this point, Tom recalls that he was one of a class of employees, and that only 1 out of every 1000 new employees has lung cancer, so he assigns 0.001 to $P(LungCancer = present)$. Then Bayes' theorem is applied as follows:

$$P(LungCancer = present \mid Test = positive)$$

$$= \frac{P(Test = positive \mid LungCancer = present)P(LungCancer = present)}{P(Test = positive)}$$

$$= \frac{P(Test = positive \mid LungCancer = present)P(LungCancer = present)}{P(Test = positive \mid present)P(present) + P(Test = positive \mid absent)P(absent)}$$

$$= \frac{0.6 \times 0.001}{0.6 \times 0.001 + 0.02 \times 0.999} = 0.029 \tag{4.7}$$

By this time, Tom feels much more relaxed, because he knows the probability to has lung cancer is only 0.029. This example demonstrates that Bayes' theorem is sufficient for an inference in two related variables. However, when there are many variables, it will become much more complex. Let's see the following example: a history of smoking has a direct influence both on bronchitis and lung cancer. In turn, bronchitis and lung cancer have a direct influence on fatigue. Also, lung cancer has a direct influence on a chest X-ray test. The states of these random variables are defined in Table 4.1.

The conditional probability for these variables are given as: $P(h1) = 0.2$; $P(b1|h1) = 0.25$, $P(b1|h2) = 0.05$; $P(l1|h1) = 0.003$, $P(l1|h2) = 0.00005$; $P(f1|b1,l1) = 0.75$, $P(f1|b1,l2) = 0.10$, $P(f1|b2,l) = 0.5$, $P(f1|b2,l2) = 0.05$; $P(c1|l1) = 0.6$, $P(c1|l2) = 0.02$. Now we want to compute the conditional probability of an individual having lung cancer given that the individual smokes, is fatigued, and has had a positive chest X-ray. This conditional probability is defined as:

Table 4.1 States of the variables (Neapolitan, R.E. 2003)

Variable	Value	When the variable takes this value
H	h1	There is a history of smoking
	h2	There is no history of smoking
B	b1	Bronchitis is present
	b2	Bronchitis is absent
L	l1	Lung cancer is present
	l2	Lung cancer is absent
F	f1	Fatigue is present
	f2	Fatigue is absent
C	c1	Chest X-ray is positive
	c2	Chest X-ray is negative

$$P(l1 \mid h1,\ f1, c1) = \frac{P(l1, h1,\ f1, c1)}{P(h1,\ f1, c1)}$$

$$= \frac{P(l1, h1,\ f1, c1, b1) + P(l1, h1,\ f1, c1, b2)}{P(l1, h1,\ f1, c1, b1) + P(l1, h1,\ f1, c1, b2) + P(l2, h1,\ f1, c1, b1) + P(l2, h1,\ f1, c1, b2)}$$

$$= \frac{\sum_{b} P(l1, h1,\ f1, c1, b)}{\sum_{b,l} P(h1,\ f1, c1, b, l)} \tag{4.8}$$

where $\sum_{b,l}$ means the sum as b and l go through all possible values. In Equation (4.8), there are an exponential number of terms in the sums. For the denominator, there are 22 terms. If there are 100 variables needing to be taken through all their possible values, there will be 2^{100} terms in the sum. We can see that when the instance is so large, this method is not practical.

The Bayesian network can address this problem when we are doing an inference with a large number of variables.

4.3 Bayesian networks

4.3.1 Definition of Bayesian Networks

Before introducing the definition of Bayesian Network, I need first to introduce some basic graph theory. The following is based on the Neapolitan's and Cowell textbooks (Neapolitan 2003, Cowell 1999), to which the reader is referred for further information.

A graph is defined as a pair (*V*, *E*), where *V* is a finite, nonempty set whose elements are called nodes or vertices, and *E* is a set of ordered pairs of distinct elements of *V*. The elements of *E* are called edges or arcs. If (α, τ) or (τ, α) belongs to *E*, we say that α and τ are joined. If both ordered pairs (α,τ) and (τ, α) belong to *E*, we can say that there is an undirected edge between α and τ. α and τ are called neighbors. If (α,τ) belongs to *E*, but (τ, α) does not, we can say that there is a direct edge between α and τ. α is called a parent of τ, and τ is called a child of α. α is called an ancestor of τ, and τ is called a descendent of α if there is a directed path from α to τ. τ is called a nondescendent of α if τ is not a descendent of α. The set of parents of τ is denoted by pa(τ), and the set of children of τ by ch(τ). The family of τ is denoted by fa(τ), and fa(τ) = { τ } $\cup$ fa(τ). A path from α to τ is a sequence $\alpha = \alpha_0, ..., \alpha_n = \tau$ of distinct nodes such that (α_{i-1}, α_i) belongs to *E* for all *i*=1,...,*n*. if the end points α and τ are identical, this path is a cycle. A graph is said to be connected if there is a path between every pair of vertices in its undirected version. A graph is acyclic if it does not possess any cycles.

If all the edges of a graph are directed, it is a directed graph. A directed graph which is acyclic is called a directed acyclic graph (DAG). The definition of a Bayesian Network is as follows (Jensen and Nielsen 2007):

- There is a set of variables represented by nodes and a set of directed edges between variables.
- Each variable has a finite set of mutually exclusive states.
- The variables together with the directed edges form an acyclic directed graph (DAG).
- To each variable *A* with parents $B_1,\ldots,B_n$, there is attached a conditional probability Table P(A| $B_1,\ldots,B_n$). If A has no parents, then the Table reduces to the unconditional probability Table *P*(*A*).

Fig. 4.1 gives the Bayesian network for the example in Section 4.2.4. The five variables H, B, L, F, and C have the same meaning as in Table 4.1. The conditional probabilities given their parents are shown near every variable.

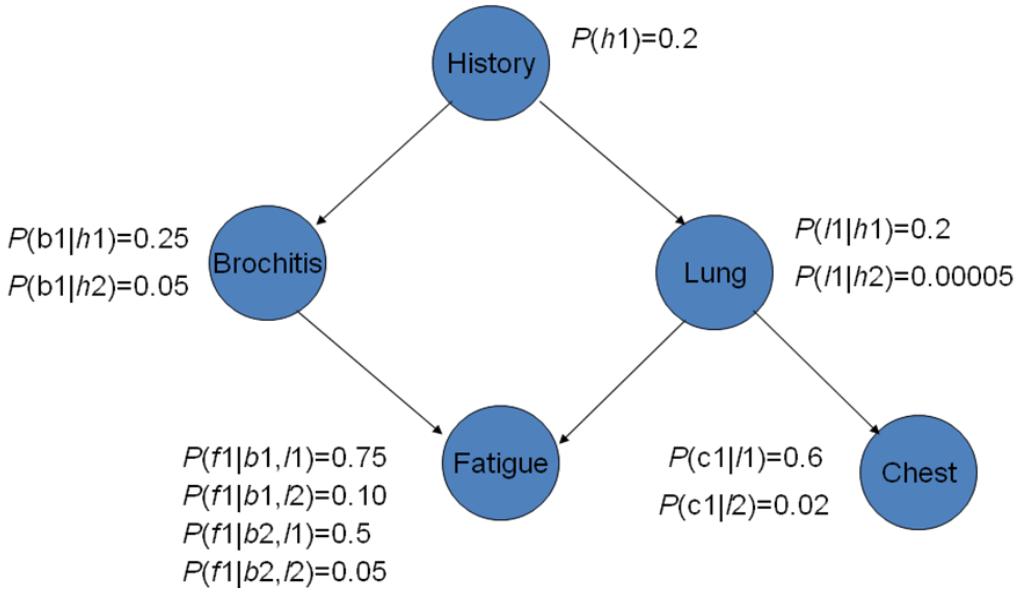

Fig. 4.1 A Bayesian Network for the example in Section 4.2.4

4.3.2 The Chain Rule for Bayesian Networks

Let $U = \{A_1,\ldots, A_n\}$ be a set of variables. From the previous Section, we know that $P(U)$ grows exponentially with the number of variables. Therefore, a compact representation of $P(U)$ is required to store information. In this case, the chain rule is used to address this problem.

Let BN be a Bayesian network over $U = \{A_1,\ldots, A_n\}$. Then BN specifies a unique joint probability distribution $P(U)$ given by the product of all conditional probability Tables specified in BN:

$$P(U) = \prod_{i=1}^{n} P(A_i \mid pa(A_i)) \tag{4.9}$$

where pa(A_i) are the parents of A_i in BN. Using the chain rule, the number of terms in $P(U)$ greatly reduced. For the Bayesian Network in fig 4.1, under the conditional independence assumption, $P(h, b, l, f, c) = P(h)\cdot P(b|h)\cdot P(l|h)\cdot P(f| b, l)\cdot P(c| l)$.

From the discussion above, we can see that the Bayesian Network has the advantage of representing the dependence relationship between variables. It incorporates graph theory and probability theory; it is a useful tool that helps perform uncertainty analysis. However, in order to facilitate the use of efficient computational algorithms, we need to do some graph manipulations on the Bayesian Network. In the next Section, we will introduce the junction tree structures which can be created from the BN and on which the computation can be manipulated.

4.4 Junction trees

Tree structures are an important class of graphs. A graph is said to be a tree if it is connected and if its undirected version has no cycles. (Cowell 1999). A tree is said to be a junction tree if it fulfills the running-intersection property. If H_i is the node set of the tree, then the running-intersection property means that the elements of the intersection set of H_1 and H_k must be included in all the cliques H_2, H_3 , …, H_{k-1} that occur between H_1 and H_k. For the definition of cliques, see section 4.4.2. For example, Fig. 4.2 is the junction tree for the Bayesian Network in Fig. 4.2. It has three node sets: *BHL*, *BFL*, and *CFL*. We call the node sets cliques of the junction tree. These cliques satisfy the running-intersection property because the intersection of cliques *BHL* and *CFL* is *L*, which is included in *BHL*, *BFL*, AND *CFL*. We call the intersection *BL* the separator between clique *BHL* and *BFL*. The cliques are generally represented by ellipses, and separators are denoted by rectangles.

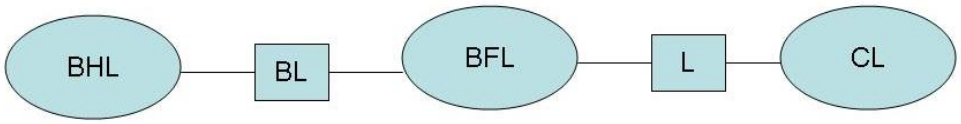

Fig. 4.2 Junction tree structure for the Bayesian Network in Fig 4.1

The junction tree is also called a Markov tree, a hypertree (Shenoy and Shafter 1990), or simply a clique tree. The junction tree structure is a compact and precise way of showing the relations between the variables. It facilitates the efficient computational algorithms, so that the inference can be performed easily and efficiently. The next Section will show how to construct a junction from a Bayesian Network.

4.4.1 Moralization

A junction tree is constructed based on the algorithm originally developed by Lauritzen and Spiegelhalter (1988). In order to convert a Bayesian Network into a junction tree, the first step is moralization, which includes two parts: adding an edge between each pair of parents which have the same children, and deleting the directions on all arcs.

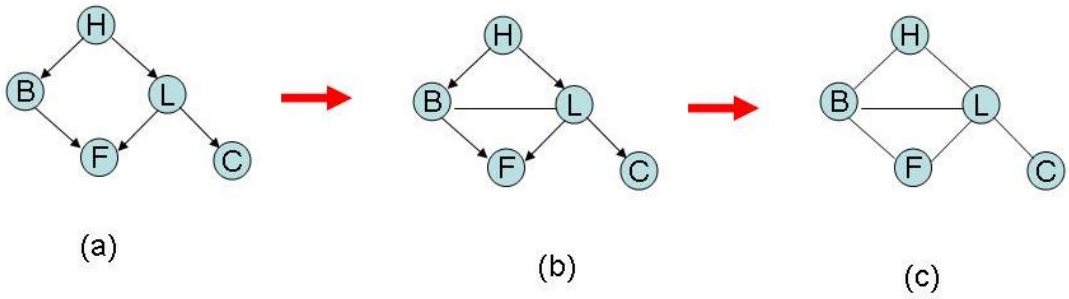

Fig. 4.3 Moralization procedures for the Bayesian Network in Fig 4.1

Fig. 4.3 shows the moralization procedures for the Bayesian Network in Fig 4.1. In Fig. 4.3a, nodes B and L have the same child F, so an edge between B and L is added in Fig. 4.3b. Finally, the directions on all edges are deleted in Fig. 4.3c.

4.4.2 Triangulation

Triangulation is the process used to identify all the cliques of the previous moralized graph. The cliques are identified by successive elimination of the variables. A variable is eliminated if all of its neighbors are mutually connected. The eliminated variable and all of its connections form a clique. If there is no such variable all of whose neighbors are connected, fill-in edges are added to create a fully connected clique, and then one of the variables in the clique is eliminated. When all the variables are identified, all cliques are identified. If a clique is a subset of an existing clique, it should be deleted.

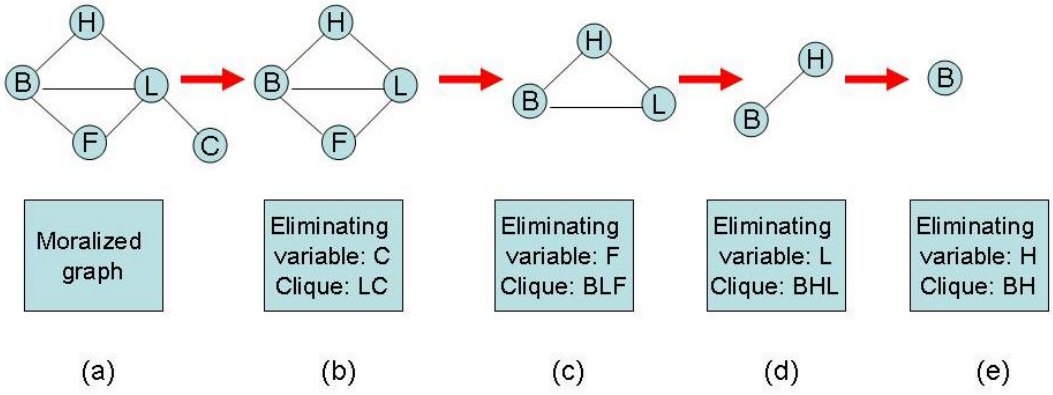

Fig. 4.4 Triangulation procedures for the Bayesian Network in Fig 4.3

Fig. 4.4 shows the elimination process for the moralized graph in Fig. 4.3. In Fig. 4.4, five variables are eliminated by the sequence of *C*, *F*, *L*, *H*, and *B*. Accordingly five cliques are generated, which are *LC*, *BCF*, *BHL*, *BH*, *B*. Since cliques *BH* and *B*

are the subset of clique BHL, they should be deleted. There are three cliques for the junction tree: *LC*, *BCF*, and *BHL*. Finally the three cliques are connected to form the junction tree based on the running-intersection property as in Fig. 4.2.

It should be noted that the elimination order is the key step in the construction of the junction tree because it determines the size of the cliques and the efficiency of the computations. If there are *N* variables in a graph, then there are *N*! possible elimination sequences. So it is not a trivial task to identify the best sequence. In fact it is *NP*-hard to find the best triangulation for an undirected graph (Yannakakis, M. 1981). For an introduction to the concept of NP (nondeterministic polynomial time) problem, the reader is referred to Sanjoy et.al (2008).

After constructing the junction tree, the inference algorithm can be applied to it. There are three architectures used in the inference: the Shafer-Shenoy architecture, the Lauritzen-Spiegelhalter architecture, and the Hugin architecture. The main differences between these architectures are the forms of messages passed, and the scheduling of messages (Lauritzen and Jensen, 1997).

4.5 Bayesian networks with conditional Gaussian distributions

The previous Section introduced the general procedures for generating a Bayesian Network, converting a Bayesian Network into a junction tree, and doing the inference on the junction tree. Since most inference algorithms can only be implemented on a discrete Bayesian Network, in this Section I will introduce the computation scheme on the Bayesian network with conditional Gaussian distributions. In chapter 5, we will generate the seismic vulnerability framework based on this kind of Bayesian Network. This local computation is based on the propagation scheme in Lauritzen & Jensen (2001), and includes the following procedures: the construction of a junction tree with a strong root, assigning potentials to cliques, sending messages towards the root in the junction tree, and then distributing a message away from the root.

4.5.1 Conditional Gaussian potentials

The basic computational object in the propagation scheme is Conditional Gaussian (CG) potential. A CG potential is represented as $\phi = [p, A, B, C]\ (H \mid T)$, where $(H \mid T)$ denotes the continuous variables in the potential with the head *H* and the tail *T*, *A*, *B*, *C* are matrix, and *p* is a vector. We assume the head *H* and the tail *T* are *r* and *s*

dimensional. An arbitrary configuration of the discrete variables is denoted by *i*. Then $p = \{p(i)\}$ is a table of nonnegative numbers: if there is no discrete variable in the potential, then $p = 1$; $A=\{A(i)\}$ is a table of $r\times 1$ vectors; $B=\{B(i)\}$ is a table of $r\times s$ vectors; $C=\{C(i)\}$ is a table of $r\times r$ symmetric matrices. Some of the parts may be absent for some potentials. The potential $[p, A, B, C]$ $(H \mid T)$ specifies the CG relationship as follows:

$$P(I = i) \propto p(i) \tag{4.10}$$

$$L(H \mid I = i, \mathrm{Z} = \mathrm{z}) = N(A(i) + B(i)z, C(i)) \tag{4.11}$$

In Equation (4.11), $N(A(i)+B(i)t, C(i))$ means normal distribution with mean value $A(i)+B(i)z$ and variation $C(i)$.

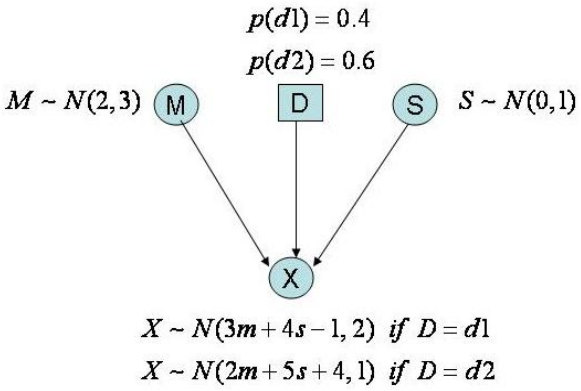

Fig. 4.5 A conditional Gaussian BN

Fig. 4.5 is a conditional Gaussian BN. *D* is a discrete variable with two states *d*1 and *d*2. *M*, *S*, *X* are continuous variables. The head variable is *X*, and the tail variables are *M* and *S*. The conditional relationships between them are:

$$L(X \mid D = d1, M = m, S = s) = N(-1+[3,4]\cdot[m; s], 2) \tag{4.12a}$$

$$L(X \mid D = d2, M = m, S = s) = N(4+[2,5]\cdot[m; s], 1) \tag{4.12b}$$

In Equation (4.12), $A(d1) = -1$, $B(d1) = [3, 4]$, $C(d1) = 2$; $A(d2) = 4$, $B(d2) = [2, 5]$, $C(d2) = 1$. So the potentials for this BN are [0.4, -1, {3, 4}, 2] $(X \mid M, S)$ and [0.6, 4, {2, 5}, 1] $(X \mid M, S)$.

4.5.2 Marginals

Marginals over continuous variables can only be calculated over head variables. If [*p*, *A*, *B*, *C*] (*H*| *T*) is decomposed as $H = (H_1, H_2)$, $A = (A_1; A_2)$, $B = (B_1; B_2)$, $C = (C_{11}, C_{12}; C_{21}, C_{22})$ corresponding to a partitioning of the head variables as $H = (H_1, H_2)$, the marginal of ϕ to H_1 is given as

$$\varphi^{\downarrow H_1} = [p, A_1, B_1, C_{11}](H_1 \mid T) \tag{4.13}$$

By the same method, the marginal of ϕ to H_2 is

$$\varphi^{\downarrow H_2} = [p, A_2, B_2, C_{22}](H_2 \mid T) \tag{4.14}$$

4.5.3 Direct combination

The direct combination of two potentials [*p*, *A*, *B*, *C*] ($H_1 \mid T_1$) and [*q*, *E*, *F*, *G*] ($H_2 \mid T_2$) is defined only if they satisfy

$$H_2 \cap (H_1 \cup T_1) = \varnothing \tag{4.15}$$

If Equation (4.15) is fulfilled, let *F* be partitioned into [F_1: F_2] corresponding to (H_1, T_1). We then define the direct combination as follows:

$$[\rho, U, V, W](H \mid T) = [p, A, B, C](H_1 \mid T_1) \otimes [q, E, F, G](H_2 \mid T_2) \tag{4.16a}$$

where $H = H_1 \cup H_2$, $T = (T_1 \cup T_2) \setminus H$, $D = D_1 \cup D_2$, and

$$\rho = pq \tag{4.16b}$$

$$U = \begin{pmatrix} A \\ E + F_1 A \end{pmatrix} \tag{4.16c}$$

$$V = \begin{pmatrix} B \\ F_2 + F_1 B \end{pmatrix} \tag{4.16d}$$

$$W = \begin{pmatrix} C & CF_1^T \\ F_1C & G + F_1CF_1^T \end{pmatrix} \tag{4.16e}$$

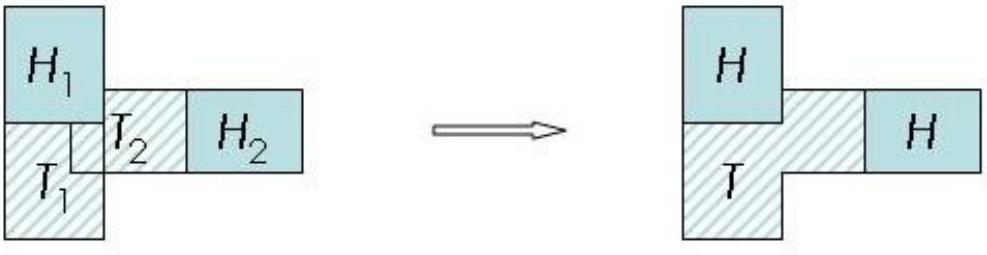

Fig. 4.6 Graphical representation of the direct combination of two potentials

If Equation (4.15) is not fulfilled, we need first to do a complement operation to the potentials. The following will introduce the complement operation.

4.5.4 Complements

If the head of a CG potential $\phi = [p, A, B, C]\ (H \mid T)$ is partitioned as

$$H = (H_1, H_2) \tag{4.17a}$$

$$A = \begin{pmatrix} A_1 \\ A_2 \end{pmatrix} \tag{4.17b}$$

$$B = \begin{pmatrix} B_1 \\ B_2 \end{pmatrix} \tag{4.17c}$$

$$C = \begin{pmatrix} C_{11} & C_{12} \\ C_{13} & C_{22} \end{pmatrix} \tag{4.17d}$$

Next, it can be decomposed into its marginal and its complement as:

$$\varphi = \varphi^{\downarrow(H_1 \cup T)} \dot{\otimes} \varphi^{|(H_1 \cup T)} \tag{4.18}$$

Where $\phi^{\downarrow(H1 \cup T)} = [m, A_1, B_1, C_{11}]\ (H_1 \mid T)$, $\phi^{|(H1 \cup T)} = [q, E, F, G]\ (H_2 \mid H_1 \cup T)$ and

$$p = mq \tag{4.19a}$$

$$E = A_2 - C_{21}C_{11}^{-}A_1 \tag{4.19b}$$

$$F = [C_{21}C_{11}^{-} : B_2 - C_{21}C_{11}^{-}B_1] \tag{4.19c}$$

$$G = C_{22} - C_{21}C_{11}^{-}C_{12} \tag{4.19d}$$

By the same method, potential ϕ can also be decomposed as:

$$\varphi = \varphi^{\downarrow(H_2 \cup T)} \dot{\otimes} \varphi^{|(H_2 \cup T)} \tag{4.20}$$

Where $\phi^{\downarrow(H2 \cup T)} = [m, A_2, B_2, C_{22}]$ $(H_2 \mid T)$, $\phi^{|(H2 \cup T)} = [q, E, F, G]$ $(H_1 \mid H_2 \cup T)$ and

$$p = mq \tag{4.21a}$$

$$E = A_1 - C_{12}C_{22}^{-}A_2 \tag{4.21b}$$

$$F = [C_{12}C_{22}^{-} : B_1 - C_{12}C_{22}^{-}B_2] \tag{4.21c}$$

$$G = C_{11} - C_{21}C_{22}^{-}C_{12} \tag{4.21d}$$

4.5.5 General combination

Consider two potentials $\phi = [p, A, B, C]$ $(H_1 \mid T_1)$ and $\psi = [q, E, F, G]$ $(H_2 \mid T_2)$. If the heads of the potentials are disjoint $(H_1 \cap H_2 = \varnothing)$, then we define the general combination as:

$$\varphi \otimes \psi = \varphi \dot{\otimes} \psi \quad \text{or} \quad \varphi \otimes \psi = \psi \dot{\otimes} \varphi \tag{4.22}$$

If neither of the direct combinations is defined, we must have

$$H_1 \cap D_2 \neq \varnothing \quad \text{and} \quad H_2 \cap D_1 \neq \varnothing \tag{4.23}$$

Let $D_{12} = H_1 \setminus D_2$ and $D_{21} = H_2 \setminus D_1$. If both D_{12} and D_{21} are empty, the combination will not be defined. Assuming $D_{12} = \varnothing$, as

$$\varphi = \varphi^{|(D_1 \setminus D_{12})} \dot{\otimes} \varphi^{\downarrow(D_1 \setminus D_{12})} = \varphi' \dot{\otimes} \varphi'' \tag{4.24}$$

and try to combine ϕ and ψ as

$$\varphi \otimes \psi = \varphi' \dot{\otimes} (\varphi'' \otimes \psi) \tag{4.25}$$

Equation (4.25) is repeated for the product $\phi'' \otimes \psi$.

4.5.6 Assignment of potentials to cliques

Every CG potential specifies the conditional distribution of a node given its parents, and it is assigned to an arbitrary clique of the junction tree that contains all of its variables. The potentials in a given clique are combined based on the operation of the general combination defined above.

Fig. 4.8 is the junction tree of the BN in Fig. 4.7. Based on the method in section 4.4.2, 6 cliques are identified in this junction tree. The variables in these 6 cliques are: C, S_1, E_{C1}, and P_a in ϕ_1; C, S_1 and S_2 in ϕ_2; C, S_2; E_{C2}, and P_b in ϕ_3; M, S_1 and S_2 in ϕ_4; M, S_1 and E_{S1} in ϕ_5; M, S_2 and E_{S2} in ϕ_6.

Since every variable is head of exactly one potential, and also there are ten variables in the BN, then there are ten CG potentials in this BN. These 10 potentials are assigned to the six cliques as in Fig. 4.8. The red variables in every clique mean that the potential with that red variable as the head variable is assigned to that clique. For example, the potential (P_a | S_1, C, E_{C1}), which has the head variable P_a is assigned to clique 1. Then, the potentials in each clique are combined based on the operations defined in Section 4.5.5. After the combinations, the new potentials in the 6 cliques are obtained.

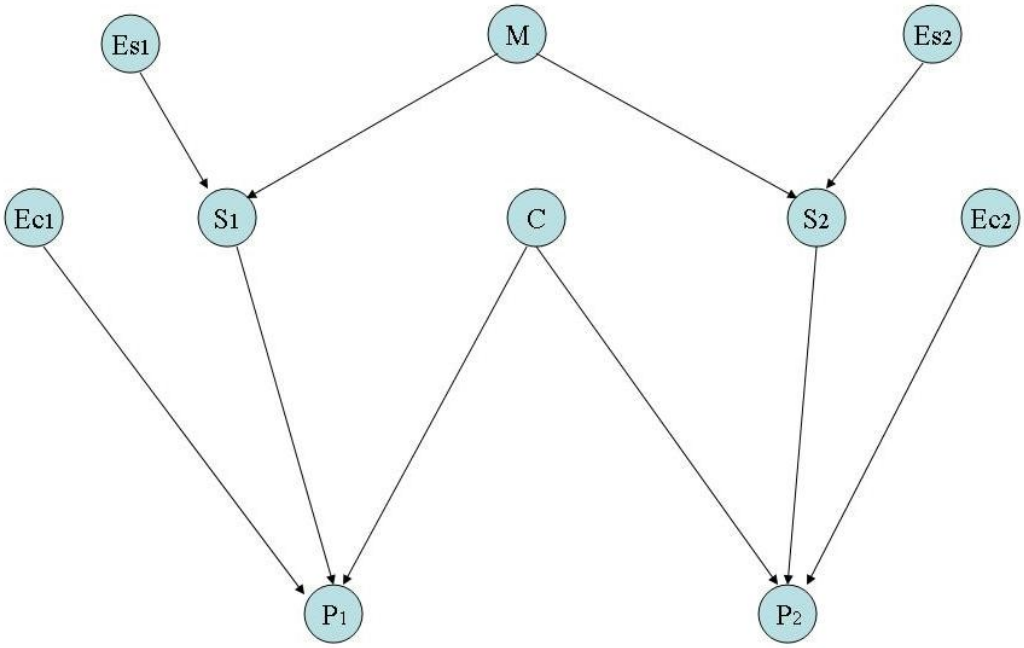

Fig. 4.7 Example of Bayesian Network

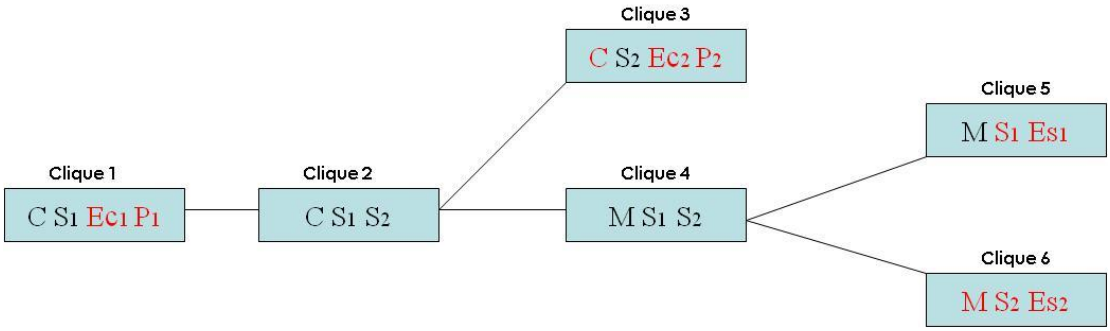

Fig. 4.8 Assignments of the potentials to the cliques

4.5.7 Collecting message

After assignment of potentials to the cliques, the next step in the propagation scheme is to send messages towards the root which can be selected randomly. A clique is allowed to send a message only if it is a leaf of the junction tree or if it has received messages from all of its neighbors further away from the root. The leaves in a junction tree are cliques which have only one neighbor clique. In Fig. 4.11, there are four leaf cliques: clique 1, clique 3, clique 5, and clique 6. Fig. 4.12 is the order of collecting messages in the junction tree.

When a message is sent from a clique C to its neighbor D towards the root with separator $S = C \cap D$, the potentials ϕ_C and ϕ_D are modified to become ϕ^*_C and ϕ^*_D, where

$$\varphi_C^* = \varphi_C^{|S}, \quad \varphi_D^* = \varphi_D \otimes \varphi_C^{\downarrow S} \tag{4.26}$$

i.e. ϕ^*_C is the complement of ϕ_C after marginalization to the separator S and ϕ^*_D is the combination of ϕ_C and the marginal of ϕ_C. After the root clique has received messages from all its neighbors, the collection of messages stops.

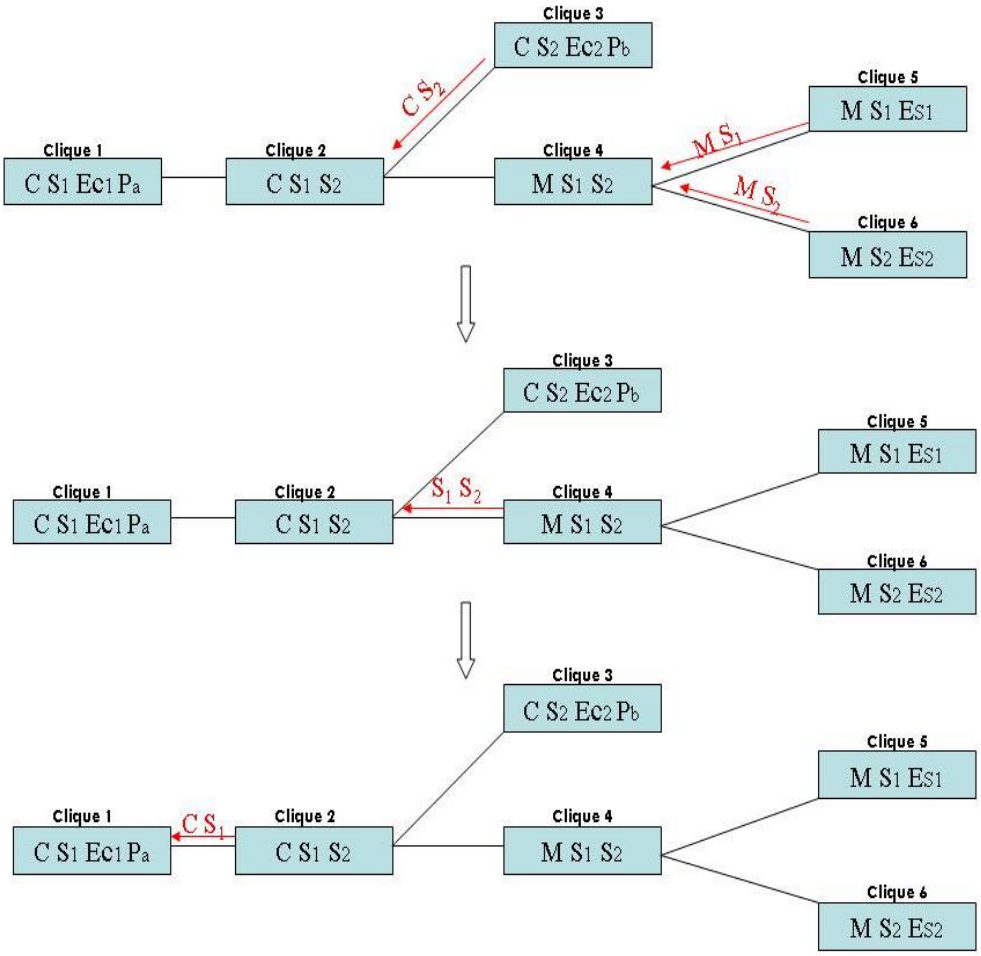

Fig. 4.9 The order of collecting messages

4.5.8 Distributing messages from the root

The next step in the calculation of marginals is sending messages away from the root. First the root clique sends messages to all its neighbors, and a clique is allowed to send a message as soon as it has received a message from its neighbors closer to the root. Fig. 4.10 gives the order of distributing messages in the junction tree.

When a clique *C* is sending a message to its neighbor *D* further away from the root with separator $S = C \cap D$, cliques *C* and *D* will stay the same, only the separator S becomes $\phi_S = (\phi_C)^{\downarrow S}$. And then when *D* is sending a message to its

neighbor E further away from the root with separator $T = D \cap E$, cliques D and E will stay the same, and the separator T will change as follows:

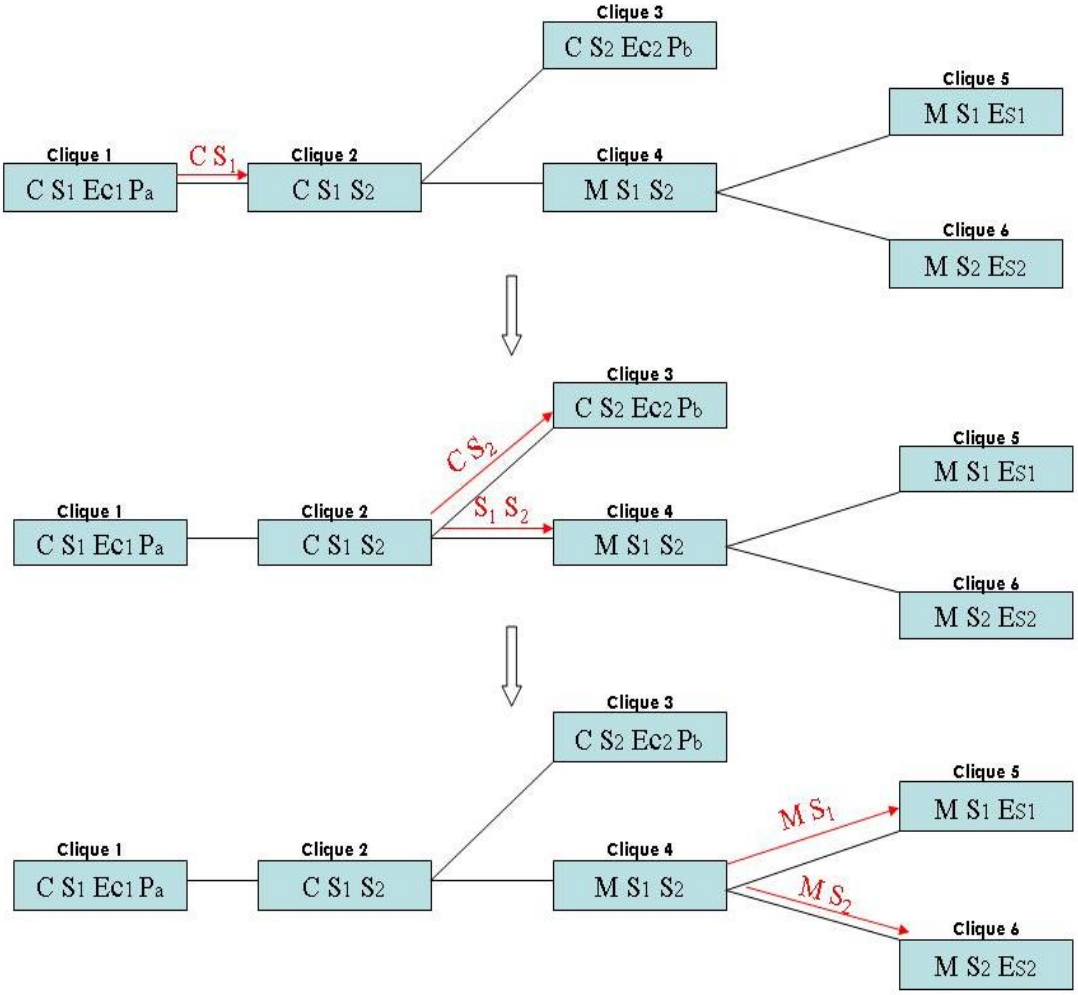

Fig. 4.10 Order of distributing messages

$$\varphi_T = (\varphi_S \dot{\otimes} \varphi_D)^{\downarrow T} \tag{4.27}$$

For example, in Fig. 4.10, when clique 1 sends a message to clique 2, the separator S between them becomes $\phi_S = (\phi_1)^{\downarrow S} = (\phi_1)^{\downarrow C, S1}$, and then when clique 2 sends a message to clique 3, the separator T between clique 2 and clique 3 becomes $\phi_T = (\phi_S \otimes \phi_2)^{\downarrow T} = (\phi_S \otimes \phi_2)^{\downarrow C, S2}$. After distributing messages, all the cliques stay the same, only the separators change.

4.5.9 Entering evidence

After distributing messages, the last step in the computation process is entering the evidence. Assuming we have an evidence for continuous variable $Y_2 = y_2$, it must be entered in all cliques where Y_2 appears. The procedures are as follows:

1. If Y_2 is in the tail, the clique changes as follows: first, Y_2 is removed from the tail; p and C stay the same; B is changed by removing the column B_2 corresponding to Y_2; and A is modified to become A+ $B_2 y_2$.
2. If Y_2 is in the head, the clique changes as follows: the head nodes are partitioned into $Y= (Y_1, Y_2)$, and the new potential changes to $[A^*, B^*, C^*]$ $(H^* \mid T^*)$; the head H^* is obtained from H by removing Y_2; the tail T^* and the B^* are empty; and $A^* = A_1 + C_{12} (y_2 - A_2)/C_{22}$, $C^* = C_{11} - C_{12}C_{21}/C_{22}$.

In this Thesis, we need to update the probability of bridge B after knowing the condition of bridge A. In the next chapter, we will generate a series of random numbers which all independently follow the posterior distribution of P_a after observing that bridge A has an operational problem. Every time we enter one evidence value into P_a, we obtain an updated distribution of P_b based on the computation scheme. For these updated distributions of P_b, we can use the mean value of the distribution as the representation value, and choose the mean value of these representation values as the final updated mean value of P_b. For the variation, we can use the mean value of the sum of all variations as the final variation. By the same method, the updated distribution of all other variables can be obtained.

4.6 Software packages for Bayesian networks

In this Section, I introduce several existing software packages for handling and calculating BNs: my search is mostly based on the information found in (Mahjoub and Kalti 2001).

Table 4.2 is a summary of these packages, and below I describe their features using as an example the decision problem shown in Fig. 4.11, which is a graph for a discrete BN. There are five variables in this BN: 'Cold' means the weather is cold, 'Tired' means Tom is tired, 'Sick' means Tom is sick, 'Home' means Tom is at home, and 'Hospital' means Tom is at the hospital. The prior and conditional probabilities of these variables are given in Fig. 4.11. Below, the example is called the 'Sick Dilemma'.

Table 4.2 List of all the software package for BNs

Tool name	Type	Source	License	Web site	Variables
BNT	Library	Matlab/ c	Free	http://code.google .com/p/bnt/	Continuous /Discrete
Hugin	Software	No	Pay/ limited	www.hugin.com	Continuous /Discrete
BayesianLab	Library	No	Pay/ limited	www.bayesia.com	Continuous /Discrete
Netica	Software	No	Pay/ limited	www.norsys.com	Continuous /Discrete
MSBNX	Software	No	Free	http://research.microsoft.com/en-us/um/redmond/groups/adapt/msbnx/	Discrete
BNet.Builder	Software	No	Pay/ limited	www.cra.com	Continuous /Discrete
SMILE	Software	C++	Free	http://genie.sis.pitt.edu/	Continuous /Discrete

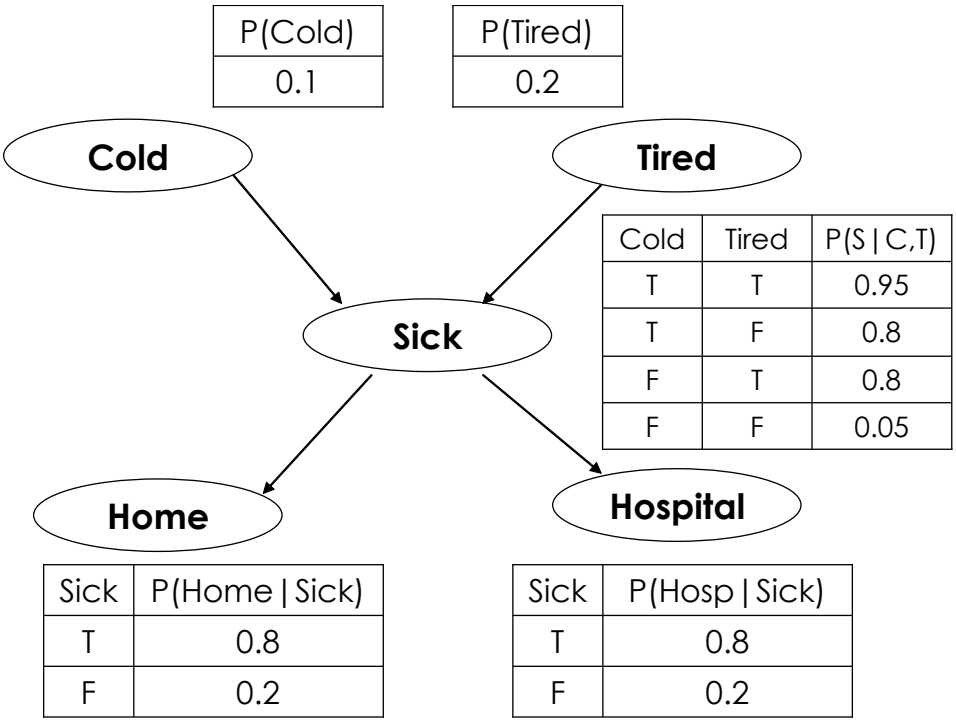

Fig. 4. 11 Example of graph structure

4.6.2 Bayesian Network Toolbox (BNT)

The Bayesian Network Toolbox (BNT) is a toolbox that runs under Matlab software (http://www.mathworks.com 2011). It was developed by Murphy (2001). The following gives the procedures for using BNT, which are taken from the web site (http://code.google.com/p/bnt/).

In BNT, an adjacency matrix is used to specify the graph structure. For example, the problem introduced in the last Section can be formalized in a directed acyclic graph as follows:

```
N = 5;
dag = zeros(N,N);
Cold = 1; Tired =2; Sick = 3; Home = 4; Hospital = 5;
dag(Cold,Sick) = 1;
dag(Tired,Sick) = 1;
dag(Sick,[Home, Hospital]) = 1;
```

The nodes are numbered as follows: Cold = 1, Tired = 2, Sick = 3, Home = 4, Hospital=5. The nodes must always be numbered in topological order, which means the parents must be before the children.

In addition to specifying the graph structure, the user must create the Bayes net shell, by specifying the size and type of each node. If a node is discrete, its size is the number of possible values each node can take on; if a node is continuous, it can be a vector, and its size is the length of this vector. If we assume all nodes are discrete and binary, then we have:

```
discrete_nodes = 1:N;
node_sizes = 2*ones(1,N);

bnet = mk_bnet(dag, node_sizes, 'discrete', discrete_nodes);
By default, all nodes are assumed to be discrete.
```

Although BNT is an open-source library and is used by many researchers, it is still difficult for non-specialists to use because it requires some knowledge of Matlab and BNT.

4.6.2 Hugin

Hugin (www.hugin.com) is a commercial product similar to BNT. It has existed since 1989 and is one of the greatest tools for advanced decision support based on complex statistical models such as Bayesian Networks. It has been used in decision

support, medical diagnostics, troubleshooting, risk analysis and safety assessment. The algorithm was developed by the group behind HUGIN EXPERT, and was published by Steffen L. Lauritzen of Aalborg and David Spiegelhalter of Cambridge in the *Journal of the Royal Statistical Association* in 1988. HUGIN EXPERT is based in Aalborg, Denmark, strategically located in the heart of the world's largest BN-community. It maintains close links with the University of Aalborg.

The supported inference algorithm of Hugin is the junction tree. The junction tree can be seen in the software for a given Bayesian Network. The learning parameters in Hugin are based on the EM algorithm. The saving formats of Hugin are 'OOBN' , 'HKB' and 'NET'. In Hugin, the users can create the network by selecting the nodes and the links. Fig. 4.12 is the example used in Fig. 4.11, and is created in Hugin simply by 5 discrete nodes and 4 links. Fig. 4.13 is the prior distributions for all the nodes after initialization.

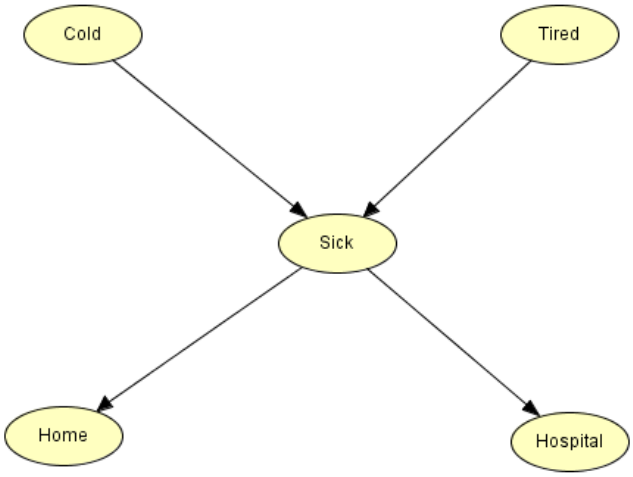

Fig. 4.12 Graphical representation of the 'Sick Dilemma' example in Hugin

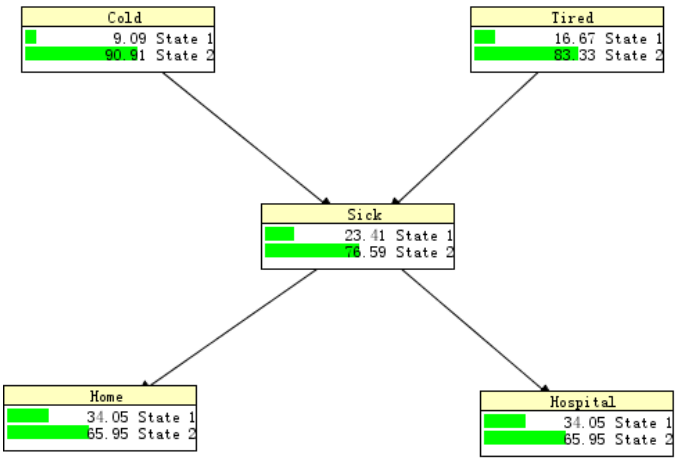

Fig. 4.13 Prior distribution of the 'Sick Dilemma' example after initialization in Hugin

4.6.3 BayesiaLab

BayesiaLab is a tool for graphical manipulation of Bayesian networks. It allows defining, modifying, using and learning models based on Bayesian networks. It was developed by the French company Bayesia (http://www.bayesia.com/), which specializes in methods for decision support and learning from artificial intelligence. BayesiaLab can incorporate discrete nodes, continuous nodes, constrained nodes, utility nodes and decision nodes. Fig. 4.14 is the graphical representation of the 'Sick Dilemma' example in BayesiaLab, and Fig. 4.15 is the node editor in BayesiaLab.

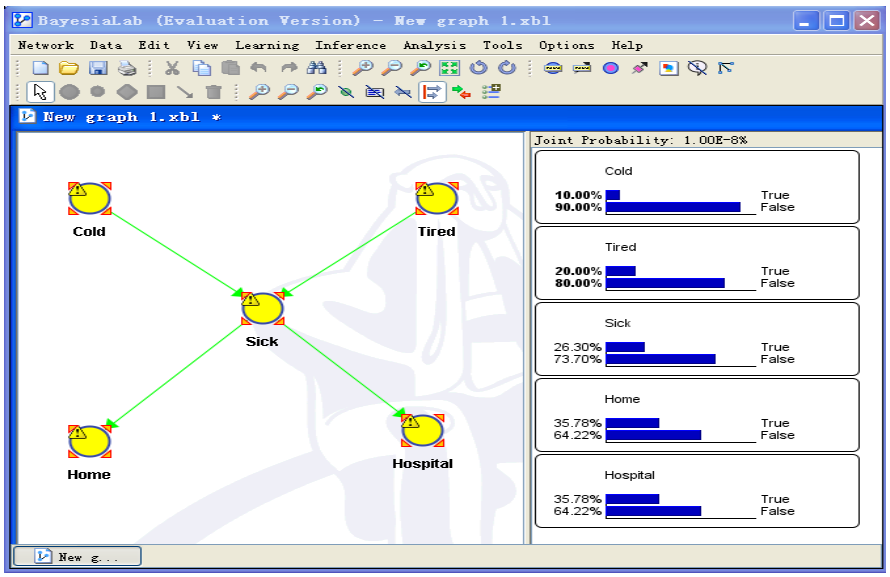

Fig. 4.14 Graphical representation of the 'Sick Dilemma' example in BayesiaLab

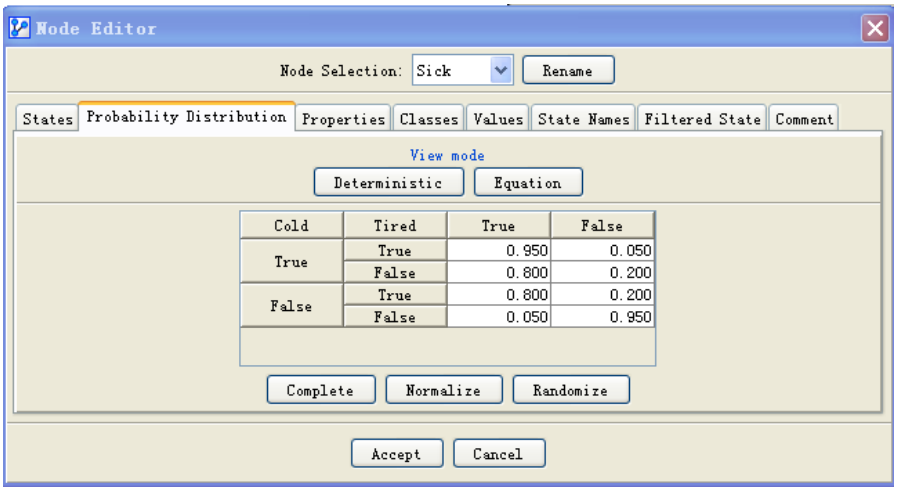

Fig. 4.15 Node editor in BayesiaLab

4.6.4 Netica

Netica (www.norsys.com) is a program for Bayesian Networks. It has an intuitive user interface for drawing the networks, and the relationships between variables may be entered as individual probabilities, in the form of equations, or learned from data files. Netica can use the networks to perform various kinds of inference. Fig. 4.16 is the network of the 'Sick Dilemma' example in Netica.

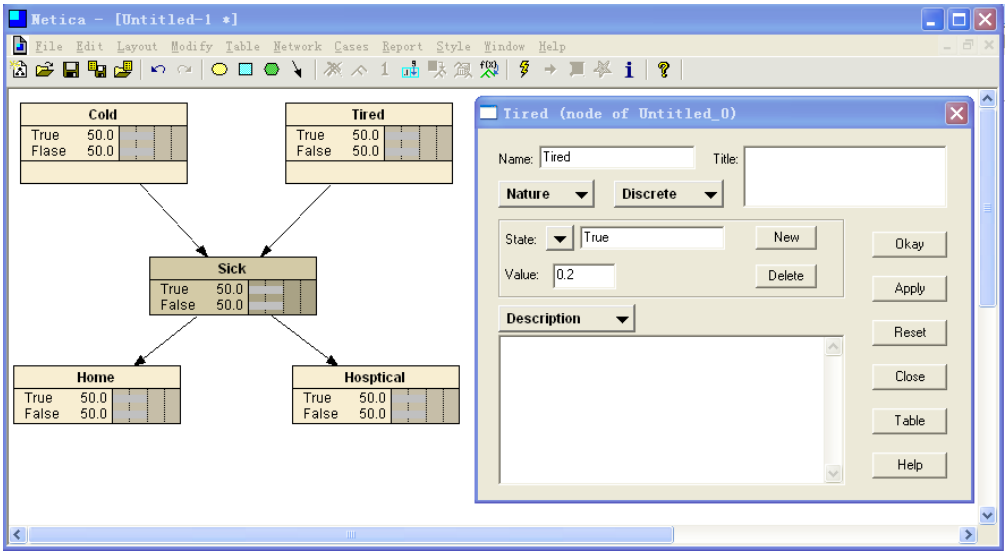

Fig. 4.16 Software window of Netica

4.6.5 MSBNX

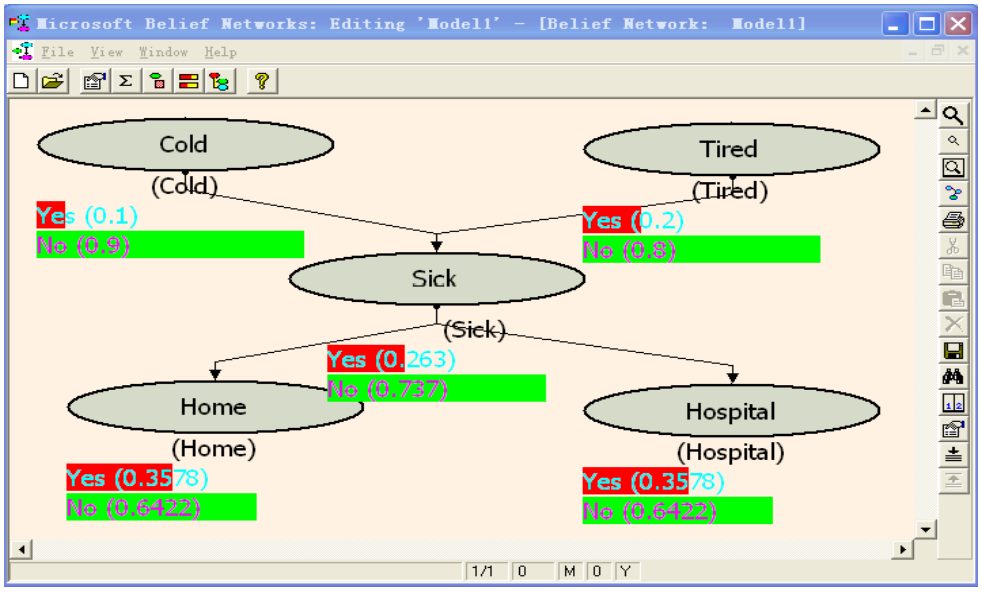

Fig. 4.17 The software window of MSBNX

MSBNX is a Microsoft Windows software application that supports the creation, manipulation and evaluation of Bayesian probability models. Each model is represented as a graph or diagram. The random variables are shown as ellipses, called nodes, and the conditional dependencies are shown as arrows, or directed arcs, between variables. Currently MSBNX only supports discrete distributions for its model variables. Models are saved to and loaded from disk-based text files in an XML-based format. The supported formats of MSVNX are 'XBN', 'DSC' and 'XML'. Fig. 4.17 is the network of the 'Sick Dilemma' example in *MSBNX*.

4.6.6 GeNIe & SMILE

GeNIe is the graphical interface of SMILE, a fully portable Bayesian inference engine developed by the Decision Systems Laboratory and thoroughly tested in the field since 1998. It has the following features (http://genie.sis.pitt.edu/about.html): Graphical editor to create and modify network models; Uses the SMILE Engine; Supports chance nodes with General, Noisy OR/MAX and Noisy AND distribution; Open multiple networks and cut and paste sections of models between them; Complete integration with MS. Excel, cut and paste data into internal spreadsheet view of GeNIe; Support for handling observation costs of nodes; Support for diagnostic case management.

Besides the above tools, there are also some other software packages like BNJ (Bayesian network tools in Java), SAMIAM, JAVABAYES, ANALYTICAOPENBUGS, and so on (Mahjoub and Kalti 2001).

5 Post-earthquake analysis using Bayesian Networks

5.1 Introduction

In Chapter 4, I introduced the related background and basic theory of BNs. Due to their distinguishing characteristics, BNs have been widely used in many areas in the last two decades. However, the general BN algorithm can effectively handle only discrete variables, while most variables in civil engineering are continuous; therefore the application of BNs to civil engineering is still at a preliminary stage.

5.1.1 BNs in civil engineering

Friis-Hansen (2000) provided one of the first publications that applied BNs to risk-related engineering issues: by solving decision problems in marine engineering, the potential of BNs in risk analysis was investigated, and their advantages such as flexibility and compatibility were demonstrated. Five different examples that ranged from inspection and maintenance planning with regard to general risk analysis aspects to the tasks of monitoring and diagnosis are used illustrate the potential of BNs in the marine industry. Moreover, traditional structural reliability methods such as the First Order Reliability Method (FORM), Second Order Reliability Method (SORM), fault tree analysis and neural networks are used to compare or combine with BNs. This research will contribute to transferring the results of the artificial intelligence community to traditional engineering fields.

Straub carried out a good deal of research work in the application of Bayesian Networks to the area of civil engineering, especially with regard to risk analysis. In Straub and Grêt-Regamey (2006), an integral probabilistic framework based on Bayesian Networks is presented for avalanche modeling. This framework can explicitly represent the different parameter uncertainties, and update the probability distribution of these uncertainties from observations of avalanches through Bayesian

inference. In Straub (2005), a general framework for natural hazard risk assessment based on Bayesian Networks is presented and applied to the assessment of rock-fall hazard risk based on indicators. This Bayesian Network model is compared with the traditional rating system, and offers the advantages of flexibility, consistency and traceability. In addition, he developed the computational framework called enhanced Bayesian network (eBN) which explored the possibility of combining Structural Reliability Methods (SRM) and Bayesian Networks for the reliability and risk analysis of engineering structures and infrastructure (Straub and Der Kiureghian 2010a; Straub and Der Kiureghian, 2010b). Enhanced Bayesian networks are a subclass of BNs that have both discrete and continuous nodes, with arbitrary distributions and interdependencies. The node elimination algorithm is used to reduce an eBN to a reduced BN (rBN) with discrete nodes only, for which exact inference can be used. In this framework, the discretization method is used on continuous random variables to reduce the complexity of the rBN. This method incorporates the advantages of both SRMs and BNs and has many potential applications in decision support for emergency response. However, it involves many complex operations when converting an eBN to rBN, which can only be performed by professionals who are familiar with BNs.

5.1.2 BNs in seismic risk analysis

Bayraktarli et al. (2005, 2006) proposed a general framework for earthquake risk management based on Bayesian Probabilistic Networks. The framework consists of three parts: firstly, the exposure model that considers the seismic hazard potential for the city or region. For example, the earthquake ground motion intensities and corresponding return periods. Secondly, the vulnerability part that is related to structural damage given the exposure event such as the spectral displacement and the state of damage. Thirdly, the robustness that is associated with the indirect consequences conditional on the exposure and a given state of damage. The framework is applied to a large part of a city for two different situations, namely before and after an earthquake. In the example, three decision actions are considered: retrofitting, rebuilding and no action. The best action is calculated both before and after the earthquake. The software package Hugin (http://www.hugin.com/) is used to construct the framework. In addition, the Geographical Information Systems (GIS) is integrated with the Bayesian Networks. All the available data are organized in a GIS platform.

Since Bayraktarli et al. (2005, 2006) aim to provide and develop a generic risk assessment framework, it does not give many details about modeling the seismic demand using a Bayesian Network. The nodes in the framework are all discrete, which will increase the computational burden when the network has a large number of variables and each variable has many states. However, they presented an

innovative framework for seismic risk assessment using a Bayesian Network.

The research team in UC Berkeley have made many contributions to the application of BNs to seismic risk analysis. Straub et al. (2008) and Bensi et al. (2009) modeled the seismic demands of an infrastructure system by constructing a BN model of ground motion intensity. In that BN model, the seismic intensities (S_i), normally characterized as peak ground accelerations (PGA) at different sites across a spatially distributed infrastructure system following an earthquake, are expressed as a function of the magnitude (M), site-to-source distance (R_i), and other characteristics of the source and site (X_i), such as the type of faulting mechanism and the site shear-wave velocity. The source-to-site distance is a function of the earthquake location and magnitude. Given the distribution of ground motion intensity at the site, the performance of infrastructure system components is modeled using fragility functions which provide the probability of exceeding some specific damage state. Then the system performance is modeled based on the performance of its components. Figure 5.1 gives the conceptual framework, taken from Bensi et al. (2009).

Bensi et. al (2011) is the first research that thoroughly investigates the Bayesian Networks in seismic risk assessment and decision support. It studies four major parts:

1. BN-based seismic demand model. The random field effects are used to consider the statistical dependence between the seismic demands of different components in the infrastructure system. The finite fault rupture and directivity effects are considered when constructing the BN model.

2. A model of the component performance using BN. The types of components considered are: point-site components such as bridges, and distributed components such as pipelines. The limit state function is used to construct the BN model. The component performance is defined as the conditional probability of failure of a component for a given ground motion intensity. A component capacity model is proposed in this part: the components are divided into different classes. For each class of component, the capacities all follow the same lognormal distribution with parameters (λ, ζ), and the parameters λ and ζ are assumed to follow some distributions but not deterministic values.

3. Models of the system performance based on component performance. The use of BNs in modeling system performance is compared with conventional methods such as fault trees, event trees, and minimal links and cut sets.

4. An influence diagram that is constructed by extending BNs to include decision and utility nodes.

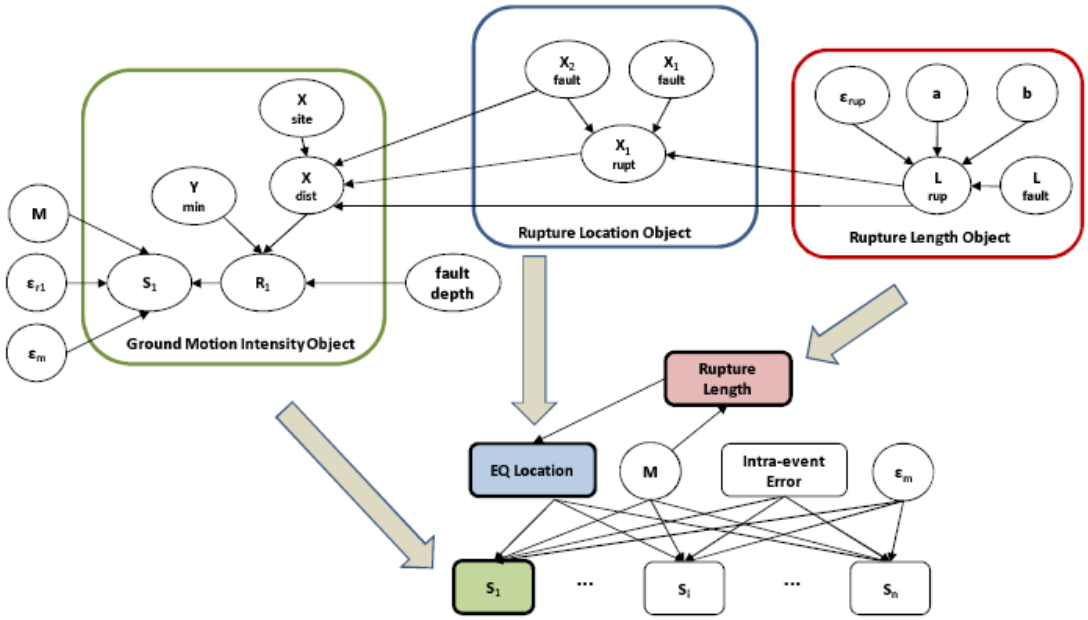

Fig. 5.1 Conceptual framework of BN in Bensi et al. (2010)

Currently, there is no exact algorithm that can be used for general continuous BNs, and the most common method for inference is discretization. In this method, a continuous variable is divided into a finite set of disjoint connected regions. Obviously, this method increases the computational burden if we want to obtain accurate results, especially for a large network with many continuous variables. Since most variables in civil engineering are continuous, there is little literature on the application of continuous BNs in this area of engineering, especially in terms of seismic risk analysis. In this Thesis, I adapt the framework in Bensi (Bensi 2010), and use the continuous BN to construct the framework. In order to apply the exact inference algorithm (Lauritzen and Jensen, 2001) rather than use discretization to deal with the continuous variable, all the continuous variables in the framework are converted into random variables with Gaussian distribution.

In the latter part of this chapter, I focus mainly on the application of BNs to seismic risk assessment for bridges. In Section 5.2, a general framework for seismic assessment based on Bayesian Network with continuous variables is first proposed. Next, in Section 5.3, a BN framework is used to address the so-called ‘twin bridges’ problem, an attempt to infer the state of a bridge based on the state of a second bridge which is highly correlated in capacity. Application to a case study is then reported in Section 5.4.

5.2 Proposed framework

The proposed framework has three main parts: the demand model, the capacity model, and the fragility function which correlates the demand and the capacity as shown. In seismic risk analysis, it is common to assume a lognormal distribution for component capacities (C) and component demands (D). If we assume that: $C \sim \ln N(\mu_C, \sigma_C^2)$; $D \sim \ln N(\mu_D, \sigma_D^2)$, then the probability of failure is:

$$F = \Pr[D - C > 0] = \Pr[\ln C - \ln D < 0] = \Phi\left(\frac{\mu_P}{\sigma_P}\right) = \Phi\left(\frac{\mu_D - \mu_C}{\sqrt{\sigma_D^2 + \sigma_C^2}}\right) \quad (5.1)$$

where Φ is the standard normal cumulative distribution function.

Fig 5.2 is the conceptual BN representing the relationship between demand and capacity. P is the intermediate variable that is related to the probability of failure, $P = \ln(D/C)$. To simplify calculation, all variables follow a normal distribution or lognormal distribution. In this simple BN, obviously we have $P \sim N(\mu_P, \sigma_P^2)$. The demand is calculated using an attenuation function depending on the local site conditions. The capacity is calculated based on some empirical or analytical models, depending on the characteristics of the bridge. Normally, the capacity model is defined based on several damage states. For each damage state, the capacity variables μ_C, σ_C will be different and, as a result, the intermediate variable P is also different.

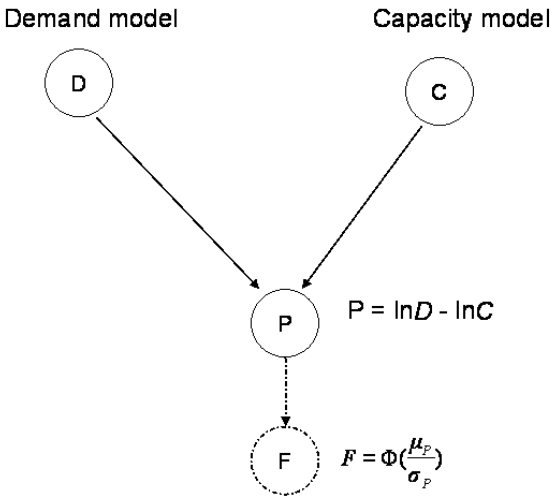

Fig. 5.2 The conceptual BN that contains the three main parts in the framework

5.2.1. The demand model

Before introducing the demand model, some basic concepts of earthquakes are introduced.

An earthquake is a rapid vibration of the earth's surface caused by shock waves generated in the Earth's interior. It can cause a natural disaster, as can tsunamis, tornadoes and ice storms. Ground vibration is the most well known and frequent manifestation. When an earthquake occurs in the seabed or in a coastal region, it can cause waves, known as tsunami. On March 11 2011, the strongest earthquake ever recorded in Japan struck the north-east coast, triggering a massive tsunami.

The distance from the observation site to the epicenter is called the epicenter distance. An earthquake is called local, when the epicenter distance is less than 100km; a near earthquake if the distance is 100km to 1,000km, and teleseismic if further than 1,000km. The greater the epicenter distance, the less the damage tends to be.

Currently there are two metrics for indicating the strength of an earthquake: magnitude and intensity. Earthquake magnitude is an objective measurement of an earthquake, and is a measure of earthquake energy, while intensity is a measure of the effects. The highest magnitude earthquake recorded was the 9.5 magnitude shock which occurred on May 22, 1960 in Chile.

The Moment Magnitude scale and the Richter scale are both measures of the magnitude of earthquakes, and refer to the seismic energy released by the earthquake. The Richter scale is the older of the two, but is now being gradually superseded by the Moment Magnitude scale.

The Richter scale was developed in 1935 by Charles F. Richter of the California Institute of Technology as a mathematical device to compare the size of earthquakes. The magnitude of an earthquake is determined from the logarithm of the amplitude of waves recorded by seismographs. Adjustments are included to take account of distances between the various seismographs and the epicenter of the earthquake. On the Richter scale, magnitude is expressed in whole numbers and decimal fractions. For example, a magnitude of 5.3 might be computed for a moderate earthquake, and a strong earthquake might be rated as magnitude 6.3. Because of the logarithmic basis of the scale, each whole number increase in magnitude represents a tenfold increase in measured amplitude. As an estimate of energy, each whole number step in the magnitude scale corresponds to the release of about 31 times more energy than the amount associated with the preceding whole number value.

The moment magnitude scale was introduced by Hanks and Kanamori (1979) as a successor to the Richter scale, and is used by seismologists to compare the energy released by earthquakes.

As suggested by many researchers (Abrahamson and Silva, 1997; Park et al., 2007; Sokolovet et al., 2010), the ground motion parameter $Y_{i,j}$ is represented by

$$\ln Y_{i,j} = f(e_i, p_i, s_{i,j}) + \eta_i + \varepsilon_{i,j} \tag{5.2}$$

where $Y_{i,j}$ is the ground motion parameter at site j during earthquake i, Peak Ground Acceleration (PGA), response Spectral Acceleration (SA), Peak Ground Velocity (PGV), or Peak Ground Displacement (PGD). In this research, I only consider the parameter PGA; f is the logarithm of the mean value of ground motion parameter that is calculated through the attenuation equation. It is a function of earthquake source (e_i), propagation path ($p_{i,j}$), and local site condition ($s_{i,j}$). The random variable η_i is the inter-event variability that follows normal distribution. It is common to all sites during the same earthquake i. The random variable $\varepsilon_{i,j}$ is the intra-event variability that also follows normal distribution. For the same earthquake i, the intra-event variables at two sites are correlated. Both inter-event variability η_i and intra-event variability $\varepsilon_{i,j}$ are random uncertainties that describe the variability. The inter-event error describes the variability between the different earthquakes, and the intra-event error captures the variability between different sites given the same earthquake event. In order to maintain consistency, 'ln' means the natural logarithm, and 'log' means the logarithm with base 10. The details of the uncertainties terms are introduced in Section 5.2.3.

Ground-motion modeling is an essential part of seismic hazard analysis. It is normally developed based on the available empirical strong-motion data. Since empirical ground-motion models have a strong dependence on the earthquake source and local site conditions, most of the existing models are applicable to a range covered by the empirical data set. According to the geographical area, current models can be divided into three classes: models applicable to California, models for Japan and models that have been developed with regard to Taiwan. The next Generation Attenuation (NGA) project developed five models in five accompanying papers that are applicable to all shallow crustal earthquakes, not only in California, but also in Europe (Campbell and Bozorgnia, 2006a; Abrahamson et al., 2008; Campbell and Bozorgnia, 2006b).

To ease computation, here we will use the attenuation relation for peak horizontal acceleration provided by Joyner & Boore (1981):

$$\log PGA = -1.02 + 0.249M - \log r - 0.00255r + 0.26\eta$$

$$r = (d^2 + 7.3^2)^{1/2} \qquad 5.0 \le M \le 7.7 \tag{5.3}$$

where M is moment magnitude. This is preferred because it corresponds to a well-defined physical property of the source; d is the closest distance to the surface projection of the fault rupture in km as shown in Fig. 5.3; η is the error term that

considers inter-event uncertainties.

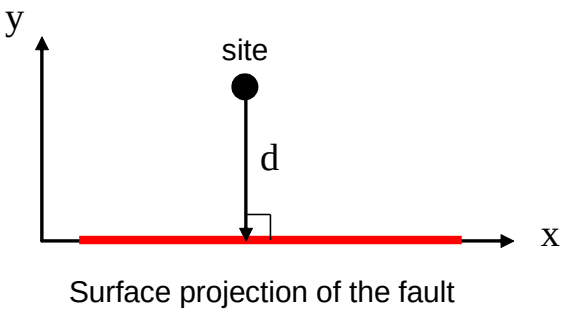

Fig. 5.3 The closest distance to the surface projection of the fault (Bensi, 2010)

5.2.2 Capacity Model

The bridge capacity model adopted in this system is based on the Hazus model (see Chapter 2 for more details). In the Hazus model, the capacity model is determined by the failure mechanism. There are two kinds of failure mechanism - failure due to the sliding of the deck (type 1) and failure of the pier (type 2).
In Equation (2.9), the capacity is given as:

$$(a_g) = \frac{2\pi}{S \cdot \eta \cdot F_0} \cdot \sqrt{\frac{C_C \cdot \Delta}{g}} \cdot \frac{K_{3D}}{T_C} = k \cdot \sqrt{C_C} \tag{5.4}$$

where C_C is the capacity coefficient of the bridge, which can be correlated, and k is the uncorrelated component of the capacity. Based on Dutta & Mander (1998), for single span bridges, or bridges seated on weak bearings with strong piers, the capacity is assumed to arise from sliding only (Basöz and Mander, 1999). In this case, C_C is given as:

$$C_C = \mu_t \tag{5.5}$$

where μ_t =coefficient of sliding friction of the bearings in the transverse direction.
For a standard bridge without wall piers, C_C can be expressed as

$$C_C = \lambda_Q \cdot k_p \cdot \frac{D}{H} \tag{5.6}$$

where λ_Q is defined as a strength reduction factor that occurs due to cyclic loading; D, H are column diameter and column height; k_p is a factor related to the reinforced concrete strength of the column $k_p = \zeta \cdot j \cdot (1+0.64 \cdot \rho_t \cdot f_y / (f_c \cdot \psi))$, where ζ is a fixity factor taken as 1 for multi-column bents and as 0.5 for single column cantilever

action; j is the internal lever arm coefficient; ρ_t is the volumetric ratio of longitudinal reinforcement; ψ is the average dead load axial stress ratio in the column; f_y is the yield stress of the longitudinal reinforcement, and f_c is the strength of the concrete. To facilitate computation, k_p is better defined as the products of several parameters. Here we assume that

$$C_C = \lambda_Q \cdot k_p \cdot \frac{D}{H} = \alpha \cdot f_y / f_c \tag{5.7}$$

where α is a factor related to ζ, j, ρ_t, ψ, f_y, and f_c. Equation 5.7 is made based on two assumptions: the resistance provided by concrete arching action is very small compared with the truss action; the volumetric ratio of longitudinal reinforcement and the average dead load axial stress ratio are determined.

5.2.3 The uncertainties terms

Consideration of uncertainty is an important part of seismic risk assessment. There are two sources of uncertainty: those related to earthquake demand; and those in structural capacity.

With regard to the uncertainty of earthquake demand, this can cause significant differences in earthquake damage for two similar structures, even though the distance between their two sites is small. It will be very useful to study the uncertainty in seismic demand; many publications have analyzed the characteristics of variability in the prediction of ground motion.

Kawakami and Mogi (2003) examined the spatial variability of PGAs (recorded at the same epicenter distance) as a function of separation distance using accelerometer arrays in Chiba (located in Tokyo), Smart-1 (located in Taiwan), and SIGNAL (located in Tokyo) databases. They conclude that the means and standard deviations have an almost linear relationship with the logarithm of the station separation distance, ranging from several meters to 100 km.

Sokolov et al. (2010) analyzed the characteristics of random variability in the prediction of peak ground acceleration in Taiwan. About 4,650 records from 66 shallow earthquakes ($M_L > 4.5$, focal depth < 30km) during 1993-2004 were used in this analysis. The results show that local geology and the peculiarities of the propagation path have a large influence on the ground motion correlation structure, and a single generalized spatial correlation model is not adequate for a large area like Taiwan.

In Equation (5.2), both the inter-event variable η and the intra-event variable ε are usually assumed to be independent and normally distributed, with a zero mean and standard deviations σ_η and σ_ε. So the total variance is given by:

$$\sigma_T^2 = \sigma_\eta^2 + \sigma_\varepsilon^2 \tag{5.8}$$

Let us consider the random variables at two sites x, y: $x=\eta+\varepsilon_x$, $y=\eta+\varepsilon_y$. The joint probability density function follows bivariate normal distribution with zero means and standard deviation σ_T (Wesson and Perkins, 2001). Since the inter-event residual is the same for the two sites in the same earthquake, the total correlation coefficient for the two sites is (see Appendix A):

$$\rho_{x,y} = \frac{\sigma_\eta^2 + \rho_\varepsilon \cdot \sigma_\varepsilon^2}{\sigma_T^2} \tag{5.9}$$

where ρ_ε is the intra-event correlation coefficient between the two sites. There are many functions developed for the intra-event correlation coefficient. For example Boore et al. (2003) proposes:

$$\rho_\varepsilon = 1 - [1 - e^{-\sqrt{0.6h}}]^2 \tag{5.10}$$

where h is the site to site distance with unit kilometer. Baker's formula (Park et al. 2007) is:

$$\rho_\varepsilon = e^{-(h/6)} \tag{5.11}$$

while Vanmarcke (1983) suggests:

$$\rho_\varepsilon = e^{-1} \tag{5.12}$$

Park et al. (2007) have compared these functions, and they conclude that the selection of the specific correlation model for simulation and loss estimate may not be critical, but the intra-event correlation cannot be completely neglected.

In this Thesis, I adopt the suggestion by Bensi (2010) that the intra-event coefficient function be given as:

$$\rho_\varepsilon = e^{-(\Delta/6)} \tag{5.13}$$

where Δ is the distance between sites x_i and x_j as with Equation (5.11).

Given the intra-event coefficient function, the inter-event uncertainty and the

intra-event uncertainty can be combined into a single uncertainty σ with zero mean and standard deviations σ_T. The total correlation coefficient is given as Equation (5.9). For the variables that follow lognormal distribution, the uncertainties are the logarithmic standard deviation or the coefficient of variation of lognormal distribution (Kennedy et al., 1980).

The term e_c is used to consider the uncertainty in the capacity model:

$$C = e_c \cdot a_g \tag{5.14}$$

e_c is assumed to follow lognormal distribution $E_c = \ln e_c \sim N(0, 0.1^2)$. Here we make the assumption that the standard deviation of $\ln e_c$ is 0.1, based on the assumption that the coefficient of variation of e_c is 0.1. For this value, we need more research into the topic.

5.2.4 BN framework for individual bridges

After introducing the three basic components of the framework, the BN framework graphs will be considered. As we have two kinds of capacity models, I provide two BN frameworks here. When the capacity of the bridge is assumed to arise from bearings, we call this kind of bridge Type 1. Fig 5.4 is the BN for bridge Type 1. It should be noted that here I determine the bridge failure type before the BN is applied for computation simplicity. In reality, we do not know the failure type before calculating the capacity. There are three parts to this framework: the demand model, the capacity model and the intersection between the demand and the capacity:

1. In the demand model, S is a parameter conceptually related to seismic demand at the site where the bridge is located: $S = \log D = \log (PGA)$. M is the earthquake magnitude; η is the inter-error term for the demand and is the same value for all the sites in one earthquake.

2. From the capacity model, we have: $\ln C = \ln(e_c \cdot e_g) = \ln(e_c \cdot k \cdot C_C) = \ln e_c + \ln k + \ln C_C$ where $E_c = \ln e_c$, e_c is the uncertainty term as defined and C_C is the resistant strength. When the bridge belongs to Type 1: $\ln C_C = \ln \mu_t = R$. μ_t is the coefficient of the sliding friction of the bearings in the transverse.

When the bridge belongs to Type 2 (pier failure): $\ln C_C = \ln \alpha \cdot f_y / f_c = \ln \alpha + \ln f_y - \ln f_c$. where $F_y = \ln f_y$, $F_c = \ln f_c$, α, f_y and f_c are defined as before.

P is the intermediate parameter related to the reliability of the bridge. From Equation (5.4) and (5.14), we have $C = e_c \cdot k \cdot C_C^{0.5}$. When the bridge belongs to type 1: $P = \ln(D/C) = 2.3\,S - E_c - \ln k - 0.5R$. When the bridge belongs to type 2: $P = \ln(D/C) = 2.3\,S - E_c - \ln k - 0.5\ln \alpha - 0.5F_y + 0.5F_c$. Given the distribution parameters (μ_P, σ_P^2) of P, the probability of failure for the bridge is $\Phi(\mu_P / \sigma_P)$.

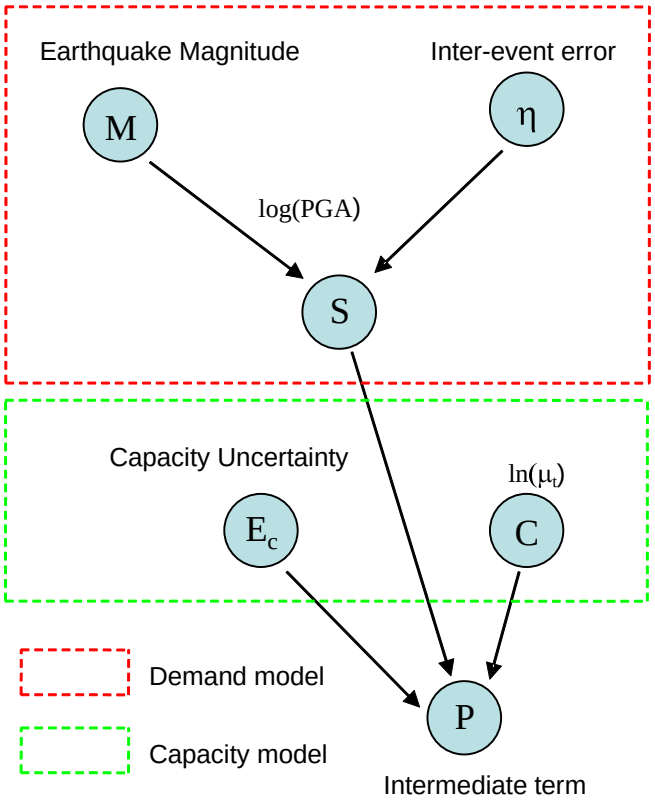

Fig. 5.4 Bayesian Network for bridge type 1

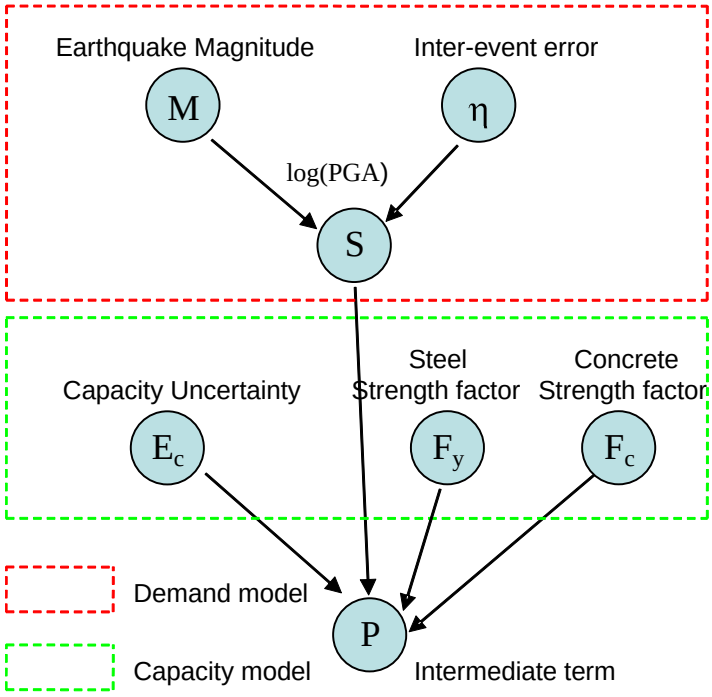

Fig. 5.5 Bayesian Network for bridge type 2

5.2.5 BN framework for twin bridges

As we can expect, the seismic vulnerabilities of any two bridges are very similar when they have similar characteristics as to type, material and construction year. On-site inspection shows that the conditions of similar bridges are also very close. Based on this observation, it is reasonable to assess the seismic vulnerability of any one bridge based on the known condition of another similar bridge. This motivates us to find the correlation of seismic vulnerabilities between similar bridges. In the previous section, I presented the BN framework for individual bridges. In this section, I want to develop the BN framework for twin bridges. Here 'twin bridges' mean that the two bridges have similar characteristics and belong to bridge Type 1 or Type 2.

Fig. 5.6 is the BN for twin bridges that belong to Type 1. Fig. 5.7 is the BN for twin bridges of Type 2. There are also three parts to this BN: demand model, capacity model and fragility curves. The two bridges are correlated through the shared variables: M, η, and C. Compared with the BN in Fig. 5.4, the main differences are the intra-error terms Z_a and Z_b in Fig. 5.6. Since there are two bridges in Fig. 5.6, the intra-error terms should be considered with regard to the two sites where the two bridges are located, while these intra-error terms are neglected in Fig. 5.4. Both Z_a and Z_b follow normal distribution. The correlation coefficient between them is defined by Equation (5.15). In order to consider this correlation in BN, two parents, U_1 and U_2 , are used as the sources of Z_a and Z_b. This idea is adopted from Bensi (2010). U_1 and U_2 are assumed to follow standard normal distribution independently. The relationship between them is as follows:

$$Z = T \cdot U = \begin{bmatrix} t_{11} & t_{12} \\ t_{21} & t_{22} \end{bmatrix} \begin{Bmatrix} U_1 \\ U_2 \end{Bmatrix} \tag{5.15}$$

where T is a 2×2 matrix. It can be obtained by Cholesky factorization, or other decomposition methods. For more details about decomposition methods, see Bensi (2010).

Similarly, Fig. 5.7 is the BN framework for twin bridges belonging to Type 2.

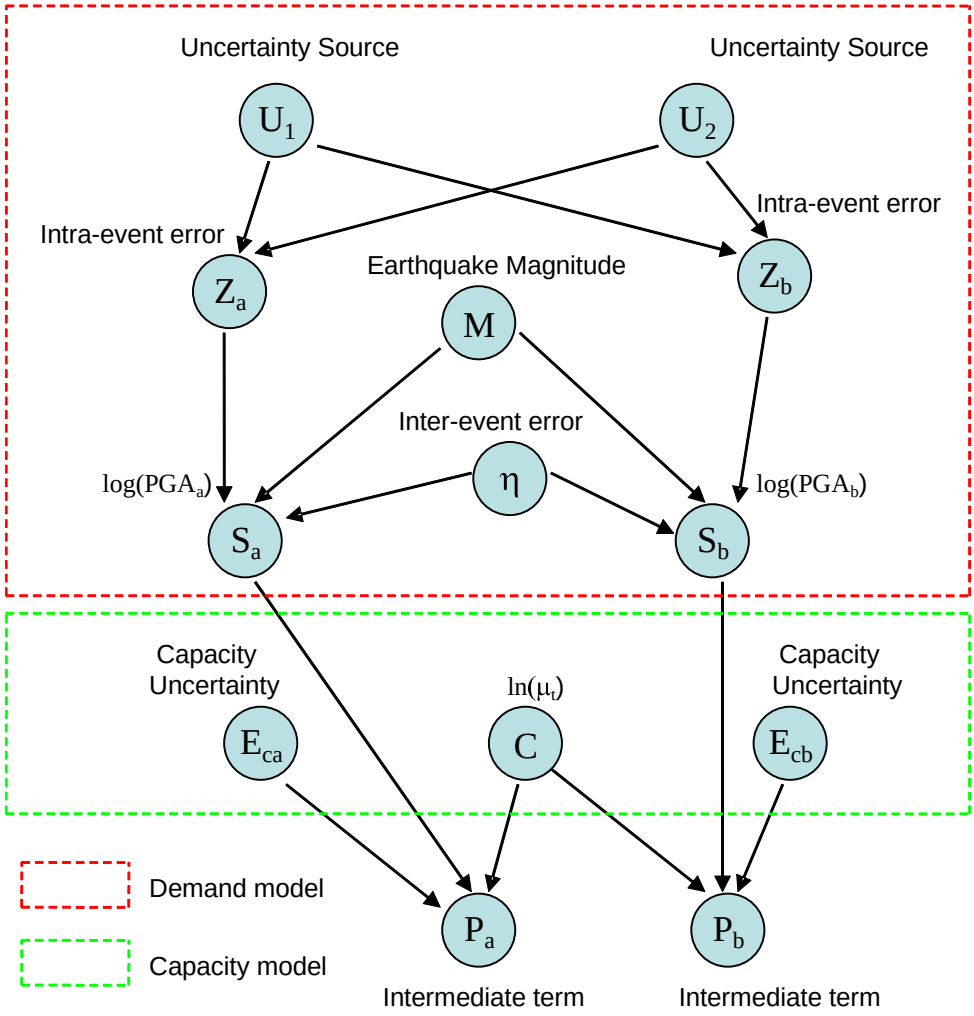

Fig. 5.6 Bayesian Network for two bridges with strong piers and weak bearings

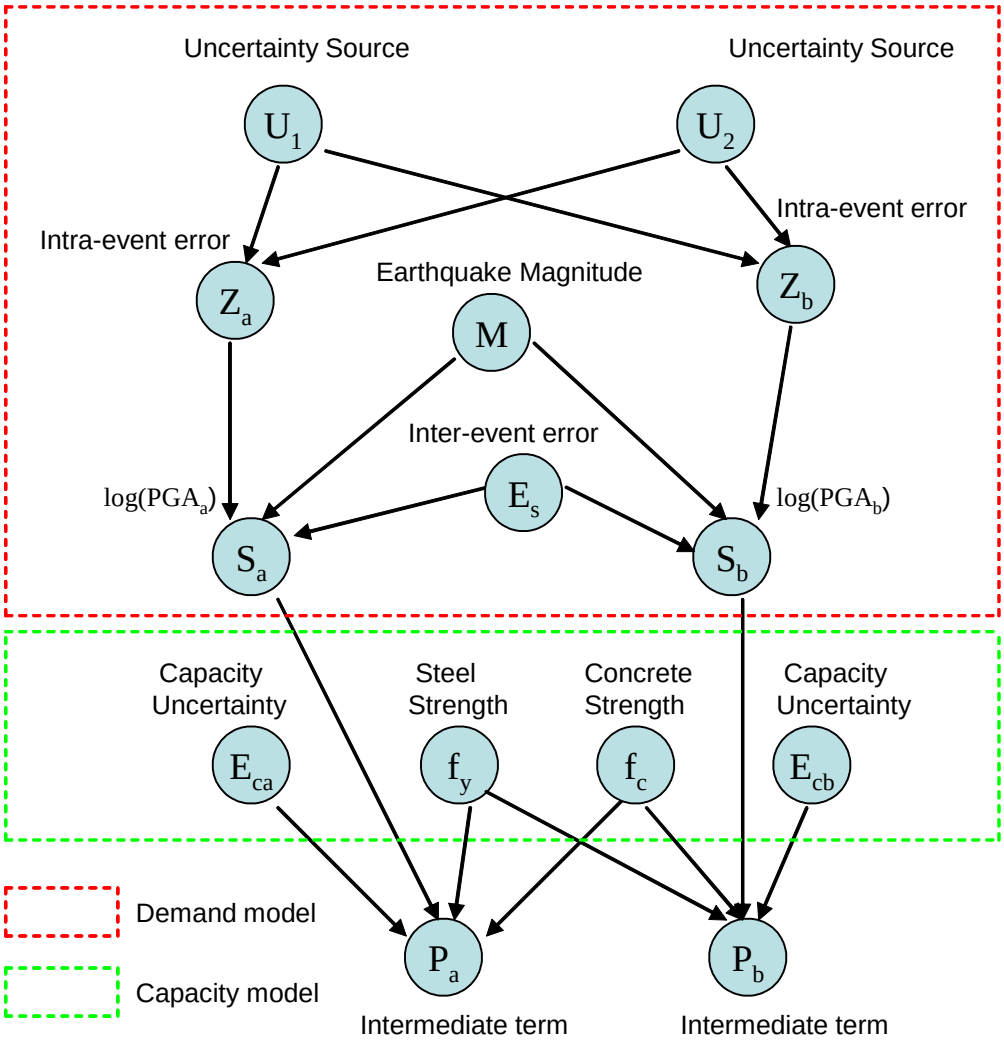

Fig. 5.7 Bayesian Network for two bridges with strong bearings and weak piers

5.3 Operations on the framework

5.3.1 Prior distribution of earthquake magnitude

For the conditional linear Gaussian Bayesian Network, there exists an exact inference algorithm when it meets the following requirements: all the continuous variables have Gaussian distribution, the continuous parents do not have discrete children, and the relationships between variables are linear. In the BNs in Figs 5.4, 5.5, 5.6 and 5.7, all the variables except *M* follow a Gaussian distribution. In order to apply the algorithm to the frameworks, we need to do some operations on them.

The earthquake magnitude was normally assumed to have a truncated exponential distribution whose PDF $f_M(m)$ is:

$$f_M(m) = \begin{cases} \dfrac{\beta \exp[-\beta(m-m_0)]}{1-\exp[-\beta(m_p-m_0)]} & m_0 \le m \le m_p \\ 0 & \text{elsewhere} \end{cases} \tag{5.16}$$

where β is the parameter that determines the shape of the distribution, and m_0 and m_p are the minimum and maximum thresholds of the magnitude. In this paper, β is assumed to be 0.76 as used by Kang et al.(2008), and the thresholds are 5.0 and 7.7 respectively based on the equation in Joyner and Boore (1981).

In order to meet the requirement that all the continuous variables follow a Gaussian distribution, we need to simulate the truncated exponential distribution using a Gaussian distribution. In this section, I use the mixtures of Gaussian (MoG) distributions to approximate arbitrary probability density functions (PDFs) based on Shenoy (2006). The logic is to find a good approximation based on minimizing some measure of distance between two distributions. The following will give the procedures to approximate $f_M(m)$.

Suppose we decide to use five components. Then we will simulate $f_M(m)$ with the mixture PDF $g_M = p_1\varphi_{\mu1,\sigma1} + \ldots + p_5\varphi_{\mu5,\sigma5}$, where $\varphi_{\mu i,\sigma i}$ denotes the PDF of a uni-variate Gaussian distribution with mean μ_i and standard deviation σ_i. It is assumed that $\mu_i > 0$, $\sigma_i > 0$, $p_i > 0$, $p_1 + \ldots + p_5 = 1$, $\mu_3 = 6.35$. Based on the symmetry of g_M around m=6.35, we can add another two constraints: $\mu_1 + \mu_5 = 12.7$; $\mu_2 + \mu_4 = 12.7$. The problem now becomes one of non-linear optimization, as follows:

Find p_1, p_2, p_3, p_4, μ_1, μ_2, σ_1, σ_2, σ_3, σ_4, σ_5 so as to minimize $\delta(f_M, g_M)$, where $\delta(f_M, g_M)$ is a distance measure between two PDFs. In this thesis, I adopt Shenoy's (2006) suggestion, and use the sum of the squared error δ_{SSE} as the distance measure: $\delta_{SSE}(f_M, g_M) = \int (f_M - g_M)^2 dx$. In practice, the magnitude range [5, 7.7] is equally divided into a large number of bins. The results are as follows: $p_1 = 0.0736$, $p_2 = 0.01$, $p_3 = 0.2619$, $p_4 = 0.4132$, $p_5 = 0.2413$, $\mu_1 = 7.1560$, $\mu_2 = 7.6064$, $\mu_3 = 6.35$, $\mu_4 =$

5.5440, μ_5 =5.0936, σ_1 = 0.1813, σ_2 = 0.0312, σ_3 = 0.3500, σ_4 = 0.3100, σ_5 = 0.1546. Fig 5.8 gives the two PDFs, the mean value and standard deviation of f_M are 5.9175 and 0.80. The mean value and standard deviation of MoG approximation are 5.7856 and 0.80. Fig. 5.9 gives the CDFs of the two distributions. It should be noted that differences between the two CDFs are larger when magnitude is close to 7.8. This is because the original distribution is truncated exponential which has lower and upper bounds.

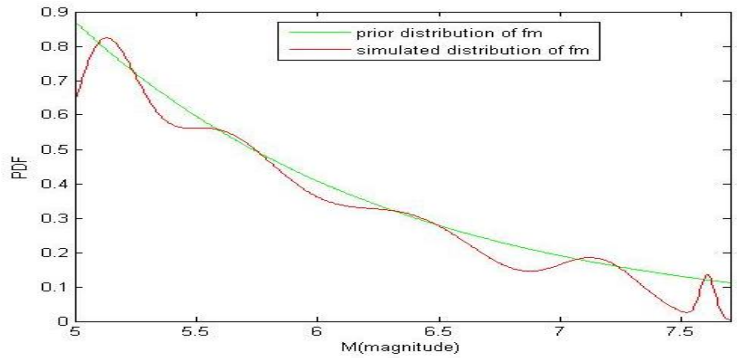

Fig. 5.8 5-component MoG Approximation of the truncated exponential distribution

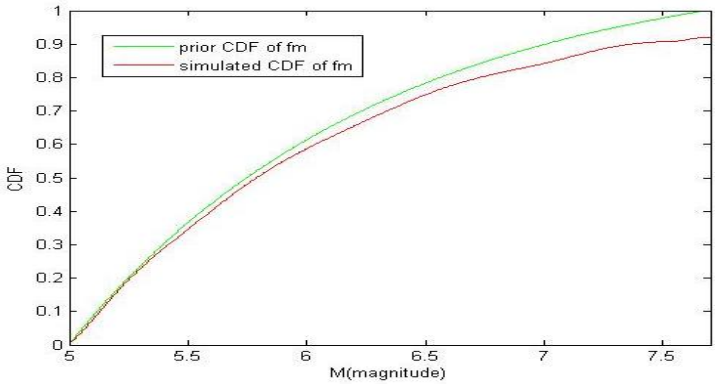

Fig. 5.9 CDFs of the truncated exponential distribution and MoG Approximation

5.3.2 Entering evidence in the BN framework

This framework aims to provide a seismic risk assessment system, both before and after the earthquake. Given the prior distributions of the variables including earthquake magnitude, capacity factor, and uncertainty terms, the prior distribution for the intermediate term *P* before the earthquake can be calculated during the initialization based on the computation scheme as described in Section 4, and then the prior probabilities of failure for the two bridges are obtained. Assume that an earthquake happens; the on-site sensor observes that bridge *A* has collapsed; now we need to update the probability of bridge *B* collapsing after the earthquake. In order to

solve this problem, we first need to enter into the framework the observation that bridge *A* has collapsed. In this case, we need to assign an evidence value to P_1.

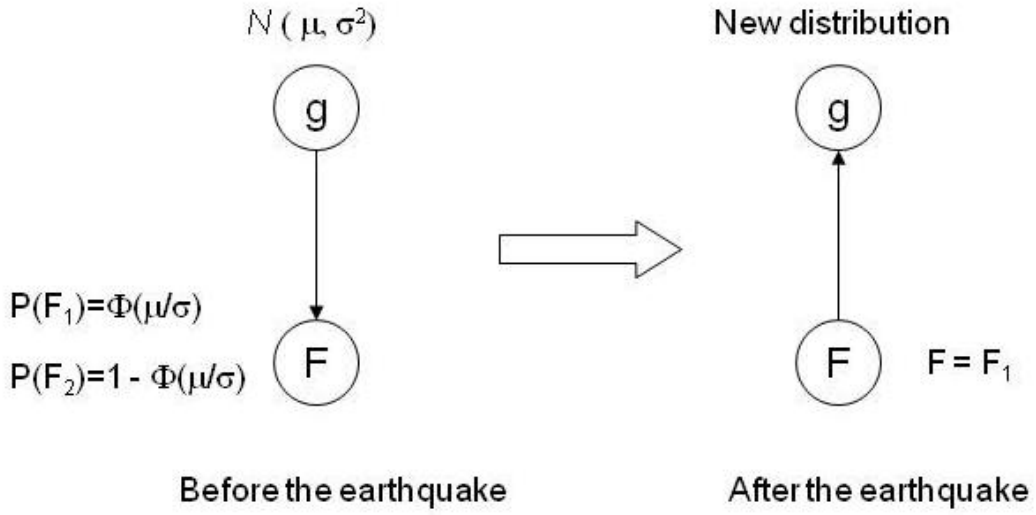

Fig. 5.10 How to incorporate into the framework the evidence about the bridge state

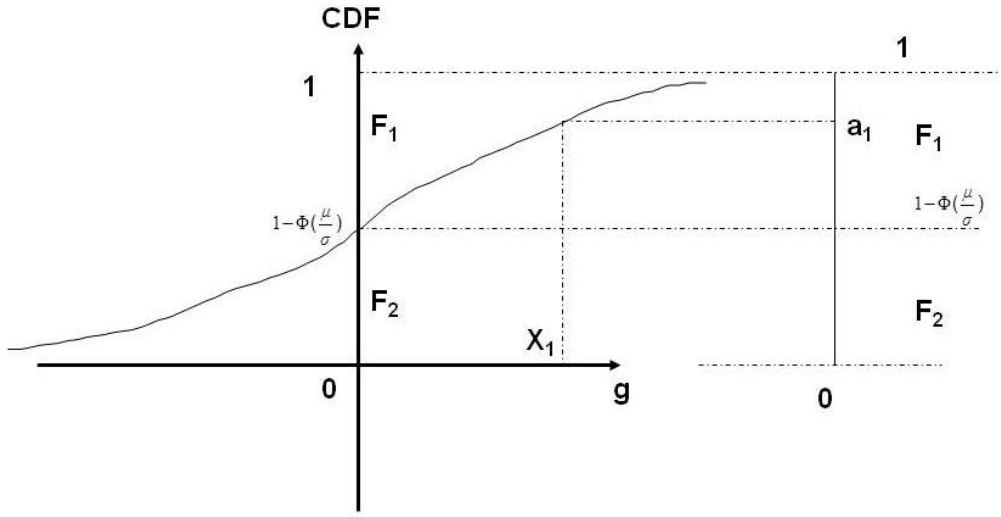

Fig. 5.11 Procedures to generate the random number X_1

In Fig. 5.10, *g* is a continuous variable. It has the prior distribution $N(\mu, \sigma^2)$, and *F* is the state of the bridge which can be F_1 (failure) or F_2 (survival). *F* is determined by *g*. If $g>0$, $F= F_1$; if $g<0$, $F= F_2$. Given the prior distribution of *g*, the probabilities for the bridge being in the two states are $\Phi(\mu / \sigma)$ and $1 - \Phi(\mu / \sigma)$. When given the evidence $F= F_1$, the posterior distribution of *g* can be obtained by Bayes theorem:

$$f(g \mid F_i) = \frac{P(F_i \mid g) f(g)}{P(F_i)} = \frac{P(F_i \mid g) f(g)}{\int P(F_i \mid g) f(g) dg} \qquad i = 1, 2 \tag{5.17}$$

where $f(g)$ is the prior distribution of g, $P(F_i|g)$ is the likelihood.

However, in the computation scheme used by Lauritzen and Jensen (2001) and introduced in Chapter 4, the evidence value can only be a number, and the distribution cannot be used as evidence. This problem can be solved by using the Monte Carlo method. For details of the Monte Carlo simulation, see Appendix D.

Using the Monte Carlo method, we can generate a series of stochastic numbers X_1, X_2, X_3, …, X_N (N = 1000) which all fulfill the evidence $F = F_1$ independently as follows (see fig. 5.11):

Step 1: Generating a random number a_1 that follows uniform distribution between 1 - Φ (μ / σ) and 1. Since $F = F_1$, we know that g>0. Then the cumulative probability of g is between 1 - Φ (μ / σ) and 1;

Step 2: X_1 = norminv(a_1, μ, σ);

Step 3: Repeat steps 1 and 2 until sufficient realization has been generated.

Then we enter these independent numbers one by one into the BN as evidence values. In the case of a binary variable, such as the collapse of a bridge, we aim to estimate a scalar value, i.e. the probability of an event. In this case, the output of each simulation (for i =1 to N) is a scalar, and we can use the sample average as an estimator.

However, when we are updating a continuous variable, the outcome of each simulation is a pair (μ_i, σ_i), which refers to the posterior Gaussian distribution of the variable.

The correct posterior can be seen as the mixture of the N Gaussian distributions, N (μ_i, σ_i) for i = 1 to N, and the weights given to each distribution is the same (because they are randomly selected using the Monte Carlo method). Now we are looking to the Gaussian "best fit", that which comes closest to the simulated mixture. A method to find it is using MC again: generate m (e.g. m = 10) samples from component in the mixture, (i.e. for every i =1 to N) and collect the $N \times m$ samples (in the example: 1,000×10=10,000). Then we compute the sample mean and variance, and take these as parameters for the posterior. The results will not converge to the real posterior (which is not Gaussian) but to the best Gaussian approximation.

In this section, the Monte Carlo simulation and Bayesian Networks are combined to get the posterior distributions of variables. However, this method has a speed limitation when the network is large. In order to approach real time updating after the earthquake, a fast computation method is needed. In this case, the continuous evidence is considered. If the posterior distribution of g can be entered as evidence, then the updating procedure will be faster. The following is a tentative way which can be improved.

If the full bridge capacity is C, then for each damage state, the capacity limit is C_i: $C_i = k_i \times C$. ($0 < k1 < k_2 < k_3 < k_4 = 1$); if we get the evidence from the inspector: the bridge is at damage state *i*, then we have the equation: $C_i - D < 0$. So we have $k_i \times C - D < 0$ and $k_{i+1} \times C - D > 0$; if $i = 4$, we can easily get $g = C - D < 0$; if $i < 4$, we have

$$(1-k_{i+1}) \cdot C < g < (1-k_i) \cdot C \tag{5.18}$$

For each bridge, the value of C is different, so if we know the prior distribution of C, the problem becomes how to convert the equation (5.18) into the distribution of g.

5.4. Case study

5.4.1 Bridges with strong piers and weak bearings

The SP135 Bridge on the River Fersina-Canezza (*A*) and the SP31 Bridge on the River Avisio (*B*) are 'twin' bridges in APT-BMS. Both are 3 span pre-stressed concrete bridges with wall piers and non-monolithic abutments; both were built in 1967. The lengths of the two bridges are 58.3m and 57.5m respectively. In Fig. 5.12 and Fig. 5.13 we can see overviews and cross sections of these structures.

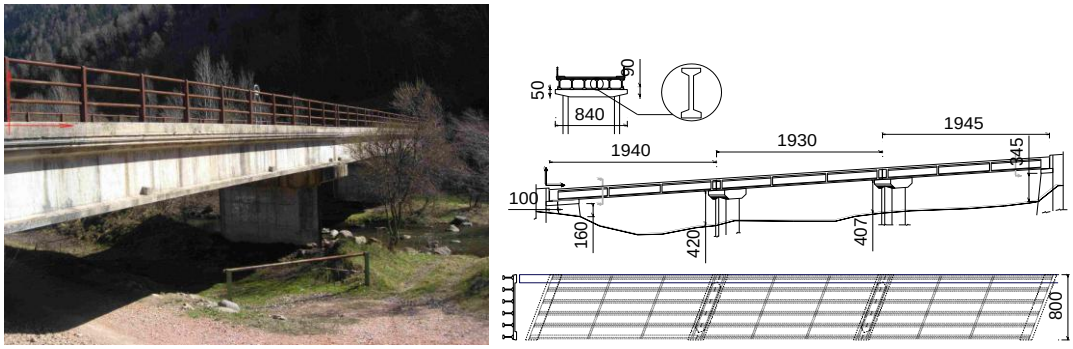

Fig. 5.12 SP135 Bridge on River Fersina-Canezza (a) overview (b) Plan view, elevation and cross-section of the deck

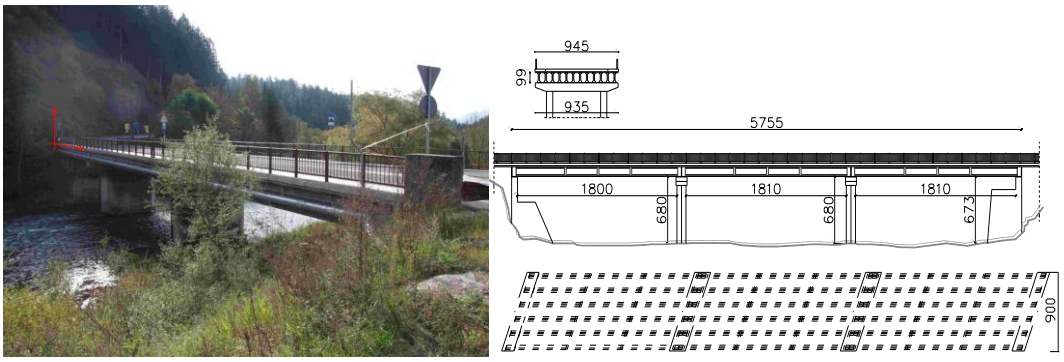

Fig. 5.13 SP31 Bridge on River Avisio (a) overview (b) Plan view, elevation and cross-section of the deck

We assume there has been an earthquake of magnitude of 7. The source to site distances for the two bridges are 15km and 10 km, and the distance between the two sites is 10km. The capacity variable μ_t is assumed to follow: $R = \ln \mu_t \sim N$ (ln0.85, 0.1^2). Entering these parameters into Equation (5.3), the seismic demand part is expressed as:

$$S_1 = -0.4913 + 0.26\eta + 0.26Z_1$$
$$S_2 = -0.3025 + 0.26\eta + 0.26Z_2$$

Since the two bridges both have wall piers, they belong to the bridge Type 1 category. According to Basöz and Mander (1999), the capacities are assumed to arise from the sliding of bearings only. Table 5.1 gives the other parameters.

Table 5.1 Parameters for calculating the median spectral acceleration in Eq (5.4)

Bridge	S	η	F_0	Δ(m)	K_{3D}	T_C (S)
Bridge A	1	0.6325	2.6848	0.3	1.21	0.3335
Bridge B	1	0.6325	2.6157	0.3	1.21	0.3629

Entering these parameters into Equation (5.4), the median spectral accelerations for collapse limit state are:

$$(a_g)_1 = 0.9584 \cdot \sqrt{(C_c)_1}$$
$$(a_g)_1 = 0.9040 \cdot \sqrt{(C_c)_1}$$

After defining the demand and capacity relationship for each bridge, the probability factors P for the two bridges can be obtained:

$$P_1 \sim (2.3 \cdot S_1 - 0.5 \cdot R - E_{c1} - 0.9908, 0.25)$$
$$P_2 \sim (2.3 \cdot S_2 - 0.5 \cdot R - E_{c2} - 0.9908, 0.25)$$

5.4.1.1 Initialization

After defining the relationship between these variables, we can use the computation scheme in Lauritzen & Jensen (2001) to calculate the prior distribution for S_a, S_b, P_a and P_b. Table 5.2 gives the results.

Table 5.2 Results after initialization

Parameters	Mean value	Var
$S_a = \log(PGA_a)$	-0.49	0.14
$S_b = \log(PGA_a)$	-0.30	0.6
P_a	-2.04	0.98
P_b	-1.61	0.98

Given the distributions of S_a and S_b, the median value of *PGA* at bridges *A* and *B* can be calculated as 0.32g and 0.50g; The probabilities of bridges *A* and *B* collapsing are 1.97% and 5.19%.

5.4.1.2 Entering evidence

After the earthquake, the on-site sensor observes that bridge *B* has collapsed. Now we need to update the probability of bridge *A* also collapsing. Since $F_b = F_1$, we can enter this evidence into the BN using the method described in Section 5.3.2 and get the posterior of other variables given in Table 5.3.

Table 5.3 Results given the evidence

Parameters	Mean value	Variation
$S_a = \log(PGA_a)$	-1.07	0.78
$S_b = \log(PGA_a)$	-0.05	0.1
P_a	0.191	0.03
P_b	-0.176	0.01

From Table 5.2 and Table 5.3, we can see that the expected median *PGA* values at the two bridges also increase from 0.32g to 0.89g for bridge *A*, and from 0.50g to 1.55g for bridge *B*. In the meantime, the expectation for the sliding coefficient μ_t reduces from 0.85 to 0.839. This can be explained by the following logic: the failure of bridge *A* shows that the capacity of the bridge is less than expected. The probability of bridge *A* collapsing increases from 1.97% to 12.4%.

5.4.2 Bridges with strong bearings and weak piers

The Viaducts Pianello (*A*) and San Silvestro (*B*) are further examples of 'twin' bridges in APT-BMS. Viadotto Pianello is a 4 span pre-stressed concrete bridge built in 1985, and Viadotto San Silvestro is a 3 span concrete bridge built in 1958. The site condition factors for the two bridges are: S = 1, η = 0.6367, T_C = 0.3172s. The lengths of the two bridges are 91.54 m and 66.15 m respectively. The column heights of the two bridges are 5.35m and 5.3m, and the diameters of the columns are 4.00m and 2.8m. In Fig 5.14 and Fig 5.15 we can see overviews and cross sections of these structures.

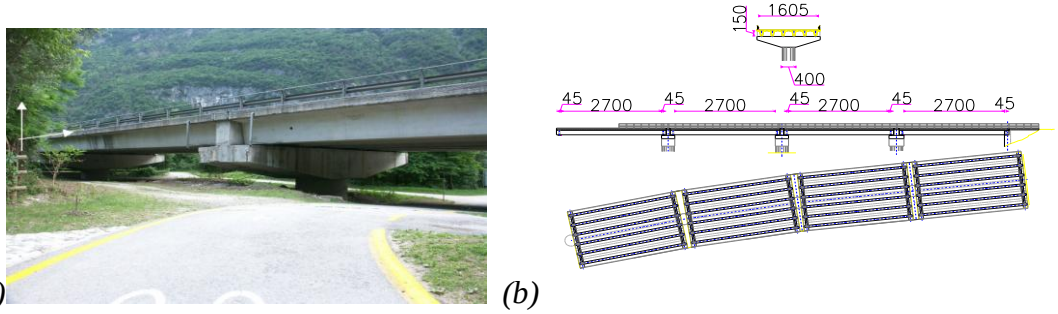

(a) *(b)*

Fig. 5.14 Viadotto Pianello: (a) overview (b) plan view, elevation and cross-section of deck

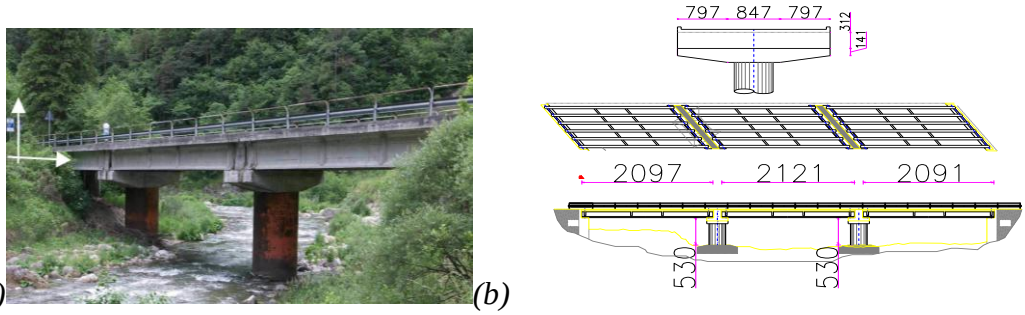

(a) *(b)*

Fig. 5.15 Viadotto San Silvestro(a) overview (b) plan view, elevation and cross-section of deck

Since both viaducts are simply supported multispan bridges, their possible damage group belongs to the type "strong bearings with weak piers". According to Basöz and Mander (1999), the capacities are assumed to arise from the piers. So we can use the BN in Fig 7. Table 5.4 gives the other parameters.

Table 5.4 Parameters for calculating median spectral acceleration

	F_0	Δ(m)	λ_Q	K_{3D}	ζ	j	ρ_t	ψ	F_y(MPa)	f_c(MPa)
A	2.451	0.05	0.6	1.125	0.5	0.8	0.01	0.05	440	28
B	2.504	0.05	0.6	1.125	0.5	0.8	0.01	0.05	330	26

For bridge *A*: $C_c = \lambda_Q \cdot k_p \cdot D/H = 0.247 \cdot (1 + 0.128 \cdot f_y / f_c)$. If we use the mean values of f_y and f_c, then $C_c = 0.743 = 0.0473 \cdot f_y / f_c$, so it is assumed that $\alpha = 0.0473$ in Equation (5.7). In the same way, for bridge *B*, we assume that $\alpha = 0.0412$. In addition, an error term e_c is used to consider the uncertainty in the capacity model: $C_C = e_c \cdot \alpha \cdot f_y / f_c$. Entering these parameters into Equation (5.4), the median spectral accelerations are:

$$(a_g)_a = 2.3597 \cdot \sqrt{(C_c)_a}$$
$$(a_g)_b = 3.8730 \cdot \sqrt{(C_c)_b}$$

For the demands on the two bridges, the earthquake magnitude is defined as in Section 5.3.1 and the fault lengths and the coordinates of the two bridges are defined as in Section 5.4.1. Given the capacity and demand, the probability factor *P* can be written as:

$$P_a = 0.922 + 2.3 \cdot S_a - 0.5 \cdot F_y + 0.5 \cdot F_c - 0.5 \cdot E_{ca}$$
$$P_b = 0.603 + 2.3 \cdot S_b - 0.5 \cdot F_y + 0.5 \cdot F_c - 0.5 \cdot E_{cb}$$

5.4.2.1 Initialization

After defining the relationship between these variables, the initial distributions are calculated based on the computation scheme in Lauritzen & Jensen (Lauritzen and Jensen, 2001) as given in Table 5.5.

Table 5.5 Prior distribution of variables after initialization

Parameters	Mean value	Standard deviation
$S_a = \log(PGA_a)$	-0.491	1.067
$S_b = \log(PGA_a)$	-0.302	1.067
P_a	-2.040	5.662
P_b	-1.605	5.662

Given the distributions of S_a, and S_b, the median value of PGA at bridges *A* and *B* can be calculated as 0.6118*g* and 0.739*g*; The probabilities of bridges *A* and *B* collapsing are 19.57% and 24.99%.

5.4.2.2 Entering evidence

Assume that an earthquake happens. The on-site sensor observes that bridge A has an operational problem. Now we need to update the probability of bridge B having a similar operational problem. The updated distributions of other variables are obtained as in Table 5.6:

Table 5.6 Posterior distributions of variables given the evidence

Parameters	Mean value	Standard deviation
M (Magnitude)	6.48	0.735
$F_y = (lnf_y)$	6.0756	0.1099
$F_c = (lnf_c)$	3.3414	0.0999
$S_a = \log(PGA_a)$	0.393	0.0538
$S_b = \log(PGA_a)$	-0.286	0.4508
P_b	-1.42	1.042

Given the distributions of conceptual variables, the mean values and standard deviations of the physical parameters can be obtained as in Table 5.7.

Table 5.7 Posterior distributions of the physical parameters given the evidence

Parameters	Mean value	Standard deviation
$PGA_a = 10^{Sa}$	2.49g	0.31g
$PGA_b = 10^{Sa}$	0.856g	1.04g
$f_y = e^{Fy}$	437.8MPa	48.3 MPa
$f_c = e^{Fc}$	28.3 MPa	0.28 MPa

From Table 5.6 and Table 5.7, we can see that the mean value for the earthquake magnitude is 6.48, which is higher than the prior value of 5.79. In addition, the *PGA* values on the two bridges also increase from 0.387g to 2.49g for bridge *A*, and from 0.329g to 0.856g for bridge *B*. The probability of bridge *B* collapsing increases from 1.43% to 8.65%.

5.5. Conclusions

This chapter proposes a framework for seismic risk assessment based on a Bayesian Network with continuous variables. First, the BN for an individual bridge is introduced, then the BN for twin bridges is developed based on the BN for the individual bridge. Using this framework, the seismic risk for an individual bridge before the earthquake can be calculated. After the earthquake, given the observation of one of the twin bridges, the condition of the other twin bridge can be predicted and updated.

However, the assumptions and limitations should be kept in mind. The framework I am proposing makes use of the assumption that all continuous variables are Gaussian. However as soon as we plug in a discrete observation, we can no longer expect the posterior distribution to be Gaussian. Nonetheless, we use a Gaussian posterior, which achieves the best fitting of the actual general distribution. The reason why we do so is that, maintaining a set of Gaussian variables allows the method to be computationally efficient. Other than this, the approximation should be kept in mind.

After each evidence processing phase, we use the MC procedure to fit the data. There are two kinds of approximation introduced here. On the one hand, there is the classic approximation of the MC technique, as we represent a distribution by a set of random samples. On the other hand the Gaussian fitting, when we impose the posterior to be Gaussian, thus keeping the variables Gaussian.

6 Network-level analysis using Bayesian Networks

In Chapter 5, I proposed a seismic vulnerability assessment framework both for a single bridge and for twin bridges based on a Bayesian Network with continuous variables. In this chapter, I will extend the framework from twin bridges to the system level. In this framework, all the bridges in the network are correlated and analyzed. Before the earthquake, the prior risks of all the bridges are calculated. After the earthquake, given the observations on some bridges, the posterior risks to the other bridges are predicted and updated.

The outline of this chapter is as follows: in Section 1, the description of the framework is introduced; each part of the framework is explained and compared with the framework for twin bridges. In Section 2, the computation scheme including initialization, entering evidence and updating, is explained. After that, the framework is applied to the bridge network in APT-BMS in Section 3. Finally, the best path between any two places within APT-BMS is identified again and compared with the results in Section 4.

6.1 Description of the framework

Fig 6.1 is the BN framework with *n* bridges. As in Section 5, this framework consists of three basic parts: the demand model, the capacity model and the fragility function.

1. The demand model includes three parts:

the first part is the earthquake demand denoted by S_1, S_2,…, S_n. These are conceptual parameters related to seismic intensities at the different sites where the

bridges are located: $S_i = \log(PGA_i)$;

the second part is the earthquake magnitude M;

the last part covers inter-error and intra-error, where η is the inter-error term for the demand, and is the same for the same earthquake; and Z_1, Z_2,…, Z_n are the intra-event error terms which are drawn from Gaussian random fields, while U_1, U_2,…, and U_n are the parents of Z_1, Z_2,…, and Z_n. U_1, U_2,…, and U_n are independent, standard normal random variables. The details of the intra-event error terms Z, will be subsequently be explained.

2. Two kinds of capacity models are included in the framework. C is the capacity factor of the bridge with strong piers and weak bearings, f_y and f_c are the strengths of the reinforcement bars and of the concrete of the bridge piers: $F_y = \ln f_y$; $F_c = \ln f_c$. In the framework, bridge 1, 2, …, i belong to Type 1 as defined in Chapter 5, while the bridge i+1, i+2,…,n belong to Type 2. The error term e_c is used to consider the epistemic uncertainty in the capacity model.

3. P_1, P_2,…, P_n are the intermediate parameters related to the reliability of a bridge. This equals the difference between demand and capacity: $P_i = \ln(PGA)_i - \ln(a_g)_i$, where PGA_i is the Peak Ground Acceleration at the site where bridge i is located, and $(a_g)_i$ is the capacity of bridge i.

The variables in the framework can be divided into two parts: global variables that are relevant to every bridge, and local variables that are related only to a specific bridge. In this framework, the following variables are global: U_1, U_2, ..., U_n, M, η, C, f_y and f_c. The others are local variables.

In the intra-error part of the demand model, vector Z can be expressed as the product of an $n \times n$ transformation matrix T and the $n \times 1$ vector U as suggested in Bensi (2010):

$$Z = TU = \begin{bmatrix} t_{11} & \cdots & t_{1n} \\ \vdots & \ddots & \vdots \\ t_{n1} & \cdots & t_{nn} \end{bmatrix} \begin{Bmatrix} U_1 \\ \vdots \\ U_n \end{Bmatrix} \tag{6.1}$$

where vector Z has zero means, unit standard deviations and correlation matrix R = $[\rho_{ij}]$, where $\rho_{ij} = e^{-(\Delta/6)}$ as defined in Section 5. The transformation matrix T can be determined using certain decomposition methods. However, since the BNs in Fig 6.1 are densely connected, when the number of bridges is large the computation will become intractable, since the largest clique becomes very large. In order to limit and solve this computational problem, Bensi (2010) proposed several methods to reduce the size of the largest clique. Generally, this is accomplished in two ways: one is by eliminating the links between vector Z and vector U. The other is by reducing the number of nodes in vector U. Node-based approaches include a node-based eigenvalue approach (NEA), a node-based Cholesky approach (NCA), and a

node-based optimization approach (NOA). Link-based approaches include a link-based eigenvalue approach (LEA), a link-based Cholesky approach (LCA), and a link-based optimization approach (LOA). The relative efficiencies of these approximation methods are measured based on the following definition:

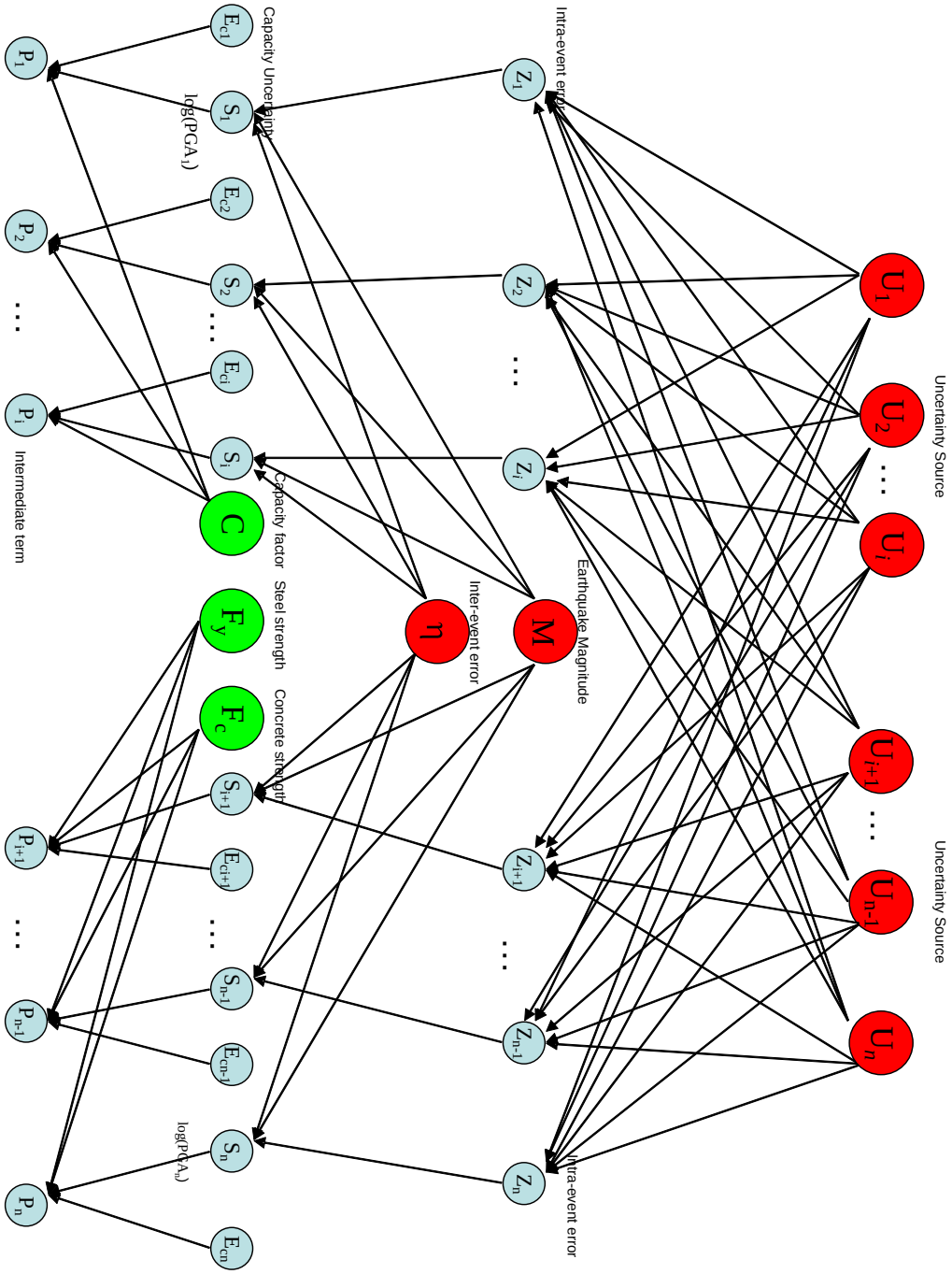

Fig. 6.1 The BN framework for the network with n bridges

$$e = \frac{\sum_{i=1}^{n-1}\sum_{j=i+1}^{n}\left|\hat{\rho}_{ij} - \rho_{ij}\right|}{\sum_{i=1}^{n-1}\sum_{j=i+1}^{n}\left|\rho_{ij}\right|} \tag{6.2}$$

where ρ_{ij} is the correlation coefficient between Z_i and Z_j as defined in Equation (5.14), and $\hat{\rho}_{ij}$ is the approximated correlation coefficient.

In this Thesis, I adopt the single node approach because it is easy to decide the size of the BN for a given number of nodes in vector U. This will facilitate the network computation, especially for a large number of bridges. The approximated vector Z_i is defined by:

$$Z_i = s_i \cdot V_i + t_i \cdot U, i = 1 \ldots n \tag{6.3}$$

where V_i and U are independent standard normal random variables, and s_i and t_i are variable-specific coefficients. Note that U is common to all Z_i, so it is the source of the correlation. The associated BN is shown in Fig 6.2.

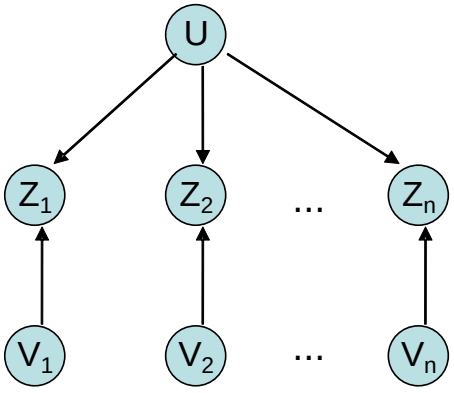

Fig. 6.2 BN model for intra-event error (Bensi, 2010)

For this model, the coefficients for approximated Z_i are: $\hat{\rho}_{ij} = t_i \cdot t_j$ for $i \neq j$ and $\hat{\rho}_{ij} = 1$ for $i = j$. Since the variance for Z_i is 1, we have:

$$s_i = (1 - t_i^2)^2, -1 \leq t_i \leq 1 \tag{6.4}$$

where the coefficient t_i is determined by minimizing the error measure for correlation coefficients as defined in Equation (6.2).

So the solution of the coefficient t_i becomes the nonlinear constrained optimization problem

$$\min \sum_{i=1}^{n-1} \sum_{j=i+1}^{n} \left| t_i t_j - \rho_{ij} \right| \tag{6.5}$$

subject to: $t_i^2 \leq 1$, $i = 1, ..., n$

In Bensi (2010), the error measures are carried out for different configurations in all node-based and link-based approaches, except the single node approach. In the following, the error measure for the single node approach is calculated. Fig 6.3 shows configurations for line layout, circle layout and grid layout. The correlation matrix for Z_i is defined based on Equation (6.3).

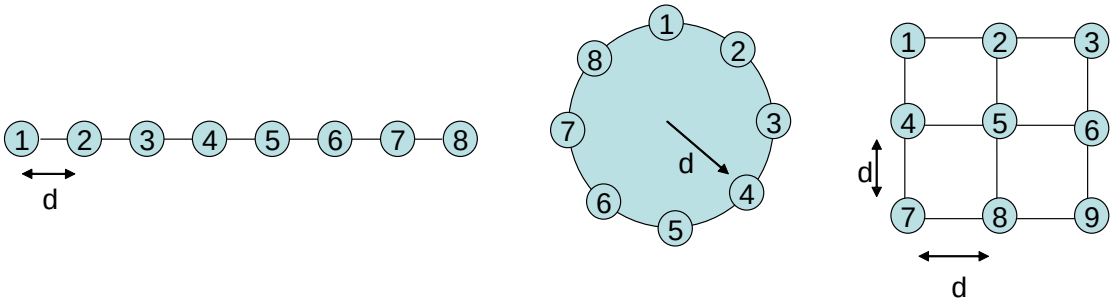

Fig 6.3 Line layout, circle layout and grid layout for numerical investigation (Bensi, 2010)

Fig. 6.4 gives the error measures for different distance unit from 0.1 to 1 (corresponding to $d = 6 \times 0.1$ and 6×1) under different bridge configurations based on Equation (6.5). The trends are the same as those in Bensi (2010): the error measure becomes larger when d increases. This is because, for larger d, the correlation coefficients are small, which results in a smaller denominator in Equation (6.2). For the same distance unit, the line layout has the largest error measure, followed by the circle layout and the grid layout. This is because the error measures of the configurations are related to their densities. The closer the bridges, the smaller the error measures.

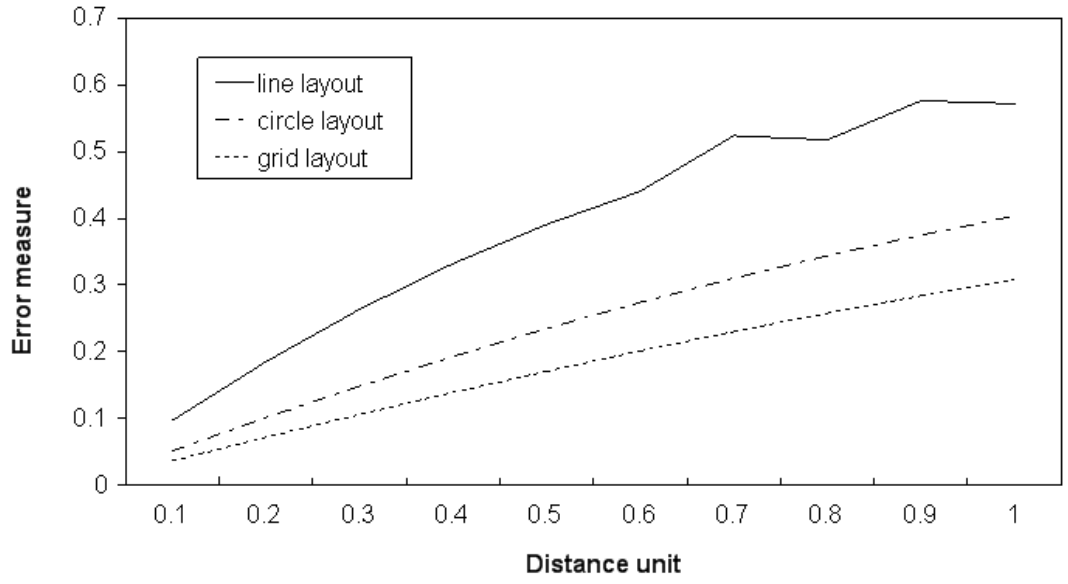

Fig. 6.4 Error measures for different configurations at different distances based on the methods in Bensi (2010)

After integrating the BN in Fig. 6.2 into the framework in Fig. 6.1, the new framework is given in Fig. 6.5. In Fig. 6.5, the number of nodes in vector U reduces from *n* to 1. In the new BN, there are only 6 global variables: U, M, E_s, C, F_y, and F_c. The others are local variables. This facilitates computation dramatically, especially for a network with a large number of bridges. The next section will introduce the computation procedures for this framework.

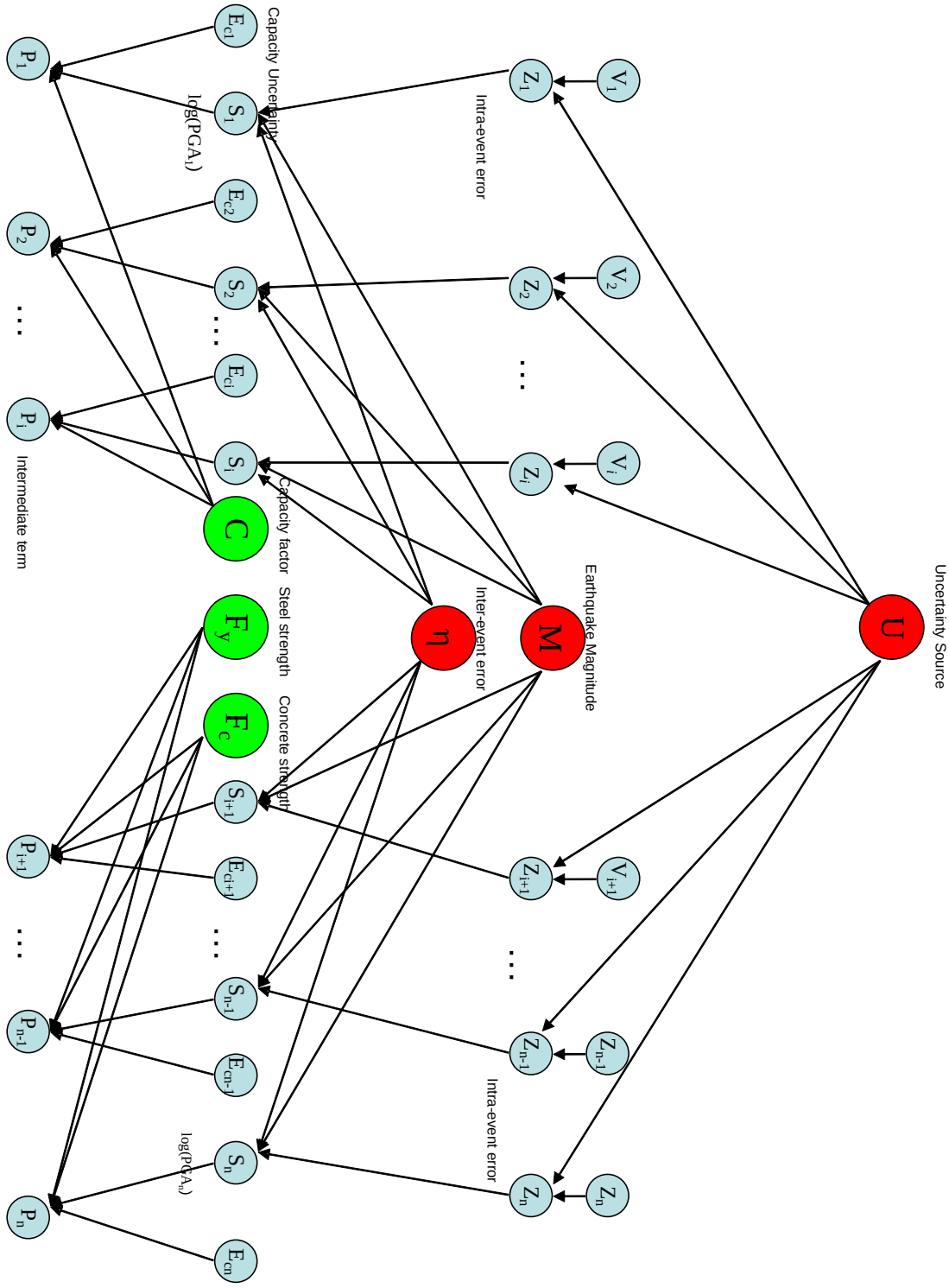

Fig. 6.5 The BN framework for a network with n bridges

6.2 Computation procedures

As in the computation scheme introduced in Chapter 4, here too there are two stages in the procedure: initialization and updating. The general procedures in this framework are the same as those introduced in Chapter 5. However, the only aspect that needs to be considered is computation efficiency. In fig. 6.4, there are 6 global variables: *U*, *E*s, *C*, *M*, f_y and f_c. They are connected to all the bridges. Besides these 6 global variables, each bridge has 4 local variables: Z_i, E_{ci}, P_i, and S_i. If there are 500 bridges in the network, then the number of total variables in the network will be 2,006. In the computation scheme as explained in Chapter 4, the potential is represented as $\phi = [p, A, B, C]$ $(H \mid T)$. If there are 2,007 variables in the network, the maximum size of the matrix would be as large as $2{,}007 \times 2{,}007$. The calculation burden would be very high during operations with these matrices. In order to reduce the computation burden and limit computation time, we must undertake some operations on the framework.

The logic of the operation is to divide the network BN into separate single BNs, each single BN corresponding to one bridge. All the single BNs share the same global variables, and the differences between them are the local variables. For the local variable Z_i in each BN, they are correlated through the nonlinear constrained optimization equation as shown in Equation (6.5). During the initialization procedure, all the local variables Z_i follow a standard normal distribution, and there is no evidence for updating the distribution. Consequently, we can directly use the standard normal distribution as the prior distribution of Z_i , and do not need to solve the optimization problem in Equation (6.5). Based on the computation scheme introduced in Chapter 4, the prior distributions of P_1, P_2, ..., and P_n are calculated as $N(\mu_1, \sigma_1)$, $N(\mu_2, \sigma_2)$, ..., and $N(\mu_n, \sigma_n)$ respectively. The probability of damage for each bridge is $\Phi(\mu_{Pi} / \sigma_i)$. During the updating procedures, the evidence is entered into each single BN, so the distributions of all the global variables, including *U*, will change. This will result in a change of Z*i* in each single BN. In order to calculate the updated distributions of Z*i*, we need to consider the correlations between Z*i* and *U*, which are achieved through the nonlinear constrained optimization condition in Equation (6.5). However, when the number of bridges is larger, the computations in solving Equation (6.5) will be very much larger. So we cannot simply divide the network BN into separate single BNs in the updating procedure. The following are the procedures to be used.

In APT-BMS, there are 986 bridges. We assume that there are observations on three bridges after an earthquake: bridge 1 and bridge 2 are damaged, and bridge 3 is not damaged. We want to predict the probabilities of the other 983 bridges being damaged. The following are the procedures:

Generate a sub-network including bridges 1, 2, 3 and 4. We then use the nonlinear constrained optimization condition in Equation (6.5) to calculate the intra-event error for these four bridges.

1. Divide the sub-network into 4 single BNs.
2. In the BN for bridge 1, do the following operations:

a: Generate a series of random numbers x independently from the prior distribution.

b: After generating the evidence for P_1, we need to enter them, one by one. For each one, we collect towards the root as during the initialization stage and get the posterior distribution of all the global variables. For each piece of evidence, we can get a posterior distribution for each global variable. We use the mean values of the posterior distribution as the updated distribution for each global variable.

3. Repeat steps a, b for bridges 2 and 3. For each observation, the distributions of global variables are updated once. When all the observations are entered and propagated, we get the final updated distributions of the global variables.
4. Enter the final updated distributions of the global variables into the single BN for bridge 4, and calculate the updated distribution for P_4.
5. Repeat the same procedures in 1-5 for bridges 5, 6, 7, ..., 986.

6.3 Application

The probabilities of APT bridges being in a damaged state have been calculated using the Hazus model in Chapter 2. In Chapter 2, the seismic demand is represented by the return period of the earthquake. In this chapter, the probability of damage to each bridge is calculated again using the framework of Fig. 6.5 during the initialization procedure. In this framework, the seismic demand is directly related to the earthquake magnitude. The prior distributions for the global variables are given in Table 6.1.

Table 6.1 Prior distribution of the global variables

The global variables	Distributions
U	N (0, 1)
η	N (0, 0.2^2)
C	N (ln 0.85, 0.15^2)
M	N (5.79, 0.8^2)
F_y	N (ln 440, 0.11^2)
F_c	N (ln 28, 0.10^2)

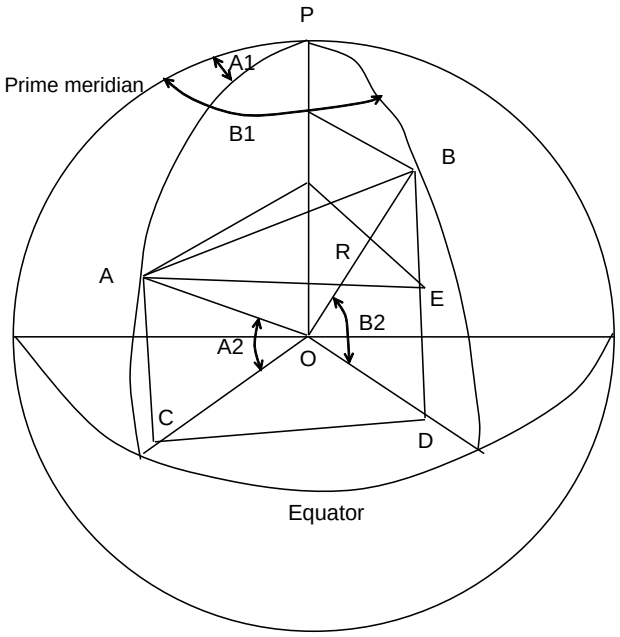

Fig. 6.6 Distance between two bridges A and B at different locations. (http://dl.zhishi.sina.com.cn/upload/31/86/74/1497318674.4175043.jpg)

In APT-BMS, the location of each bridge is denoted by its longitude and latitude. Here we introduce the method to calculate the distance, given the location of the two bridges.

Fig. 6.6 gives the locations of two bridges, A and B. The longitudes and latitudes for bridges A and B are (A1, A2) and (B1, B2). *O* is the center of the earth, *P* is the North Pole. The distance between bridge A and bridge B is the length of arc along the spherical surface.

In triangle OAC:

$$AC = R \cdot \sin(A2) \quad OC = R \cdot \cos(A2) \tag{6.6}$$

In triangle OBD:

$$BD = R \cdot \sin(B2) \quad OD = R \cdot \cos(B2) \tag{6.7}$$

In triangle OCD:

$$CD = \sqrt{OC^2 + OD^2 - 2 \cdot OC \cdot OD \cdot \cos(B1 - A1)} \tag{6.8}$$

In triangle ABE:

$$AB = \sqrt{AE^2 + BE^2} = R \cdot \sqrt{2 - 2 \cdot \cos(A2) \cdot \cos(B2) \cdot \cos(B1 - A1) - 2 \cdot \sin(B2) \cdot \sin(A2)} \tag{6.9}$$

So the distance between bridge *A* and bridge *B* along the spherical surface is:

$$r = R \cdot \arccos(\cos(A2) \cdot \cos(B2) \cos(B1 - A1) + \sin(B2) \sin(A2)) \tag{6.10}$$

Now, assume that an earthquake of magnitude 7.0 happens in the town of Salò (E10.519935,N45.603110, red dot in Fig. 6.7). This a town located 70 km South-West of Trento, on the shore of Lake Garda, in the nearby province of Brescia. The same location was actually the epicenter of a 5.4 magnitude earthquake in November 2004 (http://www.iesn.org/speciali/garda/garda.htm), and for this reason has been chosen for this simulation. Using the computation scheme introduced in Chapter 4, the initial seismic risk of each bridge is calculated once again and the results are shown in Fig 6.7. Since the seismic demand is larger than that in Chapter 2, the probabilities for the bridges being in a damaged state are also higher. So in this chapter, the category range for each color is different: green ($P<10^{-3}$), yellow ($10^{-3}<P<10^{-2}$), orange ($10^{-2}<P<10^{-1}$) and red ($P>10^{-1}$). From the figure, it is easy to see that the seismic vulnerabilities of the bridges near the epicenter are relatively high, and the bridges far from the epicenter have low probabilities of being damaged. Fig. 6.8 gives the number of bridges in each probabilistic range.

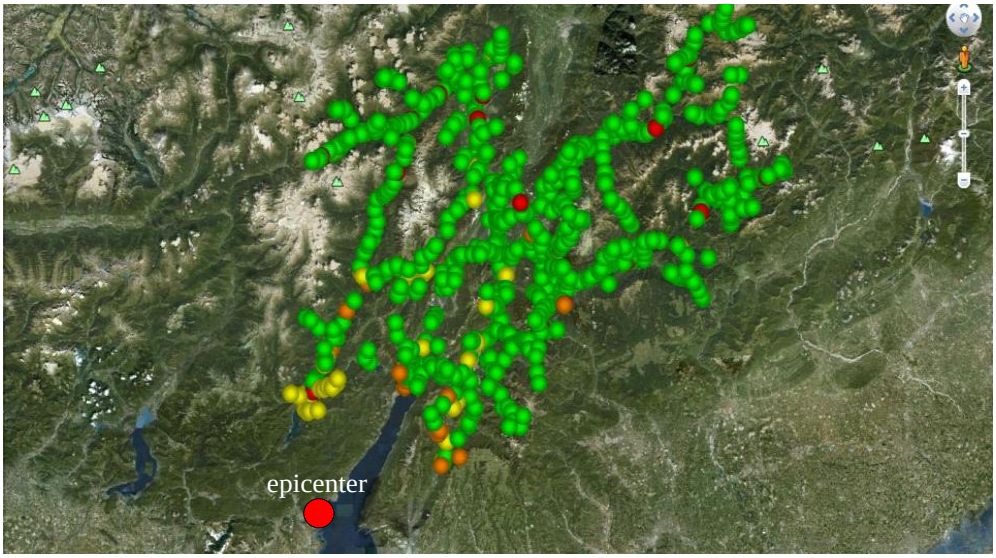

Fig. 6.7 Prior seismic vulnerability in APT bridge stock for a 7.0 magnitude earthquake with epicenter in Salò (E10.519935,N45.603110.)

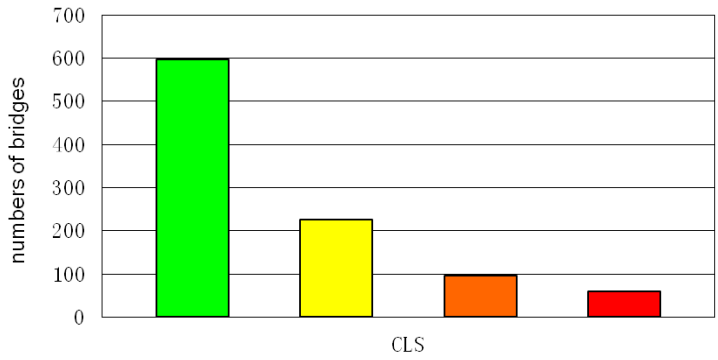

Fig. 6.8 Prior distribution of probability of collapse in APT bridge stock for a 7.0 magnitude earthquake with epicenter in Salò (E10.519935,N45.603110)

After the earthquake, we get some observations from the on-site sensors: bridge 1 and bridge 2 have collapsed during the earthquake, while bridge 3 is safe after the earthquake. Now we want to calculate the updated probability of other bridges being damaged given these observations.

Using the computation procedures in the last section, we first try to update the seismic vulnerability of bridge 4 based on the observations. After entering the evidence on bridge 1, the distributions of 6 global variables are updated, based on this observation. Table 6.2 gives the results.

Table 6.2 Posterior distributions of the global variables based on the evidence that bridge 1 has collapsed

Global variables	Distributions
U	N (2.332, 0.487^2)
η	N (0.064, 0.011^2)
C	N (ln 0.824, 0.149^2)
M	N (6.749, 0.711^2)
F_y	N (ln 440, 0.11^2)
F_c	N (ln 28, 0.099^2)

From the results, we find that the earthquake magnitude is estimated at 6.749. This means that the earthquake magnitude is expected to be much higher than the initial value In Table 6.1. For the global variable C, which is related to the sliding coefficient, the updated value is lower than the prior value. This means that the damage to bridge 1 denotes a lower sliding coefficient. Since the failure mechanism of bridge 1 belongs to type 1, the variables f_y and f_c remain the same, given the evidence.

Table 6.3 gives the updated distributions of global variables after entering the evidence with regard to bridge 2.

Table 6.3 Posterior distributions of the global variables based on evidence that bridge 2 has collapsed

Global variables	Distributions
U	N (2.357, 0.343^2)
η	N (0.064, 0.001^2)
C	N (ln 0.824, 0.149^2)
M	N (6.767, 0.524^2)
F_y	N (ln 440, 0.11^2)
F_c	N (ln 28, 0.099^2)

From Table 6.3, the earthquake magnitude increases over the value in Table 6.2. This means that the observation on bridge 2 increases the estimate of the earthquake magnitude again. The other global variables are almost the same as those in Table 6.2.

Table 6.4 shows the results after entering the evidence that bridge 3 is safe. This evidence increases the estimate of the bridge's capacity, which can be shown by variable *C*, and reduces the estimate of earthquake demand. This can be shown by earthquake magnitude *M*.

Table 6.4 Posterior distributions of the global variables based on the evidence that bridge 3 is safe

Global variables	Distributions
U	N (2.048, 0.251^2)
η	N (0.064, 0.001^2)
C	N (ln 0.852, 0.465^2)
M	N (6.282, 0.384^2)
F_y	N (ln 440, 0.11^2)
F_c	N (ln 28, 0.099^2)

After entering all the 3 pieces of evidence, the final updated distributions of the global variables are obtained, and the updated seismic vulnerability for bridge 4 is calculated.

Using the same procedures, the updated seismic vulnerabilities for all the other bridges are calculated, and the results are shown in Fig 6.9. Fig 6.10 gives the number of bridges in different probability levels.

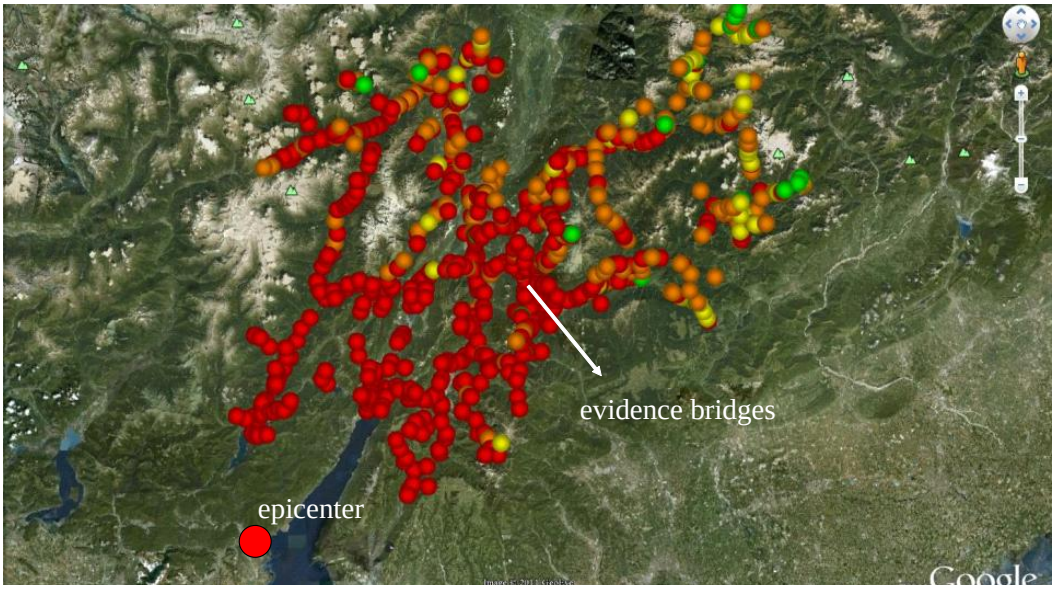

Fig. 6.9 Posterior seismic vulnerability in APT bridge stock for a 7.0 magnitude earthquake with the epicenter in Salò (E 10.519935,N 45.60311)

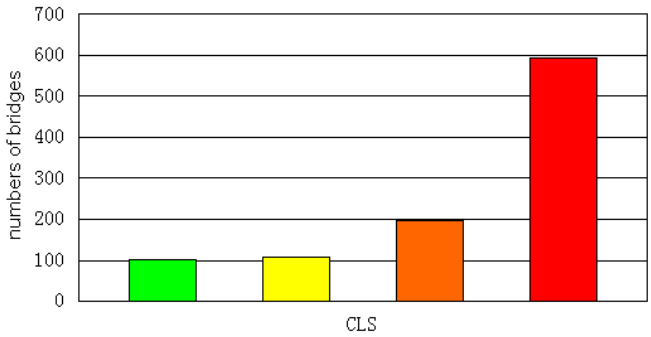

Fig. 6.10 Posterior distribution of probability of collapse in APT bridge stock for a 7.0 magnitude earthquake with the epicenter in Salò (E10.519935, N45.603110)

6.4 Identifying the best path

In Chapter 3, the network level assessment is carried out in APT-BMS. Dijkstra's algorithm is used to find the best path between any two given places. In Chapter 3, the best path is identified without considering the correlation between different bridges. In this section, we will again find the best path between any two nodes within the network. The correlation between the bridges is considered using the framework used in aforementioned sections. The results in this section are compared with those in Chapter 3.

6.4.1 The link value

Fig. 6.11 Link composed by bridge A and bridge B in series

Fig. 6.11 is a link composed of bridge *A* and bridge *B* in series. Here we use *P* (*A*) to indicate the probability of bridge *A* being safe, and *P* ($\overline{A}$) to indicate the probability of it being damaged. As for the link, *P* (*L*) means the probability of the link being safe, and *P* ($\overline{L}$) means the probability of the link being damaged. Since the link has two bridges in series, the value of *P* (*L*) equals the probability that neither bridge A nor bridge *B* is damaged, and the value of *P* ($\overline{L}$) equals the probability that there is at least one bridge of A and B is damaged. Obviously we have *P* (*L*) + *P* ($\overline{L}$) =1.

When not taking correlation into account:

$$P(L) = P(AB) = P(A) \cdot P(B \mid A) = P(A) \cdot P(B) \tag{6.11a}$$

$$P(\overline{L}) = 1 - P(L) \tag{6.11b}$$

If we consider the correlation between the two bridges, *P* (*L*) and *P* ($\overline{L}$) can be obtained by:

$$P(L) = P(AB) = P(A) \cdot P(B \mid A) \tag{6.12a}$$

$$P(\overline{L}) = 1 - P(L) \tag{6.12b}$$

Fig. 6.12 is the link formed by n bridges in series. P (L) and P ($\bar{L}$) is calculated as follows:

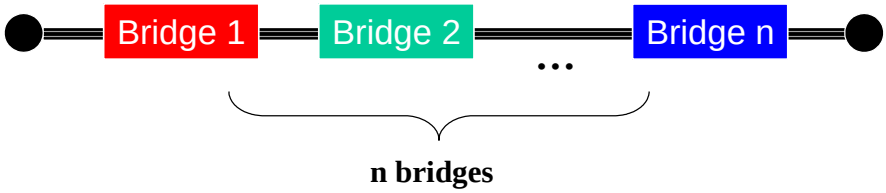

Fig. 6.12 Link formed by n bridges in series

When not taking correlation into account:

$$\begin{aligned} P(L) &= P(B_1 B_2 \ldots B_n) \\ &= P(B_1)\cdot P(B_2 \mid B_1)\cdot P(B_3 \mid B_1 \cdot B_2)\cdot \ldots \cdot P(B_n \mid B_1 \cdot B_2 \cdot B_3 \cdot \ldots \cdot B_{n-1}) \\ &= P(B_1)\cdot P(B_2)\cdot P(B_3)\cdot \ldots \cdot P(B_{n-1})\cdot P(B_n) \end{aligned} \quad (6.13.a)$$

$$P(\bar{L}) = 1 - P(L) \quad (6.13.b)$$

When consider the correlation between the bridges, P (L) and P ($\bar{L}$) can be calculated as:

$$P(L) = P(B_1)\cdot P(B_2 \mid B_1)\cdot P(B_3 \mid B_1 \cdot B_2)\cdot \ldots \cdot P(B_n \mid B_1 \cdot B_2 \cdot B_3 \cdot \ldots \cdot B_{n-1}) \quad (6.14.a)$$

$$P(\bar{L}) = 1 - P(L) \quad (6.14.b)$$

In Equation (4a), $P(B_n \mid B_1 \cdot B_2 \cdot B_3 \cdot \ldots \cdot B_{n-1})$ means the probability of bridge n being safe given the evidence that bridges 1, 2, 3, … , (n-1) are all safe. This can be obtained using the framework in Fig 6.5 of Chapter 6. The procedures are:

1. Generate a sub-network including bridges 1, 2, 3, ..., n. Use the nonlinear constrained optimization condition in Equation (6.5) to calculate the intra-event error for these n bridges.
2. Divide the sub-network into n single BNs which includes all variables that are related with an individual bridge.
3. In the BN for bridge 1, do the following operations:

Step1: generate a series of random numbers x independently from the posterior distributions of P_1 using the Monte-Carlo method.

Step 2: Repeat step 1 until the required number of realizations are generated.

Step 3: After generating the evidence for P_1, we need to enter them one by one.

For each one, we collect towards the root as during the initialization, and get the posterior distribution of all the global variables. For each piece of evidence, we can get a posterior distribution for each global variable. Use the mean values of the posterior distribution as the updated distribution for each global variable.
4. Repeat steps 1 - 3 for bridges 2, 3, ..., *n*-1. For each observation, the distributions of global variables are updated once. When all the observations are entered and propagated, we get the final updated distributions of the global variables. It should be noted that the final distributions after evidence has been provided are not Gaussian, but here we forcing them to be Gaussian.
5. Enter the final updated distributions of the global variables into the single BN for bridge *n*, and calculate the updated distribution for P_n.
In the same way, the other elements in Equation (6.14.a) can be calculated and the value of link $P(\overline{L})$ can be obtained.

6.4.2 The sum of different link values

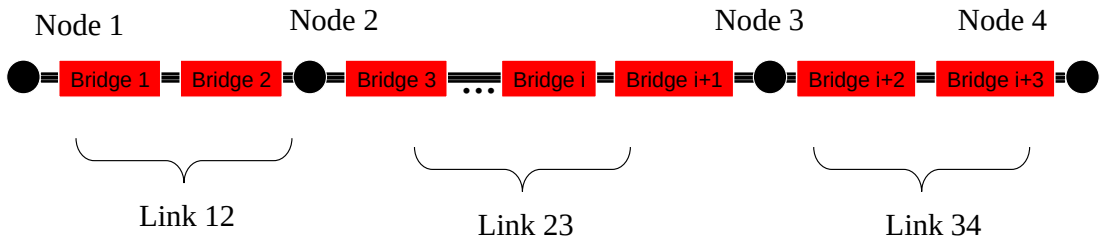

Fig. 6.13 Different links between two nodes

After calculating the link value, we need to get the sum of different link values when identifying the best path. Take Fig 6.13 for example. We want to calculate the value between link node 1 and node 4. Based on the method used in the previous section, the values of link 12, link 23, and link 34 can be obtained respectively. In order to find the value between node 1 and node 4, we can first calculate the value between node 1 and node 3. When considering the correlation between all the bridges on this link, the value of link 13 is:

$$P(L_{13}) = P(B_1) \cdot P(B_2 \mid B_1) \cdot P(B_3 \mid B_1 \cdot B_2) \cdot \ldots \cdot P(B_{i+1} \mid B_1 \cdot B_2 \cdot B_3 \cdot \ldots \cdot B_i) \qquad (6.15.a)$$

$$P(\overline{L_{13}}) = 1 - P(L_{13}) \qquad (6.15.b)$$

In the same way, the link between node 1 and node 4 is given as follows:

$$P(L_{14}) = P(B_1) \cdot P(B_2 \mid B_1) \cdot P(B_3 \mid B_1 \cdot B_2) \cdot \ldots \cdot P(B_{i+3} \mid B_1 \cdot B_2 \cdot B_3 \cdot \ldots \cdot B_{i+1} \cdot B_{i+2})$$

(6.16.b)

$$P(\overline{L_{14}}) = 1 - P(L_{14}) \qquad (6.16.b)$$

From this example, we find that the calculation of Equation (6.15) does not give us any help with the result of Equation (6.16). The value of the link is only related to all bridges on the link. The calculation of the sub-link value does not help us to find the value of the whole link. This means that each time we want to obtain the value between two nodes, we have to use Equation (6.14) once, no matter how many bridges are located between the two nodes. However, in the procedure associated with identifying the best path using Dijkstra's algorithm, we need to get the value between two nodes many times. This would increase the computation burden greatly. In order to facilitate computation, we will only consider the correlation of bridges within the same link. Based on this logic, the value between node 1 and node 4 is as follows:

$$P(L_{14}) = P(L_{12}) + P(L_{23}) + P(L_{34}) \qquad (6.17)$$

where $P(L_{12})$, $P(L_{23})$ and $P(L_{34})$ can be calculated based on the method used in the previous section.

6.4.3 Application

In Section 3 we identified the best path in the APT-BMS network, given any start node and end node, using the Dijkstra algorithm. In that section, the value of every link is calculated simply as the sum of probabilities of the bridges being in a damaged state. This ignores the correlation between the probabilities of the bridges being damaged. In the previous section, I introduced the methods used to calculate the link value and the sum of the link value. In this section, we will identify the best path again.

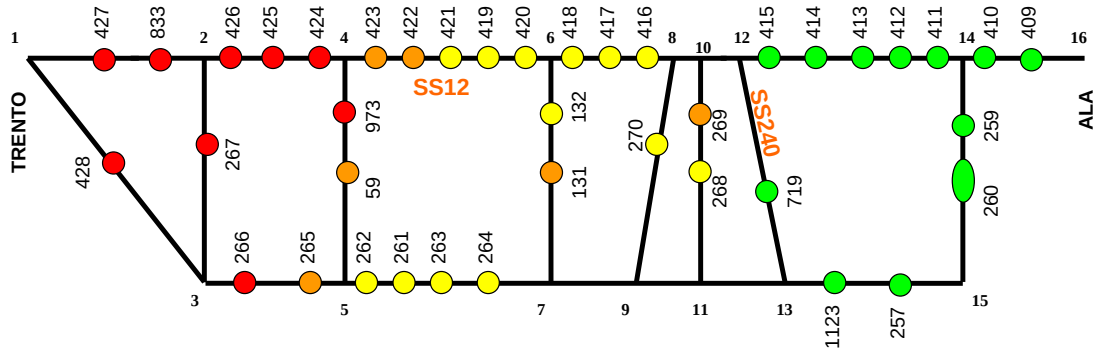

Fig. 6.14 The network between Trento and Ala

The network between Trento and Ala in Fig. 6.14 is used again to illustrate the procedures. In Fig. 3, the color of the dot means the probability of the bridge collapsing after the earthquake, as assumed in Section 6.3. The epicenter of the earthquake is located in the city center of Trento. The number beside every bridge in Fig. 14 indicates the ID of the bridge. From Fig 14, we find that bridges on the same link have very similar seismic risk. This is because the seismic demand on these bridges is similar due to their proximity to one another. In addition, the bridges near Trento have a higher seismic risk than the bridges far from Trento. This as the epicenter is assumed to be in Trento city center.

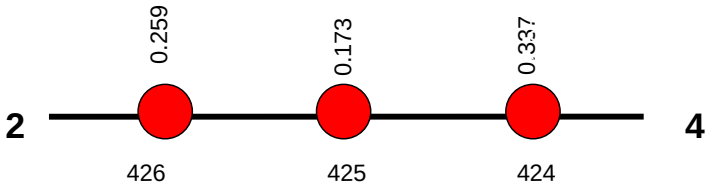

Fig. 6.15 The link between node 2 and node 4

First, the value of each link is calculated. We take the link between node 2 and node 4 as an example, shown in Fig 6.15. The number above the bridges is the probability of them being damaged. Based on Equation (6.14 a):

$$P(L) = P(B_{424}) \cdot P(B_{425} \mid B_{424}) \cdot P(B_{426} \mid B_{425} \cdot B_{424}) \tag{6.18}$$

where $P(B_{424})$ is the prior probability of bridge 424 being safe, $P(B_{425}|B_{424})$ is the conditional probability of bridge 425 being safe given that bridge 424 is safe, and $P(B_{426}|B_{425}\cdot B_{424})$ is the conditional probability of bridge 426 being safe given that bridges 425 and 424 are safe. Bridge 424 and 425 have different failure mechanisms, so the value of $P(B_{425}|B_{424})$ can be calculated using the BN in Fig. 6.16. In the same way, the value of $P(B_{426}|B_{425}\cdot B_{424})$ can be calculated using the BN in Fig. 6.17.

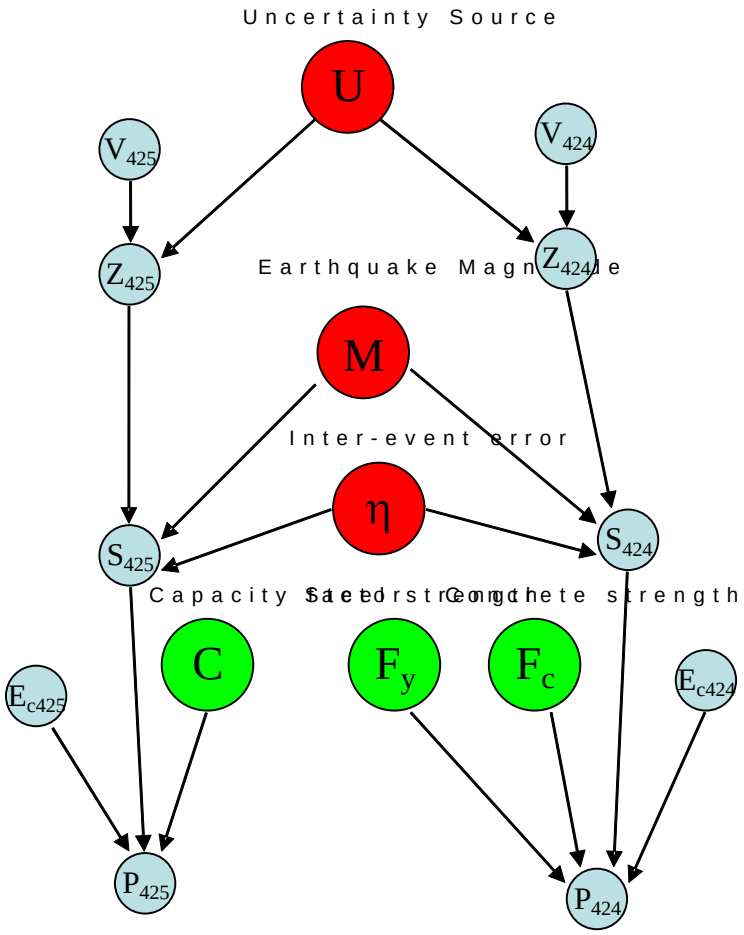

Fig. 6.16 The BN used to calculate the value of P(B425|B424)

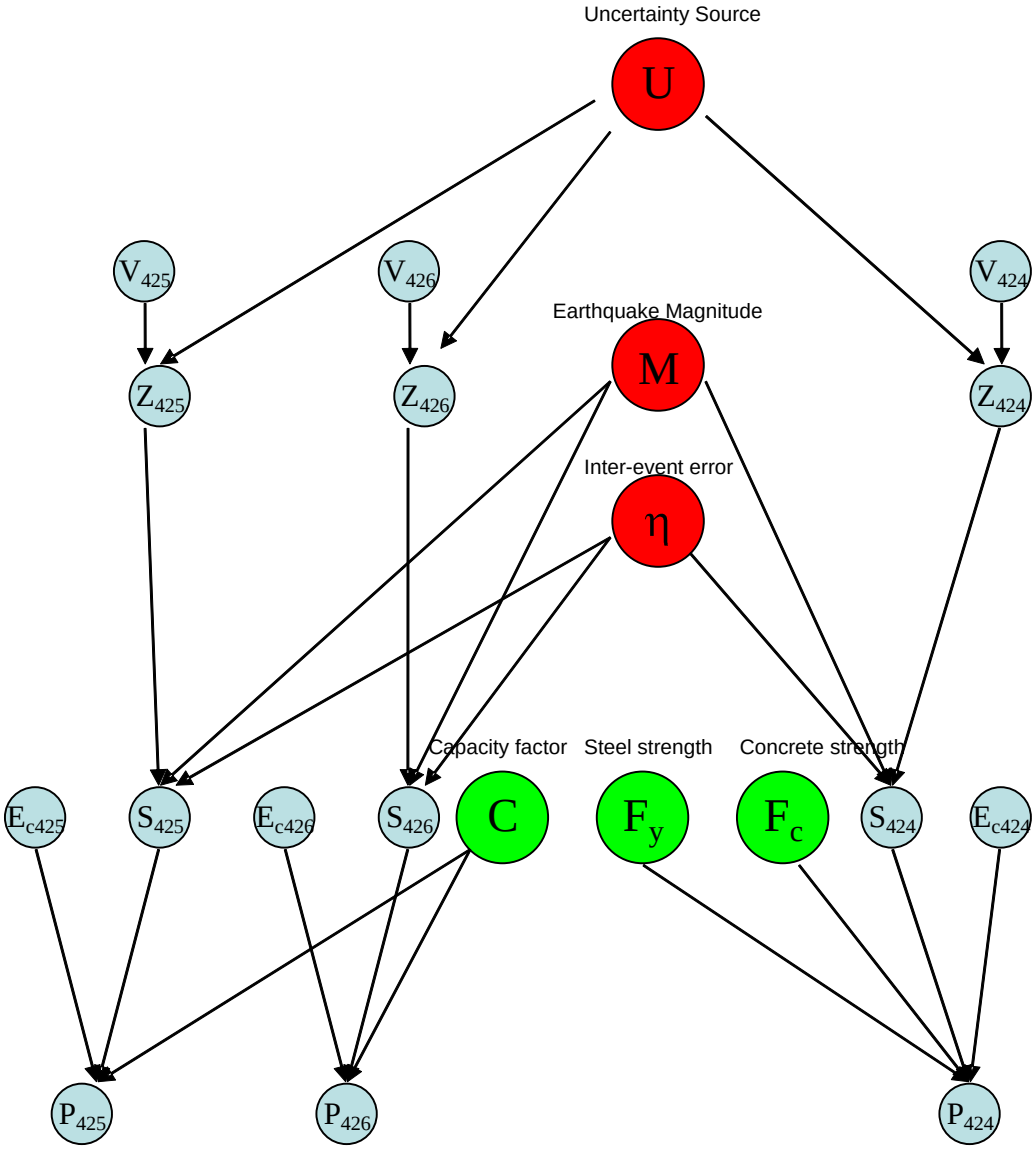

Fig. 6.17 The BN used to calculate the value of P(B426|B425·B424)

Based on the BN in Fig 6.16 and Fig 6.17, the value of $P(B_{425}|B_{424})$ and $P(B_{426}|B_{425}\cdot B_{424})$ are calculated as 0.994 and 0.90 respectively. Using Equation (6.14),

$$P(L) = P(B_{424}) \cdot P(B_{425} \mid B_{424}) \cdot P(B_{426} \mid B_{425} \cdot B_{424}) = (1 - 0.337) \cdot 0.994 \cdot 0.99 = 0.652$$

$$P(\bar{L}) = 1 - P(L) = 0.348$$

So the value of this link is 0.348. It is much smaller than 0.769, which is the sum of all probabilities of bridges on the link. In the same way, the values of all links are obtained, and the best path between node 1 and node 16 is identified as shown in Fig 6.18.

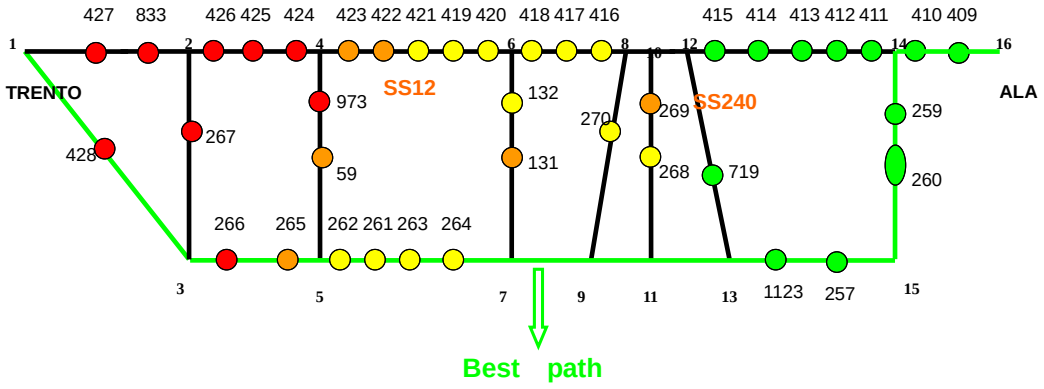

Fig. 6.18 Best path between Trento and Ala

6.4.4 Results

Finally, Dijkstra's algorithm is applied to the APT network and the best path between any two nodes is identified. Fig. 6.19 is the result between Passo Lavazè and Riccomassimo.

Fig. 6.19 The best path between Passo Lavazè and Riccomassimo

6.5 Conclusions

In this chapter, the seismic assessment framework is extended from individual bridges to the system level. This framework can provide the seismic risk analysis for all the bridges in the network. In order to consider the correlation of intra-error terms between the different sites, the single source BN model is adopted in this chapter. The correlation between all bridges can be analyzed using this framework. Based on this correlation, the link value is calculated again, and the best path between any two nodes within the network is identified. The results show that the best path identified here is very similar to that in Chapter 3. I conclude that the approximate methods used in Chapter 3 can be used to identify the best path.

It should be noted that here there are some approximations when entering the three sets of evidence one by one, as after entering evidence 1, we get the posterior for all the global variables. At this time, all the global variables should be correlated due to the same evidence 1. However, when we enter the second evidence, these posteriors will be used as the prior ones which are considered uncorrelated. In order to consider these correlations between global variables, we need to find the covariance matrix after entering each set of evidence, and use this covariance matrix as the prior information for the second entry. See Appendix E for more detail.

I mention here the assumptions and limitations of this chapter. First, we neglected the correlation between the global variables after using the evidence. We have developed a method to include the correlation (see appendix *E*) but we did not make use of this method in the simulations because it needs a great deal of time to modify and run the Matlab Program. I will finish the simulation in subsequent research.

Secondly, we neglect the correlation between the damaged states of bridges on different links. There are two reasons for this: on the one hand, when identifying the best path using Dijkstra's algorithm, we need to calculate the seismic vulnerability between any two nodes. If every time we consider the correlations between all the bridges within the two nodes, the computation will be very large; on the other hand, the bridges on different links are also far apart, so the correlations between them are not so strong as that of bridges in the same link.

7 Conclusions and Future work

Based on the work carried out, we can draw the following conclusions:

- Because of the limited information needed, the Hazus method has been chosen as the most suitable model for generating fragility curves for each bridge of the APT stock. Risk analysis has been performed under the return periods of 72, 475 and 2,475 years, accounting for four possible limit states: operational, damage, life loss, and collapse. The results show that most bridges in the APT have a very low risk of collapse, and that direct risk of loss of life is negligible. This outcome is consistent with the fact that the APT is a low seismicity region, where the design PGA for a 475 year return period is of the order of 0.075*g*. Conversely, the operational state of the network after an earthquake is of concern.
- The connectivity reliability of the road network has been analyzed. Algorithms ORDER and ORDER-II are used to enumerate the most probable network states. The results show that the APT network has a relatively high connectivity. The best path between any two given sites within the network is identified using Dijkstra's algorithm. It is to be noted that the algorithm does not take into account the correlation between the failure of different bridges. Because of this, the results may underestimate the actual connectivity. Nonetheless, the algorithm quickly provides a useful estimate. This is a graph search algorithm used to solve the shortest path problem in a non-directional graph, with non-negative path cost. These results are very helpful for bridge managers and government officials in understanding the network status, and can assist them in making rapid decisions with regard to distributing the available human and material rescue resources to the disaster centre in near-real time, under post-earthquake conditions.
- A Bayesian Network is used to consider the logical interaction between the components within the system. The framework incorporates a demand model, a capacity model and a fragility function. The uncertainty terms are considered in

both the capacity and the demand model. In order to apply the propagation scheme for a Bayesian Network with conditional Gaussian distributions to this framework, all the variables in the framework are assumed to follow a Gaussian distribution. For the variables which do not follow a Gaussian distribution, the Mixture of Gaussian (MoG) distribution is used to approximate the probability density functions (PDFs).

- The Monte-Carlo simulation is incorporated into the scheme during the procedure for entering evidence. Before an earthquake, the system is initialized by calculation of the prior probabilities of bridges being in, or exceeding, a specific limit state. After an earthquake, observations of the state of a limited number of bridges allow us to update the probabilistic knowledge of the state of the other bridges in the stock, and of the network. Again, the results are approximate. After processing the observations, the posterior joint probability of the random variables may be non-Gaussian. In this thesis, I propose application of a Gaussian approximation to the posterior, and of Monte Carlo simulations to derive that approximation. Using this framework, the observations on a few bridges can be applied to the whole bridge network. I have shown how this method could support quick decision making by authorities, as to opening a bridge in a post-earthquake situation. The simulation study shows that the bridges in the APT stock have a low probability of collapsing, even after a local earthquake of magnitude 7.
- The best path between any two places within the APT network is identified by taking account of the mutual correlation in capacity and demand between the different bridges in the stock. The result is similar to the approximate method in Chapter 3 which uses the sum of specific limit state probabilities as the link value. It concludes that the approximate method can be used to identify the best path after an earthquake.

Every step presented in this dissertation is part of the systematically organized plan in our research group, and there are still many fields needing further improvement and study. The quality of the approximations proposed in this thesis has not been assessed systematically. The reason is that exact computation is impossible for very large networks. The quality of the approximation can only be inferred by the many arguments I gave in support. A further research project, currently under way, deals with the comparison of the results of the approximation and that resulting by direct MC simulation on simple models.

- In Chapter 3 and Chapter 6, the connectivity reliability of the system is calculated and the best path is identified. The bridge elements are the only vulnerable parts of the network, and the roads between any two bridges are assumed never to fail. In future research, the influence of roads and bridge

traffic capacities should be considered in the network analysis.

- In the seismic assessment framework based on Bayesian Networks, the seismic demand model is developed using an attenuation function which is highly dependent on local site conditions. In this study, the attenuation equation used is derived from empirical data from California, while the case studies in this paper are refer to bridges in Trentino, Italy; a more sophisticated model for this specific region is needed in future research.
- This paper aims to develop a generic framework for seismic risk assessment, designed to support emergency response in a post-earthquake scenario. Additional research is needed to extend the Bayesian Network with utility and decision nodes for decision support in post-earthquake scenario.
- In order to apply the methodology described in this study to a practical project, the framework must be integrated with the external sources which can supply evidence to Bayesian Networks.
- In this study, all the calculations are carried out using Matlab program. In order to present the results to those who are not proficient in Bayesian Networks, a user-friendly interface for the program is needed. This program can present the probabilistic output in intuitive charts, graphs or curves.

Appendix A: Joint distribution for uncertainties in two sites

The random uncertainties in two sites are given as:

$$x = \eta + \varepsilon_x \tag{A.1a}$$

$$y = \eta + \varepsilon_y \tag{A.1b}$$

where η, ε are drawn from independent normal distributions with zero mean:

$$f(\eta) = \frac{1}{\sqrt{2\pi}\sigma_\eta} \exp(-\frac{\eta^2}{2\sigma_\eta^2}) \tag{A.2a}$$

$$f(\varepsilon) = \frac{1}{\sqrt{2\pi}\sigma_\varepsilon} \exp(-\frac{\varepsilon^2}{2\sigma_\varepsilon^2}) \tag{A.2b}$$

Then the mean values for *x* and *y* are:

$$\mu_x = \mu_\eta + \mu_\varepsilon = 0 \tag{A.3a}$$

$$\mu_y = \mu_\eta + \mu_\varepsilon = 0 \tag{A.3b}$$

and the variations for *x* and *y* are:

$$\sigma_x^2 = \sigma_\eta^2 + \sigma_\varepsilon^2 \tag{A.4a}$$

$$\sigma_y^2 = \sigma_\eta^2 + \sigma_\varepsilon^2 \tag{A.4b}$$

Then the probability density functions for *x* and *y* are:

$$f(x) = \frac{1}{\sqrt{2\pi}\sigma_x} \exp(-\frac{x^2}{2\sigma_x^2}) \tag{A.5a}$$

$$f(y) = \frac{1}{\sqrt{2\pi}\sigma_y} \exp(-\frac{y^2}{2\sigma_y^2}) \tag{A.5b}$$

Based on the definition of correlation coefficient

$$\rho_{x,y} = \frac{\mathrm{cov}(x,y)}{\sqrt{\mathrm{var}\, x \cdot \mathrm{var}\, y}} = \frac{\mathrm{cov}(x,y)}{\sigma_\eta^2 + \sigma_\varepsilon^2} \tag{A.6}$$

where

$$\mathrm{cov}(x,y) = E[(x-\mu_x)\cdot(y-\mu_y)]$$

$$= E[x \cdot y]$$

$$= E[(\eta+\varepsilon_x)\cdot(\eta+\varepsilon_y)]$$

$$= E[\eta^2 + \eta\cdot(\varepsilon_x+\varepsilon_y) + \varepsilon_x\cdot\varepsilon_y]$$

$$= E[\eta^2] + E[\eta]\cdot E[\varepsilon_x+\varepsilon_y] + E[\varepsilon_x\cdot\varepsilon_x]$$

$$= \sigma_\eta^2 + E[\varepsilon_x\cdot\varepsilon_x] \tag{A.7}$$

If the correlation coefficient between variable ε_x and ε_y are ρ_ε, then

$$\rho_\varepsilon = \frac{\mathrm{cov}(\varepsilon_x,\varepsilon_y)}{\sqrt{\mathrm{var}\,\varepsilon_x \cdot \mathrm{var}\,\varepsilon_y}} = \frac{\mathrm{cov}(\varepsilon_x,\varepsilon_y)}{\sigma_\varepsilon^2} \tag{A.8}$$

where

$$\text{cov}(\varepsilon_x, \varepsilon_y) = E[(\varepsilon_x - \mu_\varepsilon) \cdot (\varepsilon_y - \mu_\varepsilon)] = E[\varepsilon_x \cdot \varepsilon_y] \tag{A.9}$$

So we have

$$E[\varepsilon_x \cdot \varepsilon_y] = \text{cov}(\varepsilon_x, \varepsilon_y) = \rho_\varepsilon \cdot \sigma_\varepsilon^2 \tag{A.10}$$

Substituting equations (A.10), and (A.7) into (A.6), we have

$$\rho_{x,y} = \frac{\sigma_\eta^2 + \rho_\varepsilon \cdot \sigma_\varepsilon^2}{\sigma_\eta^2 + \sigma_\varepsilon^2} \tag{A.11}$$

For the special condition that the site to site correlation ρ_ε is zero, the total correlation coefficient is

$$\rho_{x,y} = \frac{\sigma_\varepsilon^2}{\sigma_\eta^2 + \sigma_\varepsilon^2} \tag{A.12}$$

Appendix B: Earthquake return period

The earthquake return period, which is also called the recurrence interval, is an estimate of the interval of time between earthquakes of a certain intensity. It is used to describe the frequency of earthquakes. The longer the return period, the lower is the probability of the earthquake.

If the return period of an earthquake is n years, then the annual probability of this earthquake is $\lambda = 1/n$. In T years, the probability P of this earthquake follows a Poisson distribution:

$$P = 1 - e^{-\lambda T} \tag{B.1a}$$

$$n = \frac{1}{\lambda} = -\frac{T}{\ln(1-P)} \tag{B.1b}$$

If the design life of a structure is 50 years, then 50 years is the basic period. The earthquake with 10% exceeding probability is:

$$P = 10\% \tag{B.2a}$$

$$n = \frac{1}{\lambda} = -\frac{T}{\ln(1-P)} = 475 \tag{B.2b}$$

So the return period for this earthquake is 475 years.

If a structure with a design life of 50 years has a return period of 50 years, then the exceeding probability for this earthquake is:

$$P = 1 - e^{-\lambda T} = 63\% \tag{B.3}$$

In the same way, the return period of a strong earthquake with exceeding probability of 2% is 2,475 years.

If the annual probability of an earthquake follows a Binomial distribution, then

$$P = 1 - (1 - \lambda)^T \tag{B.4a}$$

$$n = \frac{1}{\lambda} = \frac{1}{1 - (1 - P)^{1/T}} \tag{B.4b}$$

When T = 50 years, the exceeding probability P is 63%, 10%, and 2% respectively, and the return period n is 50.8 years, 475 years, and 2,475 years respectively. The results are the same with the calculations based on a Poisson distribution.

$$n = \frac{1}{1 - (1 - P)^{1/T}} = \frac{1}{1 - (1 - 63\%)^{1/50}} = 50.8 \tag{B.5a}$$

$$n = \frac{1}{1 - (1 - P)^{1/T}} = \frac{1}{1 - (1 - 10\%)^{1/50}} = 475 \tag{B.5b}$$

$$n = \frac{1}{1 - (1 - P)^{1/T}} = \frac{1}{1 - (1 - 2\%)^{1/50}} = 2475 \tag{B.5c}$$

Appendix C: Gaussian random fields

An N-dimensional random field is a set of random variables $Y(\mathbf{x})$, $\mathbf{x} \in \mathbf{R}^N$, which has a collection of distribution functions for any number of points

$$F(Y(x_1) \le y_1, ..., Y(x_n) \le y_n)$$

Where $Y(\mathbf{x_i})$ is the random variable, y_i denotes a particular value or outcome of the random variable, and $\mathbf{x_i}$ denotes spatial coordinates.

For a Gaussian stochastic process Y_G with average y_c and dispersion σ, the probability for $Y_G = [y, y+dy]$ is given by

$$P(y)dy = \frac{1}{\sqrt{2\pi}\sigma} \cdot \exp\{-\frac{(y-y_c)^2}{2\sigma^2}\}dy$$

When the stochastic process concerns an entire region of space, we talk of a Gaussian random field. A general random Gaussian field gives the knowledge of *n*-point probability distributions:

$$P(y_1, ..., y_n)dy_1...dy_n = \left((2\pi)^{\frac{N}{2}} \cdot \sqrt{|\mathbf{\Sigma}|} \right)^{-1} \cdot \exp\left(-\frac{1}{2} \cdot (\mathbf{x}-\boldsymbol{\mu})^T \cdot \mathbf{\Sigma}^{-1} \cdot (\mathbf{x}-\boldsymbol{\mu}) \right) dy_1...dy_n$$

where $\mathbf{x}$: [*N* x 1] is the random variable;
$\boldsymbol{\mu}$: [*N* x 1] is the mean value vector;
$\mathbf{\Sigma}$: [*N* x *N*] is the covariance matrix;

The product of two Gaussian distributions is an un-normalized Gaussian distribution:

$\text{Normal}(\mathbf{x};\boldsymbol{\mu}_a,\mathbf{\Sigma}_a) \cdot \text{Normal}(\mathbf{x};\boldsymbol{\mu}_b,\mathbf{\Sigma}_b) = n_c \cdot \text{Normal}(\mathbf{x};\boldsymbol{\mu}_c,\mathbf{\Sigma}_c)$;

where $\mathbf{\Sigma}_c = (\mathbf{\Sigma}_a^{-1} + \mathbf{\Sigma}_b^{-1})^{-1}$;

$\boldsymbol{\mu}_c = \mathbf{\Sigma}_c (\mathbf{\Sigma}_a^{-1} \boldsymbol{\mu}_a + \mathbf{\Sigma}_b^{-1} \boldsymbol{\mu}_b)$;

$n_c = (2\pi)^{-N/2} |\mathbf{\Sigma}_c|^{1/2} |\mathbf{\Sigma}_a|^{-1/2} |\mathbf{\Sigma}_b|^{-1/2} \cdot ...$

$... \cdot \exp[-1/2 (\boldsymbol{\mu}_a^T \mathbf{\Sigma}_a^{-1} \boldsymbol{\mu}_a + \boldsymbol{\mu}_b^T \mathbf{\Sigma}_b^{-1} \boldsymbol{\mu}_b - \boldsymbol{\mu}_c^T \mathbf{\Sigma}_c^{-1} \boldsymbol{\mu}_c)]$;

Appendix D: Monte Carlo simulation

The Monte Carlo method is also called a statistical simulation method. It is a numerical simulation method using random numbers which are random variables with a uniform distribution in (0, 1). This method was proposed by Metropolis in the Second World War and used in the Manhattan Project. Monte Carlo is the capital city of Monaco, and it is famous for its casino. The basic idea of the Monte Carlo method is to simulate stochastic processes on the computer, and then undertake statistical sampling. Compared with other traditional mathematical methods, it has the advantages of intuitiveness and easy computing.

The Monte Carlo method can be used in many areas. Generally, regarding the characteristics of the stochastic process that it incorporates, the applications of Monte Carlo method can be divided into two types: deterministic problems and random problems. For a deterministic problem, we first built a probability model related to the solution, so that the required solution equals the probability distribution or expectation of the model. We then generate a random variable, and last use the arithmetic mean as the approximation of the solution. Calculating the integral and solving linear equations are associated with this type of problem. For the second type of problem, we normally use a direct simulation method. The following is an application example of the Monte Carlo method.

Assume $f(x)$ is a continuous function in [0, 1], and $0 \le f(x) \le 1$. We now need to calculate the integral $I = \int_0^1 f(x)dx$ which equals the area of the shadow part in fig D.1. If we randomly throw point (a, b) into the unit square, the probability that point (a, b) is under the curve $y = f(x)$ is:

$$P\{y \le f(x)\} = \int_0^1 f(x)dx = I \tag{D.1}$$

The procedure for approximate results using the Monte Carlo method is the following:

Step1: generate two groups of random number x_i, y_i, i=1, 2, ..., N within the range [0, 1], and use [x_i, y_i] as the coordinates of point [a, b];

Step2: for every pair of coordinates [x_i, y_i], if $y_i \leq f(x_i,)$, then record one time.

Assume that there are n times that coordinates [x_i, y_i] are under the curve $y = f(x)$ in N times test, then n /N approximately equals the probability that point (a, b) is under the curve $y = f(x)$, which is also the integral result I.

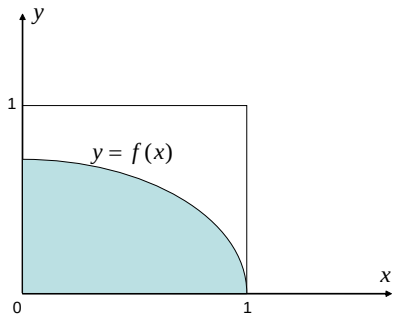

Fig. D.1 The integral of f(x) using the Monte Carlo method

Appendix E: How to consider the correlation between global variables

Suppose we have 3 sets of evidence and for each set there are N = 1,000 simulations. Then we have 1,000 mean vectors and 1,000 covariance matrices for the global variables.

Evidence 1: For each simulation, we can generate m (e.g. m=10) sample vectors based on the corresponding mean vector Vi and a covariance matrix Mi. So we can collect N×m samples (1,000×10=10,000), Then compute the sample mean and covariance matrix, and take them as parameters for the posterior.

For evidence 2, we can use the posterior of the global variables as the new prior input, and repeat the procedures in evidence 1. In this way we obtain the new posterior of the global variables.

In the same way, all the sets of evidence are entered and incorporated into the framework, and all the global variables are updated.

References

Abrahamson, N., Atkinson, G., Boore, D., Bozorgnia, Y., Campbell, K., Chiou, B., Idriss, I. M., Silva, W., and Youngs, R. (2008). *Comparisons of the NGA ground-motion relations.* Earthquake Spectra, 24(1), 45-66.

Abrahamson, N. A., and Silva, W. J. (1997). *Empirical response spectral attenuation relations for shallow crustal earthquakes.* Seism. Res. Lett., 68(1), 94-127.

Astudillo R. B. (2002): *Basis for an european bridge management system*. In: Casas J, Frangopol D and Nowak A, (eds), First International Conference on Bridge Maintenance, Safety and Management (IABMAS), Barcelona, Spain, 14-17 July 2002. Barcelona: CIMNE.

ATC (1985). *Earthquake Damage Evaluation Data for California*. Report No. ATC-13, Applied Technology Council. Redwood City, CA.

Basöz, N., and Kiremidjian, A. S. (1995). *Prioritization of bridges for seismic retrofitting, Technical Report NCEER-95-0007*. Multidisciplinary Center for Earthquake Engineering Research, Buffalo, New York.

Basöz, N., and Mander, J. B. (1999). *Enhancement of the Highway Transportation Lifeline Module in HAZUS*. Buffalo, New York: University at Buffalo, State University of New York.

BayesiaLab. (2011). http://www.bayesia.com/. October 29, 2011.

Bayraktarli, Y. Y., Ulfkjaer, J. P., Yazgan, U., and Faber, M. H. (2005). *On the Application of Bayesian Probabilistic Networks for Earthquake Risk Management.* Proceedings of the 9th International Conference on Structural Safety and Reliability, June 19-23, 2005. Rome, Italy.

Bayraktarli, Y. Y., Yazgan, U., Dazio, A., and Faber, M. H. (2006). *Capabilities of the Bayesian probabilistic networks approach for earthquake risk management.* Proceedings of First European Conference on Earthquake Engineering and Seismology, September 3-8 2006. Geneva, Switzerland.

Bensi, M. T., Kiureghian, A. D., and Straub, D. (2009). *A Bayesian Network Framework for Post-earthquake Infrastructure System Performance Assessment*. Paper presented at the Lifeline Earthquake Engineering in a Multihazard Environment. June 28- July 1, 2009, Oakland, California.

Bensi, M. T. (2010). *A Bayesian Network Methodology for Infrastructure Seismic Risk Assessment and Decision Support. Ph.D thesis, University of California, Berkeley, Berkeley, CA.*

Bensi, M. T., Kiureghian, A. D., and Straub, D. (2011). *A Bayesian Network Methodology for Infrastructure Seismic Risk Assessment and Decision Support. PEER 2011/02*

BNT (2011). http://code.google.com/p/bnt/. October 29, 2011.

Boore, D. M., Gibbs, J. F., Joyner, W. B., Tinsley, J. C., and Ponti, D. J. (2003). *Estimated ground motion from the 1994 Northridge, California, earthquake at the site of the interstate 10 and La Cienega Boulevard Bridge collapse, west Los Angeles, California*. Bulletin of the Seismological Society of America, *93*(6), 2737-2751.

Bortot, F. (2006). *Reliability-Based Decision-Making in Infrastructure Management.* Ph.D thesis, Univeristy of Trento, Trento.

Campbell, K. W., and Bozorgnia, Y. (2006a). *Campbell-Bozorgnia NGA Ground Motion Model for the Average Horizontal Component of PGA, PGV, PGD and SA at Selected Spectral Periods Ranging from 0.01-10.0 Seconds*. Version 1.0. NGA Report: Oct. 16, 2006.

Campbell, K. W., and Bozorgnia, Y. (2006b). *Next generation attenuation (NGA) empirical ground motion models: Can they be used in Europe?* The First European Conference on Earthquake Engineering and Seismology, September 3-8, 2006, Geneva, Switzerland.

Cowell, R. G. (Ed.). (1999). *Probabilistic Networks and Expert Systems.* London: Springer.

D., M. (2008). *Norme tecniche per le costruzioni*. Italian code.

Dijkstra, E. W. (1959). *A Note on Two Problems in Connexion with Graphs*. Numerische Mathematik, *1*, 269 - 271.
Dunnett, C. W., and Sobel, M. (1955). *Approximations to the Probability Integral and Certain Percentage Points of a Multivariate Analogue of Student's t-Distribution*. Biometrika, 42(1/2), 258-260.

Dutta, A. (1999). *On Energy-Based Seismic Analysis and Design of Highway Bridges.* Ph.D thesis, the State University of New York at Buffalo, New York.

Dutta, A., and Mander, J. B. (1998). *Capacity design and fatigue of confined concrete columns*. Buffalo, New York: University at Buffalo, State University of New York.

Eurocode 8 (2004): *Design of structures for earthquake resistance, Part 1: General rules, seismic actions and rules for buildings*. 2004.

FEMA (2003). *Multi-hazard Loss Estimate Methodology* (*Earthquake Model*). Technical Manual, Department of Homeland Security, Emergency Preparedness and Response Directorate, FEMA Mitigation Division, Washington, D.C.

FHWA (2006). *Seismic Retrofitting Manual for Highway Structures: Part 1*. US Department of Transportation, Federal Highway Administration. McLean, VA.

Frangopol, D. M., and Liu, M. (2007). *Bridge network maintenance optimization using stochastic dynamic programming*. Journal of Structural Engineering-Asce, 133(12), 1772-1782.

Frangopol, D. M., and Neves LC. *Probabilistic performance prediction of deteriorating structures under different maintenance strategies: Condition, safety and cost.* In Frangopol, D. M., Bruhwiler E, Faber MH and Adey B, (eds), Life-Cycle Performance of Deteriorating Structures: Assessment, Design and Management. ASCE, Reston, Virginia. 2004. 9-18.

Gardoni, P., Kiureghian, A. D., and Mosalam, K. M. (2002). *Probabilistic Models and Fragility Estimates for Bridge Components and Systems*. PEER Report 2002/13, Pacific Earthquake Engineering Research Center, Berkeley, CA: University of California, Berkeley.

Ghasemi, H., Otsuka, H., Cooper, J. D., and Nakajima, H. (1996). *Aftermath of the*

Kobe Earthquake. Public Roads, 60(2).

Hanks, T. C., and Kanamori, H. (1979). *A moment magnitude scale*. Journal of Geophysical Research, *V84, N85*. 2348-2350.

Hansen, A. F. (2000). *Bayesian Networks as a decision support tool in marine application.* Ph.D thesis, Technical University of Denmark.

Hguin. (2011). from http://www.hugin.com/, October 29, 2011.

Http://dl.zhishi.sina.com.cn/upload/31/86/74/1497318674.4175043.jpg, October 29, 2011.

Jensen, F. V., and Nielsen, T. D. (2007). *Bayesian Networks and Decision Graphs* (second ed.): Spring Verlag, London.

Jernigan, J. B., and Hwang, H. (2002). *Development of Bridge Fragility Curves.* Paper presented at the 7th US National Conference on Earthquake Engineering, July 21-25, 2002, Boston, Massachusetts.

Joyner, W. B., and Boore, D. M. (1981). *Peak Horizontal Acceleration and Velocity from Strong-Motion Records Including Records from the 1979 Imperial-Valley, California, Earthquake*. Bulletin of the Seismological Society of America, 71(6), 2011-2038.

Kang, W. H., Song, J. H., and Gardoni, P. L. (2008). *Matrix-based system reliability method and applications to bridge networks*. Reliability Engineering and System Safety, 93(11), 1584-1593.

Karim, K. R., and Yamazaki, F. (2001). *Effect of earthquake ground motions on fragility curves of highway bridge piers based on numerical simulation*. Earthquake Engineering and Structural Dynamics, 30(12), 1839-1856.

Karim, K. R., and Yamazaki, F. (2003). *A simplified method of constructing fragility curves for highway bridges*. Earthquake Engineering and Structural Dynamics, 32(10), 1603-1626.

Kawakami, H., and Mogi, H. (2003). *Analyzing spatial intraevent variability of peak ground accelerations as a function of separation distance.* Bulletin of the Seismological Society of America, 93(3), 1079-1090.

Kennedy, R. P., Cornell, C. A., Campbell, R. D., Kaplan, S., and Perla, H. F. (1980).

Probabilistic Seismic Safety of an Existing Nuclear Power Plant. Journal of Nuclear Engineering and Design, 59, 315-338.

Lam, Y. F., and Li, V. O. K. (1986). *An Improved Algorithm for Performance Analysis of Networks with Unreliable Components*. IEEE Transactions on Communications, *34*(5), 496-497.

Lauritzen, S. L., and Jensen, F. (2001). *Stable local computation with conditional Gaussian distributions*. Statistics and Computing, 11(2), 191-203.

Lauritzen, S. L., and Jensen, F. V. (1997). *Local computation with valuations from a commutative semigroup*. Annals of Mathematics and Artificial Intelligence, 21(1), 51-69.

Lauritzen, S. L., and Spiegelhalter, D. J. (1988). *Local Computations with Probabilities on Graphical Structures and Their Application to Expert Systems*. Journal of the Royal Statistical Society Series B-Methodological, 50(2), 157-224.

Li, V. O. K., and Silvester, J. A. (1984). *Performance Analysis of Networks with Unreliable Components*. IEEE Transactions on Communications, 32(10), 1105-1110.

Liu, M., and Frangopol, D. M. (2006). *Probability-based bridge network performance evaluation*. Journal of Bridge Engineering, 11(5), 633-641.

Mander, J. B. (1999). *Fragility curves development for assessing the seismic vulnerability of highway bridges*. MCEER Highway Project Report, FHWA National Institute of Building Sciences (NIBS), Buffalo, New York.

Matlab. (2011). http://www.mathworks.com/products/matlab/index.html , October 29, 2011.

Murphy, K. P. (2001). *The Bayes Net Toolbox for Matlab*. Computing Science and Statistics, 33. 1-20.

Neapolitan, R. E. (Ed.). (2003). *Learning Bayesian Networks*. NJ: Prentice Hall, Upper Saddle River.

Netica, www.norsys.com. October 29, 2011.

Nielson, B. G. (2005). *Analytical fragility curves for highway bridges for moderate seismic zones.* Ph.D thesis, Georgia institute of technology, Atlanta.

Nielson, B. G., and DesRoches, R. (2007). *Seismic fragility methodology for*

highway bridges using a component level approach. Earthquake Engineering and Structural Dynamics, 36(6), 823-839.

Nojima, N. (1998). *Prioritization in upgrading seismic performance of road network based on system reliability analysis.* Proc. Third China-Japan-US Trilateral Symposium on Lifeline Earthquake Engineering, August 1998, Kunming, China.

Nuti, C. (2004). *Prioritization techniques.* FIB TG 7.4 Seismic Design and Assessment Procedures for Bridges 5th Meeting, May 30, 2004. Pavia, Italy.

Park, J., Bazzurro, P., and Baker, J. W. (2007). *Modeling spatial correlation of ground motion intensity measures for regional seismic hazard and portfolio loss estimate*. Proceedings of Applications of Statistics and Probability in Civil Engineering, July 18, 2007. Kanda, Takada & Furuta (eds), Taylor & Francis Group, London.

Sanjoy Dasgupta, Christos H. Papadimitriou, and Umesh V. Vazirani (2008). Algorithms. McGraw-Hill.

Shenoy, P. P. (2006). *Inference in hybrid Bayesian networks using mixtures of Gaussians*, R. Dechter, T. Richardson, Editors , Uncertainty in Artificial Intelligence: Proceedings of the Twenty-Second Conference (UAI-06), AUAI Press, Corvallis, OR July 13-16 , 2006, 428–436.

Shinozuka, M., Feng, M. Q., Kim, H. K., and Kim, S. H. (2000c). *Nonlinear static procedure for fragility curve development*. Journal of Engineering Mechanics-Asce, 126(12), 1287-1295.

Shinozuka, M., Feng, M. Q., Lee, J., and Naganuma, T. (2000b). *Statistical analysis of fragility curves*. Journal of Engineering Mechanics-Asce, 126(12), 1224-1231.

Shinozuka, M., Grigoriu, M., Ingraffea, A. R., Sarah, Billington, L., and Feenstra, P. (2000a). *Development of Fragility Information for Structures and Nonstructural Components*. Buffalo, New York: University at Buffalo, State University of New York.

Sokolov, V., Wenzel, F., Jean, W. Y., and Wen, K. L. (2010). Uncertainty and Spatial Correlation of Earthquake Ground Motion in Taiwan. *Terrestrial Atmospheric and Oceanic Sciences*, *21*(6), 905-921.

Straub, D. (2005). *Natural hazards risk assessment using Bayesian networks.* Paper presented at the Safety and Reliability of Engineering Systems and Structures (Proc.

ICOSSAR 05), JUNE 19-23, 2005. Rome. Augusti et al. (eds), Millpress, pp. 2535-2542

Straub, D., Bensi, M. T., and Kiureghian, A. D. (2008). *Spatial Modeling of Earthquake Hazard and Infrastructure Performance Through Bayesian Networks.* Proc. EM'08, Inaugural International Conference of the Engineering Mechanics Institute, May 18-21, 2008. University of Minnesota, Minneapolis.

Straub, D., and Gret-Regamey, A. (2006). *A Bayesian probabilistic framework for avalanche modeling based on observations*. Cold Regions Science and Technology, 46(3), 192-203.

Straub, D., and Kiureghian, A. D. (2008). *An investigation into the combination of Bayesian network with structural reliability methods.* Paper presented at the Proc. IFIP WG 7.5 Working conference, Reliability and optimization of structural systems, August 6 - 9 2008, Toluca, Mexico.

Straub, D., and Kiureghian, A. D. (2010a). *Bayesian Network Enhanced with Structural Reliability Methods: Methodology*. Journal of Engineering Mechanics-Asce, 136(10), 1248-1258.

Straub, D., and Kiureghian, A. D. (2010b). *Bayesian Network Enhanced with Structural Reliability Methods*: *Application*. Journal of Engineering Mechanics-Asce, 136(10), 1259-1270.

Thompson P. D., Small E. P., Johnson M and Marshall AR. *The Pontis bridge management system*. Structural Engineering International, 1998, 8(4): 303-308.

USGS. (2011). http://earthquake.usgs.gov/earthquakes/eqarchives/year/byyear.php. October 29, 2011.

Vanmarcke, E. (Ed.). (1983). *Random fields, analysis, synthesis*. Cambridge, Mass: MIT press.

Wesson, R. L., and Perkins, D. M. (2001). *Spatial correlation of probabilistic earthquake ground motion and loss*. Bulletin of the Seismological Society of America, 91(6), 1498-1515.

Zonta, D., Zandonini, R., and Bortot, F. (2007). *A reliability-based bridge management concept*. Structure and Infrastructure Engineering, 3(3), 215-235.

Publications

Yue Y. C, M. Pozzi, D. Zonta, F. Bortot and R. Zandonini, "Application of continuous Bayesian Networks to seismic vulnerability assessment". Proc. "6th International Conf. on Bridge Maintenance, Safety and Management (IABMAS2012)",Como, Italy, 8-12 July 2012.

Y. C. Yue, M. Pozzi, D. Zonta, F. Bortot and R. Zandonini, 'Network-level seismic risk assessment based on the Bayesian Network'. the International Symposium on Reliability Engineering and Risk Management (ISRERM'2012). August 5-8, 2012, Kanagawa University, Yokohama, Japan. (abstract accepted).

Yue Y. C, D. Zonta, M. Pozzi, F. Bortot and R. Zandonini. 'System reliability analysis of a Bridge Management System under earthquake hazards'. 6th International ASRANet Conference on Network for Integrating Structural Analysis, Risk and Reliability. 2-4 July 2012 at London, Croydon.

Yue Y. C, D. Zonta, M. Pozzi, F. Bortot and R. Zandonini "Application of the Bayesian network to seismic vulnerability assessment in Bridge Management System". , 2007. Proc. "XIV Convegno Nazionale: L'Ingegneria Sismica in Italia ANIDIS 2007", Bari, 18-22 September 2011.

Yue Y. C, Zonta D., Bortot F., Zandonini R., "Assessment of the operation level of a bridge network in post-earthquake scenarios". Proc. "5th International Conf. on Bridge Maintenance, Safety and Management (IABMAS2010)",Philadelphia, 11-15 Jul 2010.

Y. C.Yue, M. Pozzi, D. Zonta, F. Bortot and R. Zandonini, "Seismic Assessment using a Bayesian Network". In: International Symposium on Reliability Engineering and Risk Management (ISRERM2010). Sept. 23-26, 2010, Shanghai, China.

Zandonini R., Yue Y., Bortot F. and Zonta D., "Network-level seismic risk management of regional road infrastructure". In: Large Structures and Infrastructures for Environmentally Constrained and Urbanised Areas, Zurich: IABSE, 2010. Proc. "IABSE Symposium", Venice, 22-24 Sep 2010.

Y. C.Yue, M. Pozzi, D. Zonta, F. Bortot and R. Zandonini, Application of the Bayesian Network to Seismic Vulnerability Assessment. 14th European Conference on Earthquake Engineering. August 30 –September 03, 2010. Ohrid, Republic of Macedonia.